

AD-A223 672

# NAVAL POSTGRADUATE SCHOOL

## Monterey, California



### THESIS

DTIC  
ELECTE  
JUL 10 1989  
S B D

COMPARE AT SEA POSITION USING  
MINI-RANGER, LORAN C (INTERNAV) IN  
THE CONTEXT OF MEASURING CURRENT  
VELOCITY WITH A SHIPBOARD ADCP  
(ACOUSTIC DOPPLER CURRENT PROFILER)

by

Ioannis S. Moschovos

December 1989

Thesis Advisor

Curtis A. Collins

Approved for public release; distribution is unlimited.

Unclassified

security classification of this page

## REPORT DOCUMENTATION PAGE

1a Report Security Classification <b>Unclassified</b>			1b Restrictive Markings		
2a Security Classification Authority			3 Distribution/Availability of Report <b>Approved for public release; distribution is unlimited.</b>		
2b Declassification Downgrading Schedule			5 Monitoring Organization Report Number(s)		
4 Performing Organization Report Number(s)			7a Name of Monitoring Organization Naval Postgraduate School		
6a Name of Performing Organization Naval Postgraduate School		6b Office Symbol (if applicable) 55	7b Address (city, state, and ZIP code) Monterey, CA 93943-5000		
6c Address (city, state, and ZIP code) Monterey, CA 93943-5000		9 Procurement Instrument Identification Number			
8a Name of Funding Sponsoring Organization		8b Office Symbol (if applicable)	10 Source of Funding Numbers		
8c Address (city, state, and ZIP code)		Program Element No   Project No   Task No   Work Unit Accession No			
11 Title (include security classification) <b>COMPARE AT SEA POSITION USING MINI-RANGER, LORAN C (INTERNAV) IN THE CONTEXT OF MEASURING CURRENT VELOCITY WITH A SHIPBOARD ADCP (ACOUSTIC DOPPLER CURRENT PROFILER) (Unclassified)</b>					
12 Personal Author(s) <b>Ioannis S. Moschovos</b>					
13a Type of Report Master's Thesis		13b Time Covered From To	14 Date of Report (year, month, day) December 1989		15 Page Count 98
16 Supplementary Notation The views expressed in this thesis are those of the author and do not reflect the official policy or position of the Department of Defense or the U.S. Government.					
17 Cosat Codes			18 Subject Terms (continue on reverse if necessary and identify by block number)		
Field	Group	Subgroup	Loran C, Mini-Ranger, ADCP		
19 Abstract (continue on reverse if necessary and identify by block number)					
<p>The scope of this thesis is to evaluate the use of the MINI RANGER, LORAN (TD) and LORAN (DISPLAY) navigation systems in order to support the collection of current profiles by an Acoustic Doppler Current Profiler Recorder (ADCP). A theoretical error analysis of these systems is undertaken in order to establish the minimum error limits which might be expected when averaging current profiles over time frames of up to 30 minutes.</p> <p>Experimental data was collected with all of these systems in the Monterey Bay and was analysed, the results being presented in this thesis. In addition GPS data was also collected but time has prohibited its analysis and subsequent inclusion. The results show that because of ship fluctuations in course and speed there is no statistically significant difference between the navigation systems when we average the data over times of about 25 - 30 minutes. However, they also show that both the MINI RANGER and Bottom Tracking with the ADCP can produce reasonable results in as little as three minutes, although the ADCP results are clearly biased.</p>					
20 Distribution Availability of Abstract <input checked="" type="checkbox"/> unclassified unlimited <input type="checkbox"/> same as report <input type="checkbox"/> DTIC users			21 Abstract Security Classification <b>Unclassified</b>		
22a Name of Responsible Individual Curtis A. Collins			22b Telephone (include Area code) (408) 646-2673		22c Office Symbol 68CO

DD FORM 1473.84 MAR

83 APR edition may be used until exhausted  
All other editions are obsolete

security classification of this page

Unclassified

Approved for public release; distribution is unlimited.

Compare at Sea Position Using Mini-Ranger, Loran C (Internav)  
in the context of measuring current velocity with a shipboard  
ADCP (Acoustic Doppler Current Profiler)

by

Ioannis S. Moschovos  
LT, Hellenic Navy  
B.S., Hellenic Naval Academy 1979

Submitted in partial fulfillment of the  
requirements for the degrees of

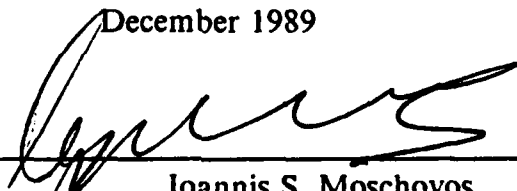
MASTER OF SCIENCE IN HYDROGRAPHY SCIENCE  
AND  
MASTER OF SCIENCE IN APPLIED MATHEMATICS

from the

NAVAL POSTGRADUATE SCHOOL

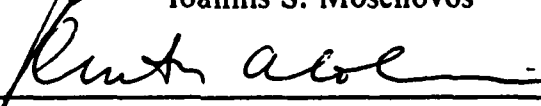
December 1989

Author:

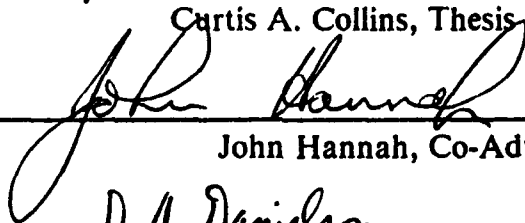


Ioannis S. Moschovos

Approved by:



Curtis A. Collins, Thesis Advisor



John Hannah, Co-Advisor



Donald Danielson, Co-Advisor



Curtis A. Collins, Chairman,  
Department of Oceanography

## ABSTRACT

The scope of this thesis is to evaluate the use of the MINI RANGER, LORAN (TD) and LORAN (DISPLAY) navigation systems in order to support the collection of current profiles by an Acoustic Doppler Current Profiler Recorder (ADCP).

A theoretical error analysis of these systems is undertaken in order to establish the minimum error limits which might be expected when averaging current profiles over time frames of up to 30 minutes.

Experimental data was collected with all of these systems in the Monterey Bay and was analysed, the results being presented in this thesis. In addition GPS data was also collected but time has prohibited its analysis and subsequent inclusion.

The results show that because of ship fluctuations in course and speed there is no statistically significant difference between the navigation systems when we average the data over times of about 25 - 30 minutes. However, they also show that both the MINI RANGER and Bottom Tracking with the ADCP can produce reasonable results in as little as three minutes, although the ADCP results are clearly biased. *Three. (CP) ←*

*Global Positioning System*



<b>Accession For</b>	
NTIS GRA&I	<input checked="" type="checkbox"/>
DTIC TAB	<input type="checkbox"/>
Unannounced	<input type="checkbox"/>
Justification	
By	
Distribution/	
<b>Availability Codes</b>	
Dist	Avail and/or Special
A-1	

## TABLE OF CONTENTS

I. INTRODUCTION .....	1
II. DATA COLLECTION .....	2
A. CRUISE .....	2
B. TIME SYNCHRONIZATION .....	2
III. ACOUSTIC DOPPLER CURRENT PROFILERS .....	5
A. INTRODUCTION .....	5
B. PRINCIPLES OF OPERATION OF THE ACOUSTIC DOPPLER CURRENT PROFILER .....	6
C. THREE DIMENSIONAL CURRENT VELOCITY VECTORS ...	8
D. DEPLOYMENT AREA .....	9
E. BOTTOM TRACKING OPERATION .....	10
F. VELOCITY PROFILES .....	11
G. ACOUSTIC DOPPLER CURRENT PROFILER DATA PROC- ESSING .....	11
IV. THEORY OF LORAN C .....	13
A. INTRODUCTION .....	13
B. SYSTEM DESCRIPTION .....	13
C. PULSES-PHASE AND CODES-CYCLE SELECTION .....	13
D. TIME DIFFERENCE EQUATIONS .....	16
E. HYPERBOLIC GRADIENT, CROSSING ANGLES .....	18
F. ERROR ANALYSIS FOR LORAN C .....	20
V. THEORY OF MINI RANGER .....	30
A. INTRODUCTION .....	30
B. REFERENCE STATIONS .....	30

C. RANGE POSITIONING .....	30
D. ERROR ANALYSIS FOR MINI RANGER .....	31
VI. RESULTS .....	36
VII. CONCLUSIONS AND RECOMMENDATIONS .....	46
APPENDIX A. STATISTICAL ANALYSIS FOR THE LC 408 DATA	47
APPENDIX B. TABLES FOR STANDARD DEVIATIONS AND COVARIANCES OF VELOCITY COMPONENTS FOR LORAN C (LC 408) .....	48
APPENDIX C. PROGRAM DRIVLR FORTRAN .....	51
A. GENERAL REMARKS .....	51
B. DESCRIPTION OF PARAMETERS: .....	51
APPENDIX D. TABLE FOR STANDARD DEVIATIONS AND COVARIANCES OF VELOCITY COMPONENTS FOR MINI RANGER	66
APPENDIX E. AVERAGE CURRENT PROFILES .....	67
APPENDIX F. CURRENT PROFILES FOR SPECIFIC TIMES .....	79
LIST OF REFERENCES .....	85
INITIAL DISTRIBUTION LIST .....	86

## LIST OF TABLES

Table 1.	COMPARISON OF CLOCKS WITH THE MINI RANGER (MR) .....	2
Table 2.	DIFFERENT TIMES BETWEEN THE CLOCKS WITH COMMON TIME BASE (ADCP) .....	2
Table 3.	LORAN C PHASE CODES .....	13
Table 4.	REFERENCE STATION SITES .....	30
Table 5.	POSITION ERROR FOR DIFFERENT CROSS ANGLES ..	32
Table 6.	MAX-MIN VALUES OF STANDARD DEVIATIONS AND COVARIANCES FOR VELOCITY COMPONENTS FOR 3 MINUTE TIME INTERVALS BETWEEN POSITIONS (MINI RANGER) .....	34
Table 7.	SHIP VELOCITY COMPONENTS FOR MINI RANGER, LORAN (TD), LORAN (DISPLAY) FROM POINT 1 TO POINT 2 AT 3 MINUTE TIME INTERVAL. ....	36
Table 8.	SHIP VELOCITY COMPONENTS FOR MINI RANGER, LORAN (TD), LORAN (DISPLAY) FROM POINT 2 TO POINT 1 AT 3 MINUTE TIME INTERVAL .....	36
Table 9.	COMPARISON BETWEEN MINI RANGER AND LORAN (TD) AND THE MINI RANGER AND LORAN (DISPLAY) FOR LEGS 1 - 2 AND 2 - 1. ....	37
Table 10.	SHIP VELOCITY COMPONENTS FOR MINI RANGER, LORAN (TD), LORAN (DISPLAY) FROM POINT 1 TO POINT 3 AT 3 MINUTE TIME INTERVAL .....	38
Table 11.	COMPARISON BETWEEN MINI RANGER AND LORAN (TD) AND THE MINI RANGER AND LORAN (DISPLAY) FOR LEG 1 - 3. ....	39
Table 12.	SHIP VELOCITY COMPONENTS FOR MINI RANGER, LORAN (TD), LORAN (DISPLAY), BOTTOM TRACKING	

FROM POINT 3 TO POINT 2 AT 3 MINUTE TIME INTER- VAL .....	39
Table 13. SHIP VELOCITY COMPONENTS FOR MINI RANGER, LORAN (TD), LORAN (DISPLAY), BOTTOM TRACKING FROM POINT 2 TO POINT 3 AT 3 MINUTE TIME INTER- VAL .....	40
Table 14. COMPARISON BETWEEN MINI RANGER AND LORAN (TD) AND THE MINI RANGER AND LORAN (DISPLAY) FOR LEGS 3 - 2 AND 2 - 3. ....	40
Table 15. SHIP VELOCITY COMPONENTS FOR MINI RANGER, LORAN (TD), LORAN (DISPLAY), BOTTOM TRACKING FROM POINT 3 TO POINT 4 AT 3 MINUTE TIME INTER- VAL .....	41
Table 16. COMPARISON BETWEEN MINI RANGER AND LORAN (TD) AND THE MINI RANGER AND LORAN (DISPLAY) FOR LEG 3 - 4. ....	43
Table 17. AVERAGE VELOCITY COMPONENTS FOR MINI RANGER, LORAN (TD), LORAN (DISPLAY), BOTTOM TRACKING .....	44
Table 18. TIME INTERVAL BETWEEN POSITIONS 3 MINUTES ...	48
Table 19. TIME INTERVAL BETWEEN POSITIONS 6 MINUTES ...	48
Table 20. TIME INTERVAL BETWEEN POSITIONS 12 MINUTES ..	49
Table 21. TIME INTERVAL BETWEEN POSITIONS 20 MINUTES ..	49
Table 22. TIME INTERVAL BETWEEN POSITIONS 40 MINUTES ..	50



## LIST OF FIGURES

Figure 1.	CHART OF THE WORK AREA .....	3
Figure 2.	VOLUME SCATTERING OF SOUND .....	6
Figure 3.	FIRST-SECOND SOUND DOPPLER SHIFT .....	7
Figure 4.	WATER VELOCITY VECTOR .....	8
Figure 5.	VELOCITY RESOLUTION WITH FOUR ADCP BEAMS ...	8
Figure 6.	SMALL AND LARGE ERROR VELOCITY .....	9
Figure 7.	ADCP AND CURRENT METERS .....	11
Figure 8.	LOCATION OF WEST COAST LORAN C STATIONS ....	14
Figure 9.	LORAN C GROUP REPETITION INTERVAL (GRI) AND TIME DIFFERENCES (TD) .....	15
Figure 10.	THIRD CYCLE TRACKING POINT .....	16
Figure 11.	TYPICAL HYPERBOLIC FIX GEOMETRY .....	17
Figure 12.	HYPERBOLIC GRADIENTS .....	19
Figure 13.	HYPERBOLIC GRADIENTS AND CROSSING ANGLES .	20
Figure 14.	SPHERICAL TRIANGLE SPANAGEL-M-NORTH POLE .	21
Figure 15.	PLANNING THE MOST DESIRABLE SITE .....	31
Figure 16.	MAXIMUM POSITION ERROR .....	33
Figure 17.	AVERAGE CURRENT PROFILE FROM POINT 1 TO POINT 3 USING NAVIGATION DATA FROM MINI RANGER .....	67
Figure 18.	AVERAGE CURRENT PROFILE FROM POINT 3 TO POINT 2 USING NAVIGATION DATA FROM MINI RANGER .....	68
Figure 19.	AVERAGE CURRENT PROFILE FROM POINT 2 TO POINT 3 USING NAVIGATION DATA FROM MINI RANGER .....	69
Figure 20.	AVERAGE CURRENT PROFILE FROM POINT 3 TO POINT 4 USING NAVIGATION DATA FROM MINI	

RANGER .....	70
Figure 21. AVERAGE CURRENT PROFILE FROM POINT 1 TO POINT 3 USING NAVIGATION DATA FROM LORAN (TD)	71
Figure 22. AVERAGE CURRENT PROFILE FROM POINT 3 TO POINT 2 USING NAVIGATION DATA FROM LORAN (TD)	72
Figure 23. AVERAGE CURRENT PROFILE FROM POINT 2 TO POINT 3 USING NAVIGATION DATA FROM LORAN (TD)	73
Figure 24. AVERAGE CURRENT PROFILE FROM POINT 3 TO POINT 4 USING NAVIGATION DATA FROM LORAN (TD)	74
Figure 25. AVERAGE CURRENT PROFILE FROM POINT 1 TO POINT 3 USING NAVIGATION DATA FROM LORAN (DISPLAY) .....	75
Figure 26. AVERAGE CURRENT PROFILE FROM POINT 3 TO POINT 2 USING NAVIGATION DATA FROM LORAN (DISPLAY) .....	76
Figure 27. AVERAGE CURRENT PROFILE FROM POINT 2 TO POINT 3 USING NAVIGATION DATA FROM LORAN (DISPLAY) .....	77
Figure 28. AVERAGE CURRENT PROFILE FROM POINT 3 TO POINT 4 USING NAVIGATION DATA FROM LORAN (DISPLAY) .....	78
Figure 29. CURRENT PROFILE FROM POINT 1 TO POINT 2 USING NAVIGATION DATA FROM MINI RANGER FOR A SPE- CIFIC TIME (14 33 11) .....	79
Figure 30. CURRENT PROFILE FROM POINT 2 TO POINT 1 USING NAVIGATION DATA FROM MINI RANGER FOR A SPE- CIFIC TIME (15 06 10) .....	80
Figure 31. CURRENT PROFILE FROM POINT 1 TO POINT 2 USING NAVIGATION DATA FROM LORAN (TD) FOR A SPE- CIFIC TIME (14 33 11) .....	81
Figure 32. CURRENT PROFILE FROM POINT 2 TO POINT 1 USING	

	NAVIGATION DATA FROM LORAN (TD) FOR A SPECIFIC TIME (15 06 10) .....	82
Figure 33.	CURRENT PROFILE FROM POINT 1 TO POINT 2 USING NAVIGATION DATA FROM LORAN (DISPLAY) FOR A SPECIFIC TIME (14 33 11) .....	83
Figure 34.	CURRENT PROFILE FROM POINT 2 TO POINT 1 USING NAVIGATION DATA FROM LORAN (DISPLAY) FOR A SPECIFIC TIME (15 06 10) .....	84

## I. INTRODUCTION

The relative accuracy of navigation data is very important in the processing of Acoustic Doppler Current Profiler (ADCP) data.

The shipboard ADCP is an instrument which measures vertical profiles of currents. The raw ADCP data is collected in 128 four meter bins, and is used in conjunction with a navigation system from which the position of the ship is recorded.

In this experiment we will try to evaluate which of the navigation systems available to us is better for use with the ADCP in order to determine the absolute current velocity. We collected data with MINI RANGER, LORAN (TD), LORAN (DISPLAY), and GPS receivers. Due to time constraints, however, the GPS data has not been included in the analysis.

Chapter 2 describes the cruise from which the data analysed in this thesis is taken. It also describes the time synchronization problems which existed between the various types of navigational equipment used.

Chapter 3 describes the ADCP and its principles of operation.

In chapters 4 and 5 we try to define the theoretical random error for the LORAN (LC 408) and the MINI RANGER respectively.

Chapter 6 gives the results from the data collected in a cruise of Monterey Bay while Chapter 7 gives a summary of the conclusions from this study together with recommendations for future work.

## **II. DATA COLLECTION**

### **A. CRUISE**

The day chosen for the cruise was 22 September 1989 with the ship R/V Point Sur. During the cruise the following equipment belonging to the NPGS and R/V Point Sur was used:

1. Motorola Mini Ranger,
2. LORAN C receiver (Internav LC 408),
3. Trimble GPS receiver,
4. HP Computer logging three data sources simultaneously, and
5. RDI ADCP with the Data Acquisition System (DAS) and IBM XT compatible computer.

The results reported in later sections will concern only the MINI RANGER and LORAN C navigational systems.

The ship navigated the runs from point 1 to point 2, 2 - 1, 1 - 3, 3 - 2, 2 - 3, and 3 - 4 (see Figure 1). The speed during the measurements was 6 knots which, from previous experience, has proven effective for ADCP data collection. In running from 1 - 2 for example, a turn was made at point 2 and then the ship steamed back to point 1 without attempting to follow the identical outward track.

The average depth in the area of the triangle 1 2 3 is 30 fathoms, and for the run 3 - 4 it varies between 20 to 300 fathoms.

### **B. TIME SYNCHRONIZATION**

During the cruise the four pieces of equipment used each had clocks which operated independently of each other. In order to synchronize all these clocks, at five times during the cruise time comparisons were made between them by using the Mini Ranger as the common time base (see for example Table 1).

These times were then converted from a MR time base to an ADCP time base (see Table 2).

The standard error in the time comparisons was at least 1 second. Once a dedicated multi-channel data logger is installed which allows all equipment out-

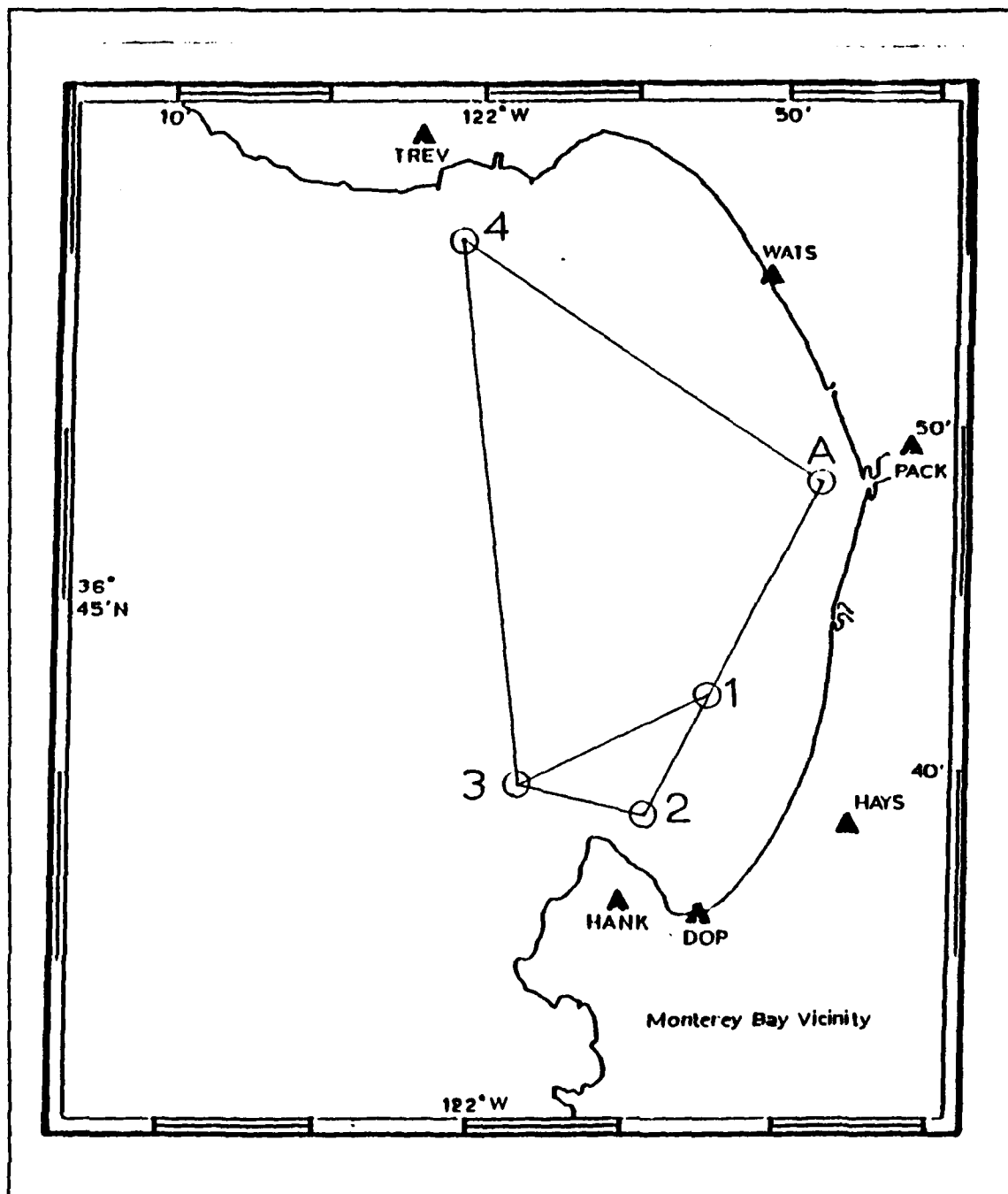


Figure 1. CHART OF THE WORK AREA

puts to be recorded on a common time base, it is anticipated that this synchronization error will be reduced to negligible levels.

**Table 1. COMPARISON OF CLOCKS WITH THE MINI RANGER (MR)**

HP	15:16:28	MR	15:16:28.6
LC 408	15:14:00	MR	15:14:00.6
ADCP	15:15:10	MR	15:15:06.6

**Table 2. DIFFERENT TIMES BETWEEN THE CLOCKS WITH COMMON TIME BASE (ADCP)**

HP	15:16:28	ADCP	15:16:32.0
LC 408	15:14:00	ADCP	15:14:04.0
MR	15:15:06.6	ADCP	15:15:10

With five tables on a common ADCP time base, a linear regression between the different times was performed for each equipment type in order to calculate the coefficients A and B of the equation:

$$Y = AX + B \quad (1)$$

The linear clock drifts were thus calculated and used to assist in interpolating the data into the ADCP time base.

### III. ACOUSTIC DOPPLER CURRENT PROFILERS

#### A. INTRODUCTION

The shipboard Acoustic Doppler Current Profiler (ADCP) from RD Instruments is a state of the art instrument which measures vertical profiles of currents of the ocean at points along the ship's path [RD Instruments, 1989]. It allows the ocean to be sampled in a way which is fundamentally different from moored currents or drifters (instruments most commonly used for current measurement).

Consider the general case of measuring the current at the water parcel whose coordinates are  $X_w(t)$  using an instrument whose location is  $X_0(t)$

$$X_w(t) = X_0(t) + r \quad (2)$$

Where  $r$  is a vector between the two locations and

$$r = X_w(t) - X_0(t) \quad (3)$$

From (2) and (3)

$$X_w(t) = X_0(t) + [X_w(t) - X_0(t)] \quad (4)$$

The current  $U$  at the measurement point  $X_0 + r$  will be:

$$U(X_0 + r) = \frac{dX_w}{dt} = \frac{dX_0}{dt} + \frac{d(X_w - X_0)}{dt} \quad (5)$$

Equation (5) can be rewritten as

$$U(X_0 + r) = \frac{dX_0}{dt} + V(r) \quad (6)$$

Where  $V(r)$  is the velocity of the water parcel relative to the instrument position and  $dX_0/dt$  is the velocity of the instrument itself with respect to the Earth.

Since the currents are a difference between two directly measured quantities  $dX_0/dt$  and  $V$ , the measurement of currents to an accuracy of 1 cm/sec from a



ship travelling at 10 knots (approximately 5.2 m/sec or 520 cm/sec) requires that both  $dX_o/dt$  and  $V$  must be measured to an accuracy of 0.2%.

## B. PRINCIPLES OF OPERATION OF THE ACOUSTIC DOPPLER CURRENT PROFILER

ADCP's use the Doppler effect by transmitting a succession of acoustic pulses at a fixed frequency and listening to the resulting backscattered water mass echoes in as many as 128 depth cells (bins) over a depth range of 30 to 700 meters. When scatterers move toward the ADCP, the echoes heard by the scatterers is Doppler shifted to a higher frequency. The amount of this shift is proportional to the relative velocity between the ADCP (ship) and scatterer Figure 2.

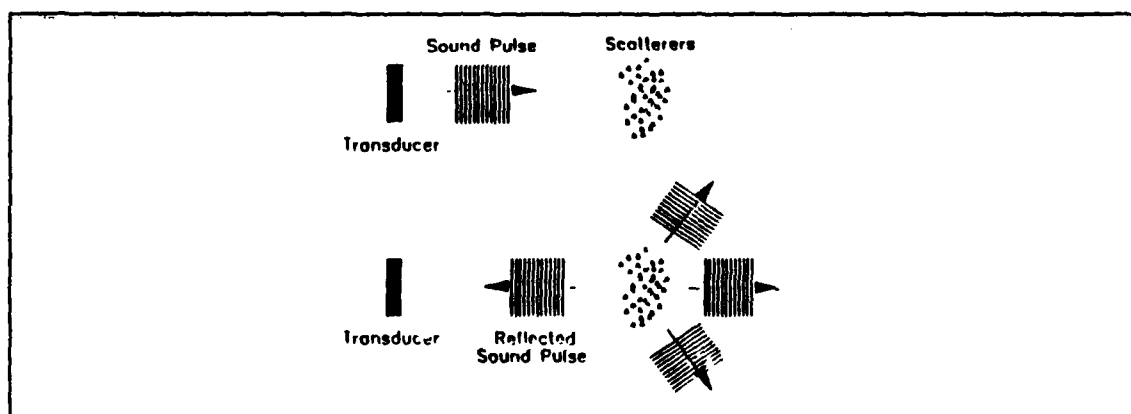


Figure 2. VOLUME SCATTERING OF SOUND

Part of these Doppler-shifted echoes reflect backwards or are backscattered to the ADCP. The backscattered echoes appear to the ADCP as if the scatterers were the source of the echoes (see Figure 3).

The ADCP hears the backscattered echoes, Doppler shifted a second time. Since the ADCP both transmits and receives, the Doppler shift is doubled, and the equation for the Doppler shift will be

$$F_D = 2F_S \frac{V}{C} \cos A \quad (7)$$

where

- $F_D$  is the Doppler shift,

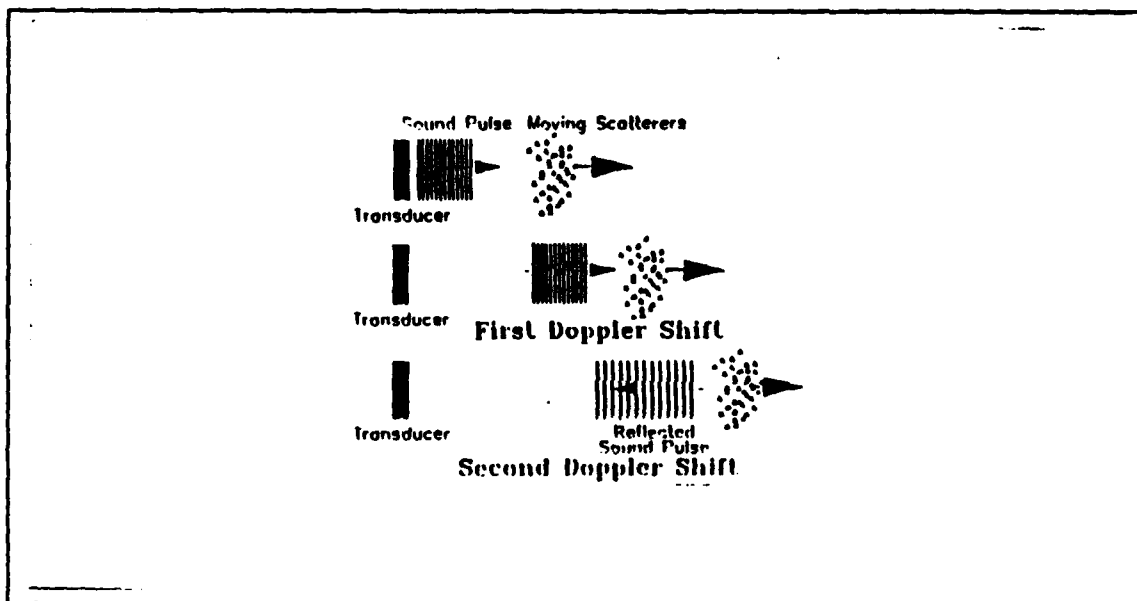


Figure 3. FIRST-SECOND SOUND DOPPLER SHIFT

- $F_s$  is the frequency of the sound when everything is still,
- $A$  is the angle between the acoustic beam and the water velocity,
- $V$  is the relative velocity between the sound source and the sound receiver, and
- $C$  is the speed of sound (m/sec) in the water at the face of the transducer, and can be calculated from the expression

$$C = 1449.2 + 4.6T - 5.510^{-2}T^2 + 2.910^{-4}T^3 + (1.34 - 10^{-2}T)(S - 35) + 1.610^{-2}D \quad (8)$$

where

- $D$  = Depth, in meters,
- $S$  = Salinity, in practical salinity units, and
- $T$  = Temperature, in degrees Celsius.

The water temperature at the face of the transducer is measured by the ADCP. The speed of sound ( $C$ ) can be calculated from this measured water temperature using nominal values for depth ( $D$ ) and salinity ( $S$ ).

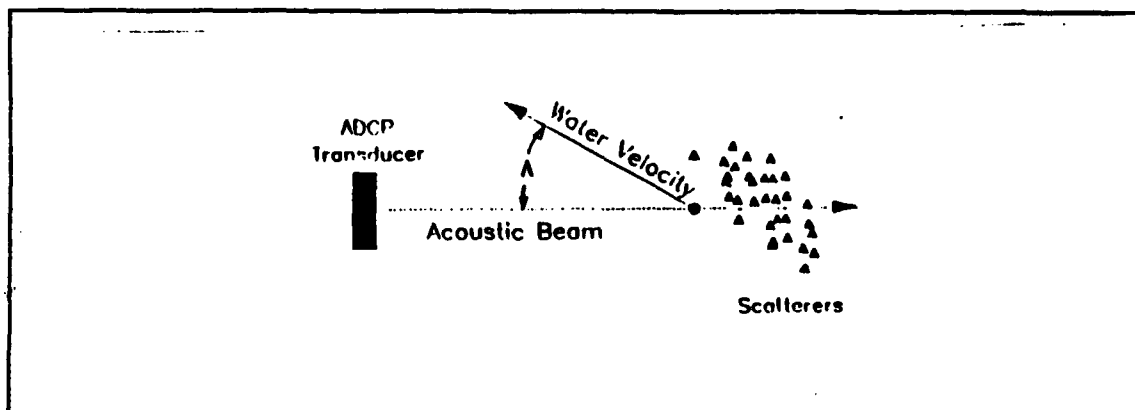


**Figure 4. WATER VELOCITY VECTOR**

Computer analysis of the Doppler frequency shift of backscattered echoes from each bin is used to generate a precise depth segmented picture (or profile) of water currents throughout the water column bounded by the path of the acoustic beams.

### **C. THREE DIMENSIONAL CURRENT VELOCITY VECTORS**

The ADCP beams each measure a single velocity component, i.e. the component of velocity toward or away from the transducer. When using multiple beams, one must make an assumption that currents are the same (homogeneous) over layers of constant depth. When the ADCP uses multiple beams pointed in different directions, it senses different velocity components.

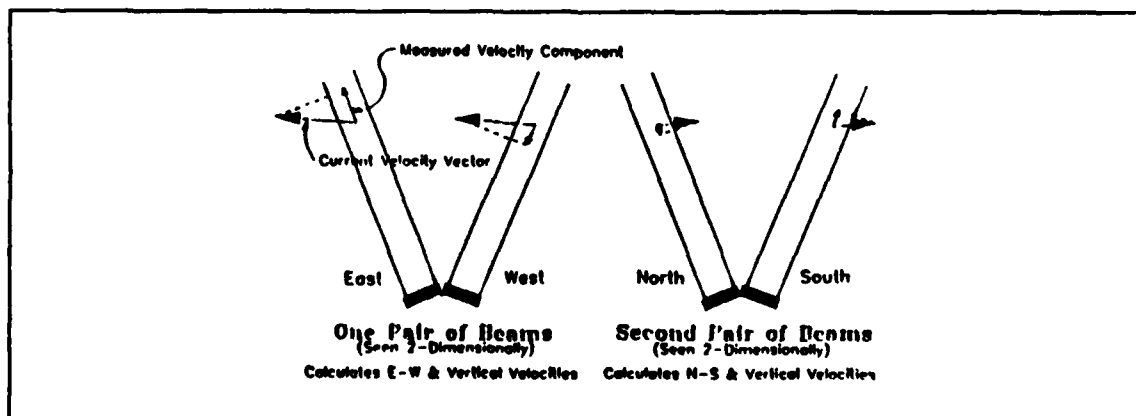


**Figure 5. VELOCITY RESOLUTION WITH FOUR ADCP BEAMS**

Figure 5 shows how the ADCP, using four acoustic beams, computes three velocity components. The first pair of beams produces one horizontal and one vertical component, the second pair produces one horizontal (perpendicular to the first horizontal) and again one vertical component.

The product  $SCALE \times (V_1 + V_2 - V_3 - V_4)$  is defined as the error velocity component, where  $V_1$  to  $V_4$  are the velocity components along the beam directions Figure 6. This sum should be close to zero. The error velocity component allows us to evaluate if the assumption for the horizontal homogeneity is reasonable. Also this is another way to estimate data quality.

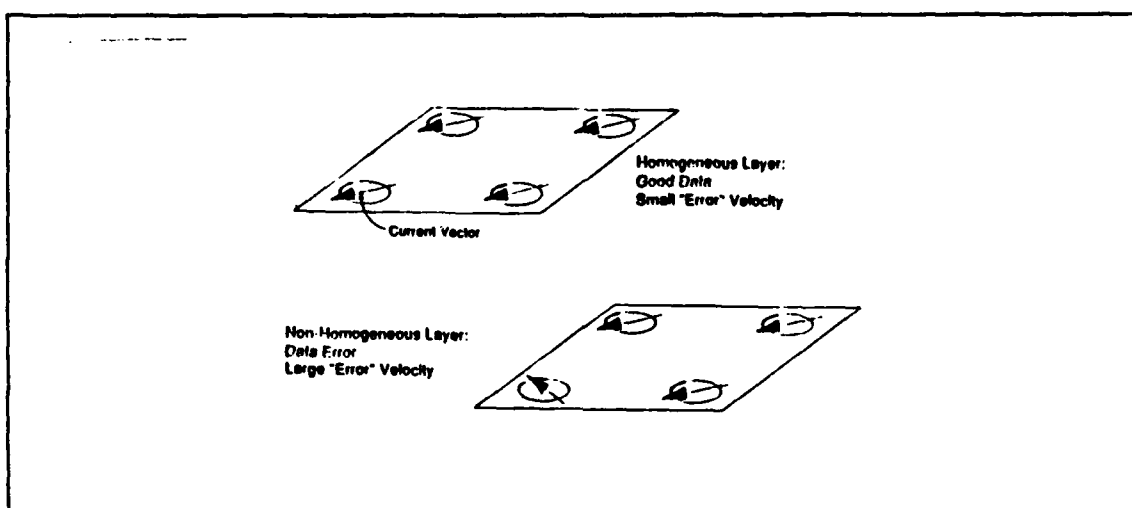


Figure 6. SMALL AND LARGE ERROR VELOCITY

In Figure 6 there are two different situations, in the first the velocity is the same in all four beams at a constant level, in the second the velocity in one beam is different. The error velocity in the second case will be on average larger than the error velocity in the first case. The difference in the error velocities can be from different currents or from errors caused by malfunctioning equipment.

#### D. DEPLOYMENT AREA

The RD Instruments ADCP remotely measures water flow velocity along the lines of position defined by the four narrow vertically inclined acoustic beams. To insure accurate current measurement it is necessary that the water mass in the

region of measurement be free of strong acoustic reflecting objects (e.g platform members, large cables, surface, etc.) within a  $\pm 15$  degrees conical sector along the direction of each of the beams. However, since only three beams are required for computation of three axes current components, in applications where potential interference objects may be close to one beam, the current vector may be calculated from the other three beams.

In shallow water vertical profiling applications, acoustic interference from the surface (upward looking ADCP) or bottom (downward looking ADCP) limit the vertical current measurement region to a maximum range defined by

$$R(\max) = D \times \cos \phi \quad (9)$$

where

- $R(\max)$  = maximum profiling range,
- $D$  = distance to surface/bottom boundary, and
- $\phi$  = acoustic beam angle relative to the vertical.

#### **E. BOTTOM TRACKING OPERATION**

The ADCP can be used in a bottom tracking mode to give direct estimates of the velocity components of the ship. In the experimental data collected for this thesis we used the bottom tracking on for the runs 3 - 2, 2 - 3, and at the first part of the run 3 - 4. In order for the ADCP to gather bottom tracking data, bottom echoes must be distinguished from other echoes. The ADCP transmits a dedicated bottom track ping between current profiling pings. The number of profiling pings can be selected by the user. Consequently, the bottom tracking ping data is separated from the current profiling data. Bottom echoes are identified by virtue of their greater echo strength (the bottom returns a stronger echo than the echo from a profiling bin).

Ship velocity (relative to the bottom) is measured in much the same way as current velocity (the Doppler shift of the backscattered bottom echo being proportional to the ship velocity). Bottom depth is detected by comparing received echo amplitude to a detection threshold which decreases with increasing range to the bottom.

## F. VELOCITY PROFILES

The most important feature of ADCP's is their ability to measure current profiles. ADCP's break up the velocity profile into uniform segments called depth cells.

Each depth cell is similar to a single current meter, but there are two basic differences. The first difference is that the depth cells in an ADCP are always uniformly spaced while current meters can be spaced irregularly, the second is that the ADCP measures average velocity over the depth range of each depth cell while the current meter measures current only at the current meter Figure 7.

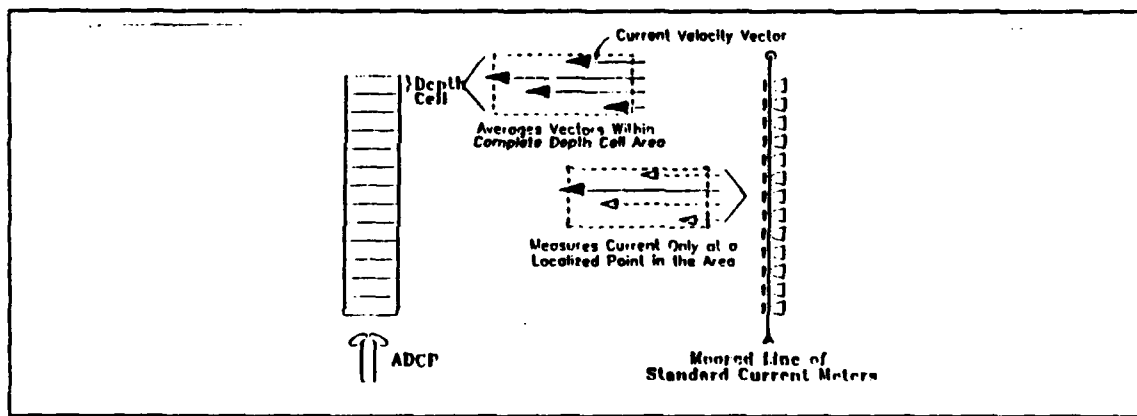


Figure 7. ADCP AND CURRENT METERS

The advantage of the ADCP averaging the velocity over the full range of a depth cell is that it reduces the effects of spatial aliasing (signals at frequencies higher than the time series can resolve are mistaken for low frequency signals).

## G. ACOUSTIC DOPPLER CURRENT PROFILER DATA PROCESSING

The raw data is collected in 128 four meter bins over a three minute ensemble interval. Generally speaking, either a MINI RANGER, LORAN C (calculated  $\phi$ ,  $\lambda$  from time differences or  $\phi$ ,  $\lambda$  recorded from the display) or a GPS receiver are used for navigation and a position recorded every 30 seconds. By interpolation a position can be calculated at the end of each ensemble.

The first steps in processing are the calculation of ship's velocity from the navigation data. From this navigation data the U and V components of ship's velocity are calculated.

The next step in processing is the initial determination of the depth to which the data of each ensemble remains reliable. For our case the 7 , 8 , 9 bins were chosen. The basic criterion comes from the good percent of return echoes (BIN STATISTICS FILE). By subtracting the ship's velocity from the average velocity within the chosen reference layer an absolute reference layer velocity for each ensemble is obtained. The series of absolute reference velocities is then filtered with a low pass Hamming window filter.

Once the absolute reference velocity is determined the velocity profiles of each ensemble with respect to the reference velocity are also determined, thus yielding the final profiles of absolute water velocity. The remaining profiles of absolute velocity are then averaged over the time interval for each run.

In appendix E there are 18 average current profiles from different navigation data.

## IV. THEORY OF LORAN C

### A. INTRODUCTION

LORAN C (LONG RANGE NAVIGATION) is a pulsed, low frequency (100 KHZ carrier) long-range hyperbolic navigation system. It operates on the principle that the difference in time of arrival of signals from two stations, observed at a point in the coverage area, is a measure of the difference in distance from the point of observation to each of the stations.

Measurements of the ship's latitude and longitude (  $\phi$  ,  $\lambda$  ) and Time Differences (TD) from a LC 408 LORAN C receiver were recorded throughout the experiment (22 September 1989) at intervals of 30 seconds.

### B. SYSTEM DESCRIPTION

LORAN C normally requires signals from at least a Master and two Secondary stations to give a positional fix.

Transmitters are grouped to form a "chain" of which one station is labelled the Master (M) and the others are called secondaries (X,Y,W) as shown in Figure 8.

The chain designators for LORAN C are 4 digit numbers which indicate the pulse Group Repetition Interval (GRI) in tens of micro-seconds. For example, the west coast LORAN C chain (Figure 8) is designated 9940 and has a GRI 99400 micro-seconds ( see Figure 9) [LC 408, Operation Manual]

### C. PULSES-PHASE AND CODES-CYCLE SELECTION

Each station of a LORAN C chain transmits groups of pulses (Table 3).

Table 3. LORAN C PHASE CODES

Master	A + + -- + - + - +	B + -- + + + + + -
Secondary	A + + + + + -- +	B + - + - + + --



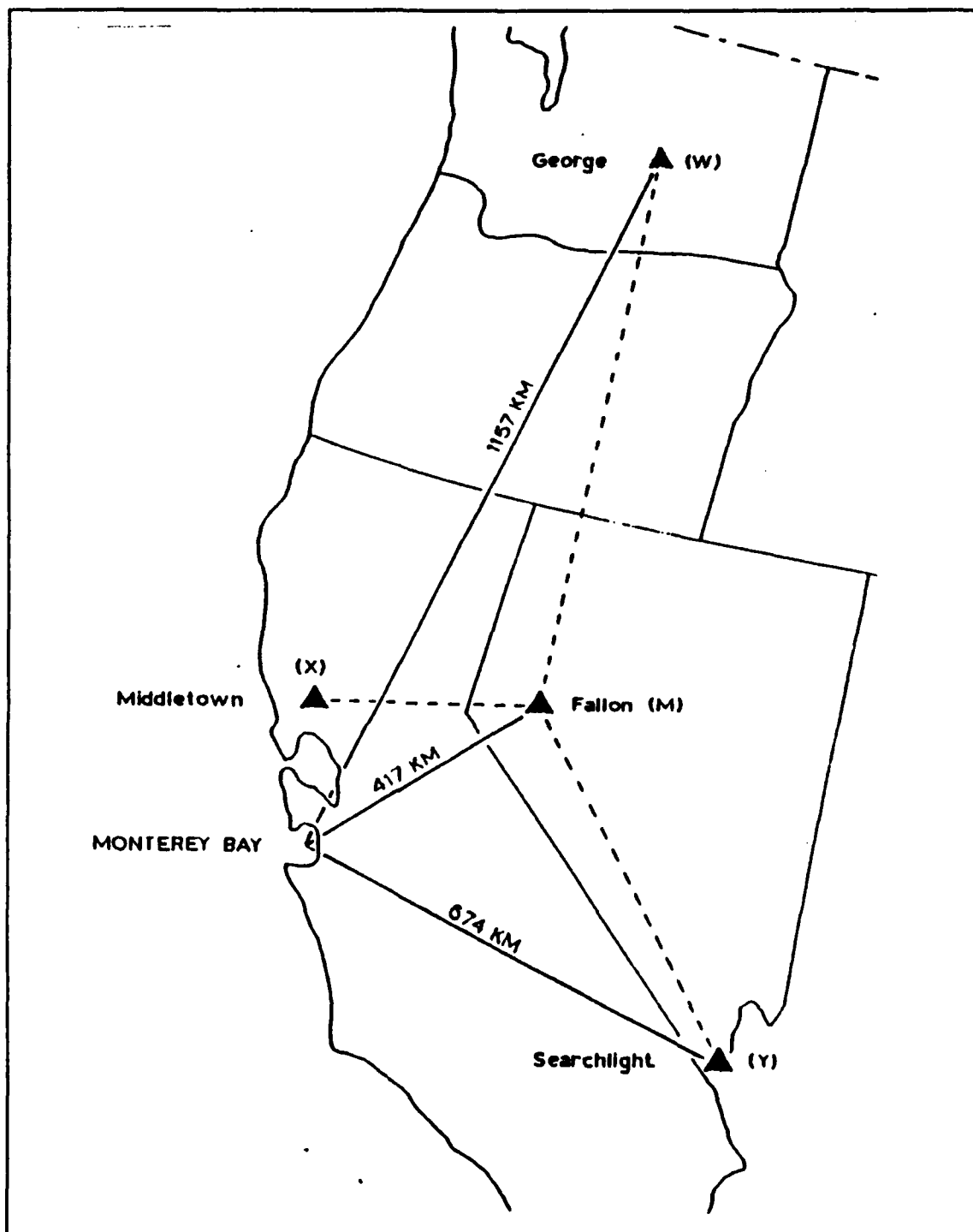


Figure 8. LOCATION OF WEST COAST LORAN C STATIONS

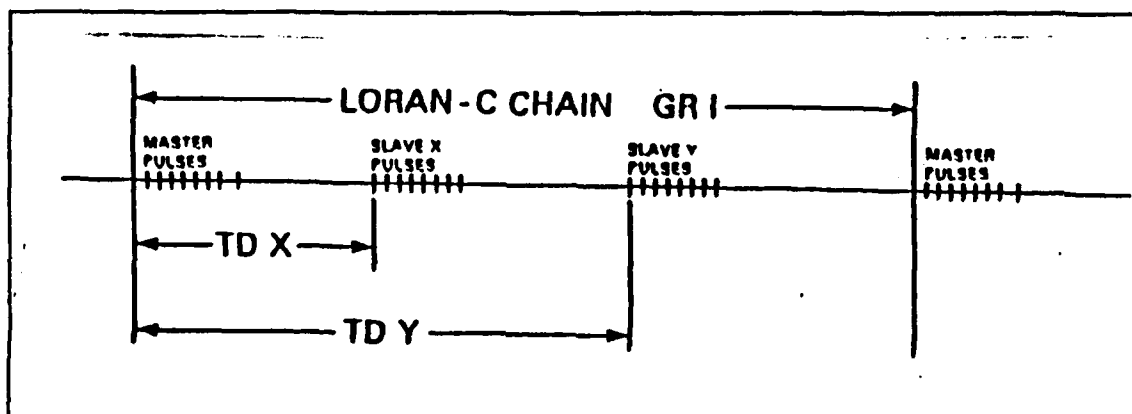


Figure 9. LORAN C GROUP REPETITION INTERVAL (GRI) AND TIME DIFFERENCES (TD)

The Secondary transmits eight pulses and the Master nine (the last pulse for identification and blink alarm). The pulses are phase coded to improve the signal to noise ratio through compression and to distinguish between Master and Secondary transmissions.

Low frequency radio signals propagate over the earth's surface at nearly the velocity of light in a vacuum. However, Maxwell's equations dictate that the ground wave (surface wave) will be influenced slightly by the surface parameters of geometry and electrical properties.

In order to make the received 100 KHz signal more stable and reliable within a given coverage area, the LORAN C radio navigation system is designed as a pulse system which separates the ground wave from the skywave.

Because the earth parameters remain nearly constant, LORAN C has demonstrated a repeatability of quite high accuracy.

The high accuracy of LORAN C, despite long ranges from transmitters, is due to a technique called "*cycle matching*" [Bowditch, 1984].

The LC 408 tracks the third cycle cross-over path point which is very consistent between transmissions and less susceptible to skywave interference than later cycles. By tracking this cycle on all pulses, high accuracy is attained. Figure 10 shows the third cycle tracking point with an example of skywave interference.

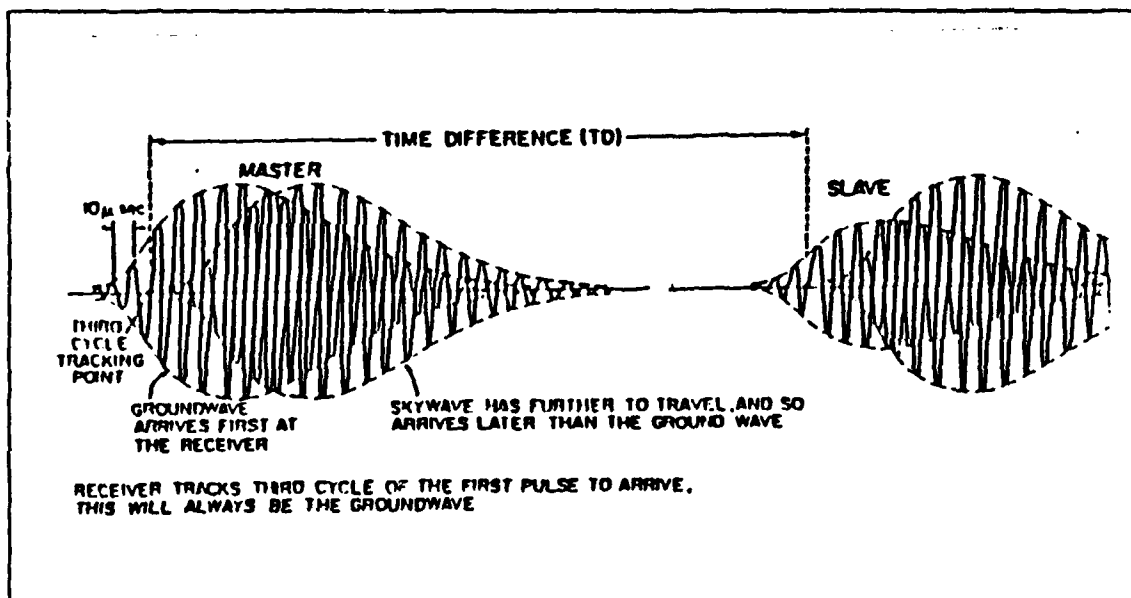


Figure 10. THIRD CYCLE TRACKING POINT

#### D. TIME DIFFERENCE EQUATIONS

The elapsed time between the arrival of the signals from the Master and a Secondary stations is called the "Time Difference" (TD). Each observed time difference, or rate, provides one hyperbolic line of position. By observing the transmissions from four stations, three hyperbolic rates are measured and the position can be determined by either graphical or analytical techniques.

The time difference observed at a receiver is the difference in arrival times for signals from the master and one secondary transmitter in the chain. Because all transmitters share the same frequencies, their signals must be separated in time to prevent interference.

The chain is synchronized so that the Master transmits first followed by each of the Secondaries. The transmission of each secondary is specified by the emission delay so that in the coverage area signals from one station will overlap another [Schenebele, 1979].

Suppose that at a point P there is a receiver. The observed time difference using the Master M and Secondaries X,Y,W are

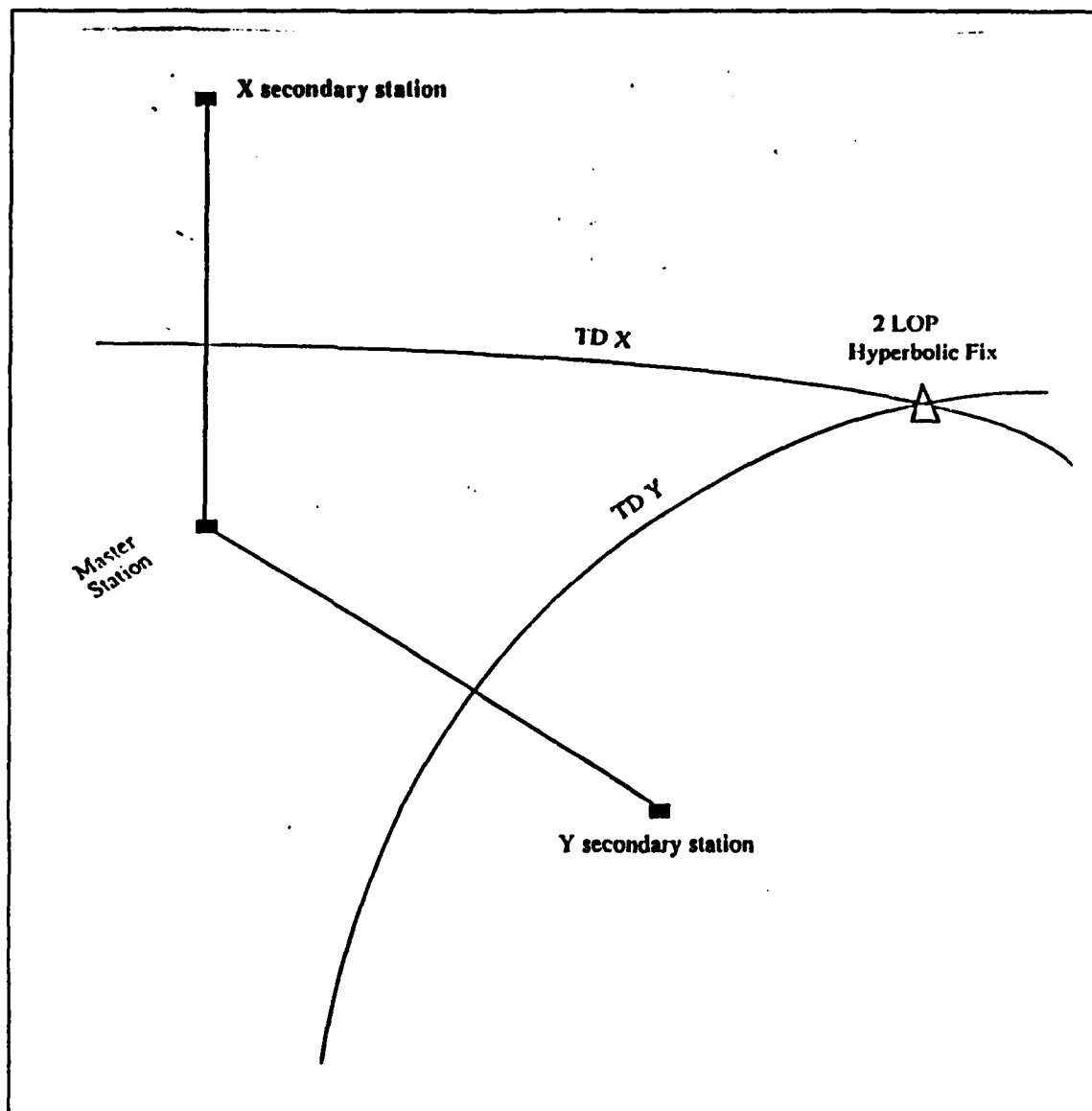


Figure 11. TYPICAL HYPERBOLIC FIX GEOMETRY

$$TDW = ED_W + t_W - t_M \quad (10)$$

$$TDX = ED_X + t_X - t_M \quad (11)$$

$$TDY = ED_Y + t_Y - t_M \quad (12)$$

where  $ED_W, ED_X, ED_Y$  are the emission delay for W, X, Y. The terms  $t_W, t_X, t_Y$  are travel times from the W, X, Y to P. The term  $t_M$  is the travel time from the Master M to P.

In order to express the time difference as a function of geographic position, the travel time  $t$  is separated into additive terms

$$t = \frac{n}{C} \times D + F \quad (13)$$

where:

- $C$  = free space propagation velocity,
- $n$  = index for refraction for a standard atmosphere,
- $D$  = geodetic distance from the transmitter to receiver, and
- $F$  = phase factor which corrects for effects of the earth's surface along the path.

Substituting the last formula into the equations (10), (11), (12), gives the equations:

$$TDW = ED_W + \frac{n}{C} \times (D_W - D_M) + F_W - F_M \quad (14)$$

$$TDX = ED_X + \frac{n}{C} \times (D_X - D_M) + F_X - F_M \quad (15)$$

$$TDY = ED_Y + \frac{n}{C} \times (D_Y - D_M) + F_Y - F_M \quad (16)$$

All these equations relate the time differences TDW, TDX, TDY to the distances from each of the four transmitters.

Since the latitude and longitude is mathematically calculated from the time difference numbers, the crossing angles, gradients, and signal to noise ratios are still important.

## E. HYPERBOLIC GRADIENT, CROSSING ANGLES

For a given pair Master, Slave a family of hyperbolas separated by a constant value can be plotted.

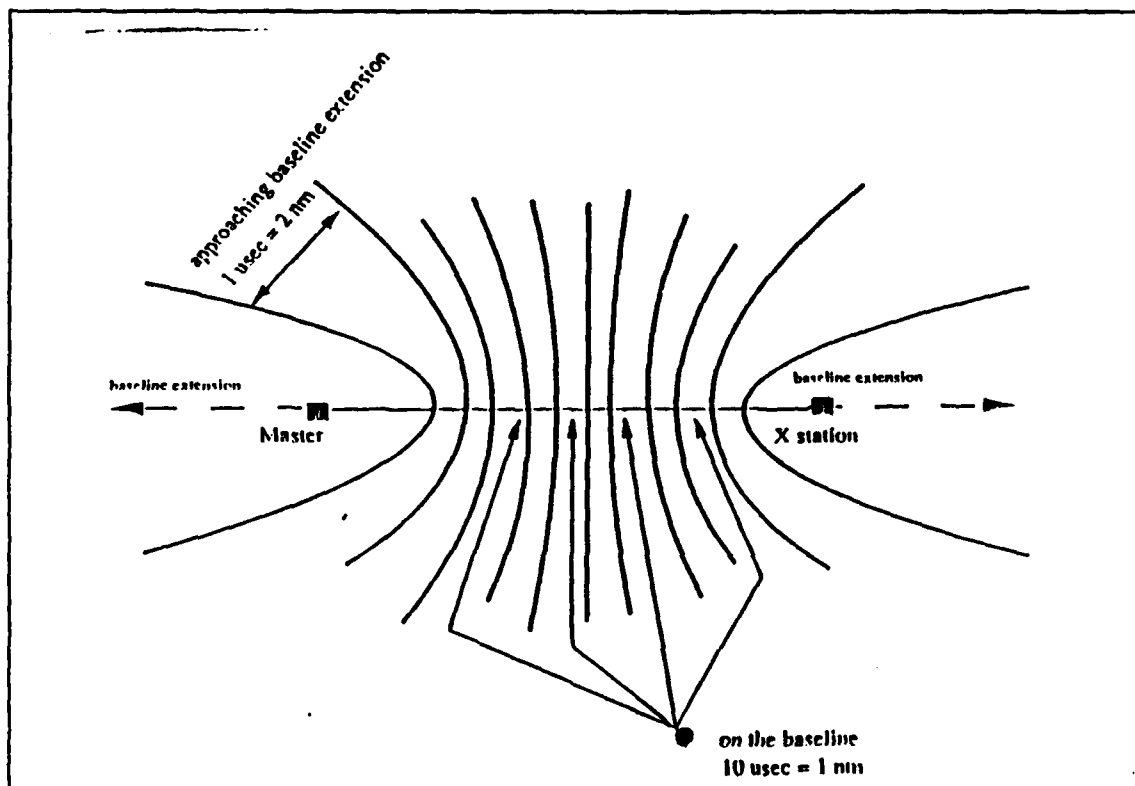


Figure 12. HYPERBOLIC GRADIENTS

The hyperbolas in Figures 12 and 13 are all separated by 10 microseconds [Gann]. That means that the distance on the baseline represents about 1852 meters. The distance between successive hyperbolas increases as one moves towards the baseline extensions or away from the baseline. This change in the accuracy of a hyperbolic Line of Position (LOP) that occurs relative to the position of the LORAN C stations is known as the gradient.

The angle between the LOPs is called the crossing angle Figure 13. The crossing angle must be bigger than 30 degrees and smaller than 150 degrees. This fact is common with any ranging positioning system, but is further limited for the LORAN C because the reception of three stations is required to define two LOPs (direct ranging navigation systems provide one LOP per station).

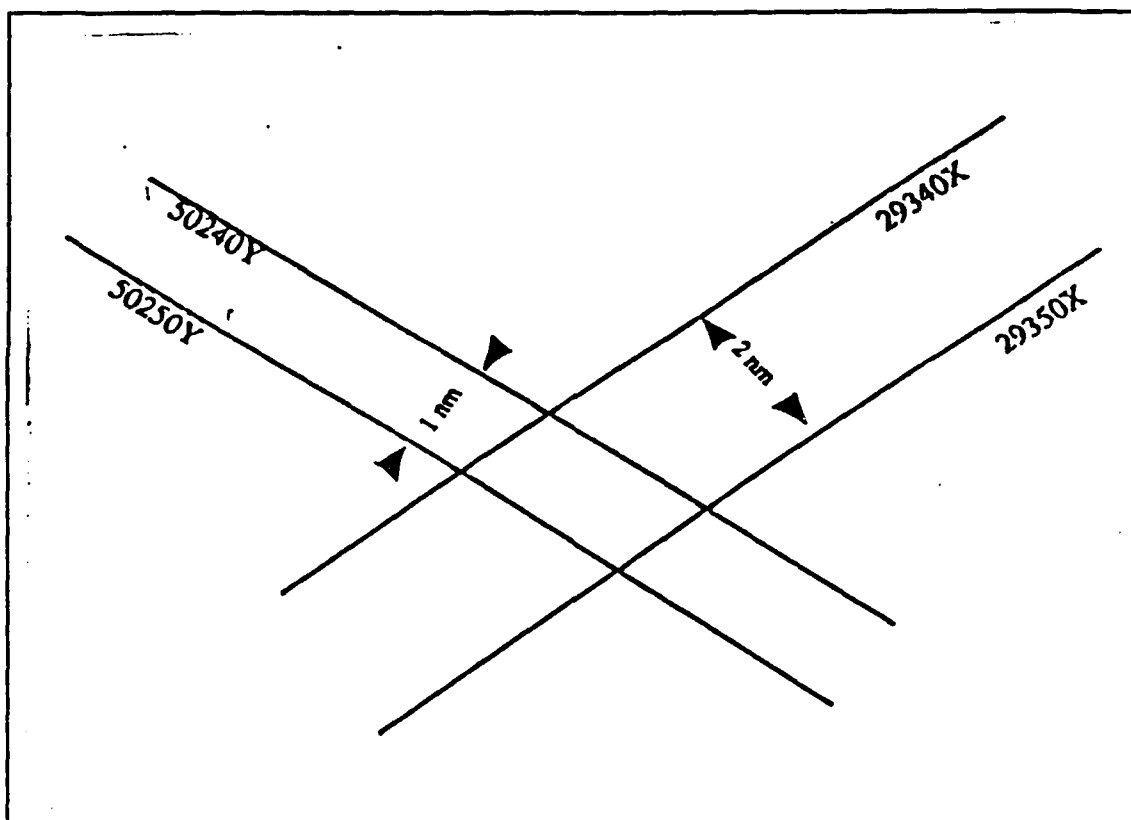


Figure 13. HYPERBOLIC GRADIENTS AND CROSSING ANGLES

#### F. ERROR ANALYSIS FOR LORAN C

Any discussion of accuracy should begin with the definition of the types of accuracy.

*Repeatable accuracy* (Repeatability, Precision) is the accuracy with which a navigator can return to a location, the coordinates of which have been previously measured using the same system.

*Random error* is one which results from basic limitations in the method. The characteristics of this error can be determined by statistical analysis of a sufficient number of measurements. This type of error affects the repeatability. These errors are identified by their Gaussian distribution.

*Absolute accuracy* is the accuracy with which a navigator can determine his point position in terms of a well defined coordinate system e.g. ( $\phi$ ,  $\lambda$ ).

*Systematic errors* result from a basic (but unrealized) fault in the method and cause the values to be consistently biased from the true value. It affects the absolute accuracy, and often cannot be detected by statistical analysis.

The LC 408 microprocessor uses an exacting spherical trigonometric formula to derive its latitude and longitude positions. Also it is important to note that the LC 408 used for the calculations assumes that the LORAN signals travel over ideal all seawater paths from the transmitter to the receiver. To correct for path over land, the LC 408 allows use of "additional secondary factors"; this is typically used only in small regions adjacent to known fixed locations.

For the error analysis given shortly, the shape of the earth is approximated by a sphere, and it is assumed that all the west longitudes are *positive*.

In order to find the standard deviations in the velocities, we established a fixed point in the roof of Spanagel Hall to enable an assesment of the standard deviations in the three time differences and after it to propagate the error at the positions and the velocities.

Consider the spherical triangle PSM (see Figure 14 [Cross, 1981]).

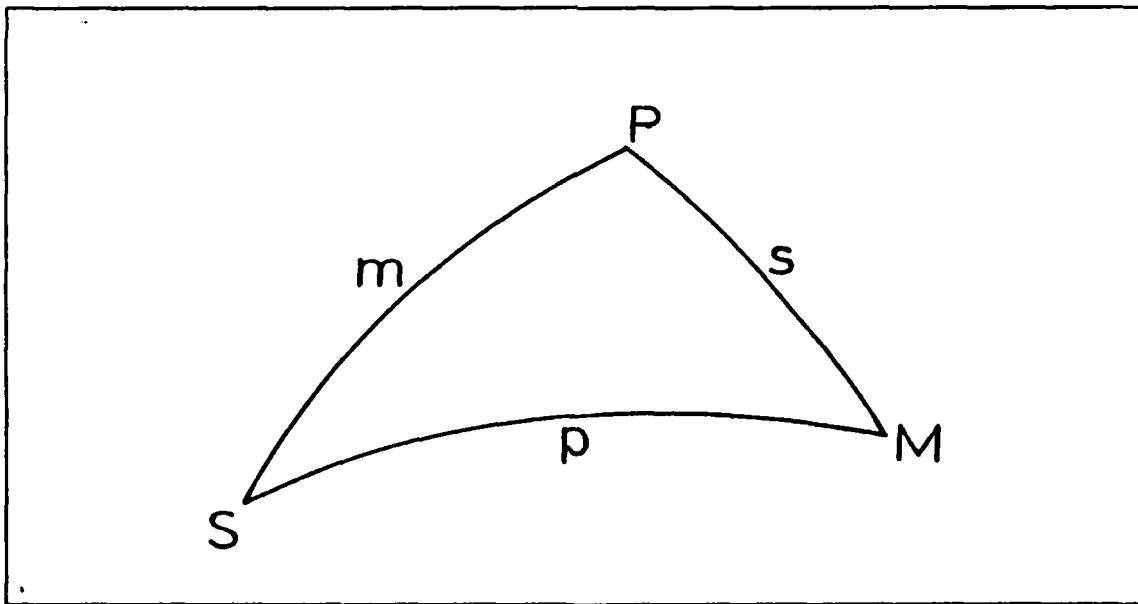


Figure 14. SPHERICAL TRIANGLE SPANAGEL-M-NORTH POLE



Where (M) can be the Master, S can be the point on the Spanagel roof, and P can be the North pole. We try to find an expression for the distance between Master and Spanagel roof with respect to  $\phi$ ,  $\lambda$  (coordinates of the point on the Spanagel roof),

$$m = 90 - \phi \quad (17)$$

$$s = 90 - \phi_M \quad (18)$$

$$P = \lambda - \lambda_M \quad (19)$$

where  $\phi_M$  and  $\lambda_M$  are the coordinates of the Master station. Using the law of cosines for the side p,

$$\cos p = \cos m \cos s + \sin m \sin s \cos P \quad (20)$$

Substitute (17), (18), (19) into (20) to yield

$$\cos p = \sin \phi_M \sin \phi + \cos \phi_M \cos \phi \cos(\lambda - \lambda_M) \quad (21)$$

Differentiate each part of (21)

$$\begin{aligned} -\sin p dp &= \cos \phi_M \sin \phi d\phi_M + \sin \phi_M \cos \phi d\phi \\ &\quad - \sin \phi_M \cos \phi \cos(\lambda - \lambda_M) d\phi_M \\ &\quad - \cos \phi_M \sin \phi \cos(\lambda - \lambda_M) d\phi \\ &\quad - \cos \phi_M \cos \phi \sin(\lambda - \lambda_M) d\lambda \\ &\quad + \cos \phi_M \cos \phi \sin(\lambda - \lambda_M) d\lambda_M \end{aligned} \quad (22)$$

Since the position of Master station is a fixed point  $d\lambda_M = d\phi_M = 0$  equation (22) becomes

$$\begin{aligned} -\sin p dp &= [\sin \phi_M \cos \phi - \cos \phi_M \sin \phi \cos(\lambda - \lambda_M)] d\phi \\ &\quad - \cos \phi_M \cos \phi \sin(\lambda - \lambda_M) d\lambda \end{aligned} \quad (23)$$

We now introduce into each term in the right part of (23) the factor  $\sin p$ . Using the relationship between two angles and three sides

$$\sin p \cos S = \cos s \sin m - \sin s \cos m \cos P \quad (24)$$

Substituting for s, m and P as appropriate, we have

$$\begin{aligned} \sin \phi_M \cos \phi - \cos \phi_M \sin \phi \cos(\lambda - \lambda_M) = \\ \cos(90 - \phi_M) \sin(90 - \phi) - \sin(90 - \phi_M) \cos(90 - \phi) \cos(\lambda - \lambda_M) = \\ \sin p \cos S \end{aligned} \quad (25)$$

From the law of sines we know that

$$\frac{\sin m}{\sin M} = \frac{\sin p}{\sin P} \quad (26)$$

OR

$$\sin m \sin P = \sin p \sin M \quad (28)$$

Substituting for m and P and multiplying both sides by  $\cos \phi_M$ , we have

$$\begin{aligned} \cos \phi_M \cos \phi \sin(\lambda - \lambda_M) = \\ \cos \phi_M \sin(90 - \phi) \sin(\lambda - \lambda_M) = \\ \sin p \sin M \cos \phi_M \end{aligned} \quad (29)$$

Substituting (25) and (29) into (23), we have

$$dp = -\cos S d\phi + \sin M \cos \phi_M d\lambda \quad (30)$$

Actually in order to convert the angle dp into distance da (arc length), using spherical approximation multiply by the mean radius of the earth R

$$da = -R \cos S d\phi + R \sin M \cos \phi_M d\lambda \quad (31)$$

From the last equation we have

$$\frac{\partial a}{\partial \phi} = -R \cos S \quad (32)$$

$$\frac{\partial a}{\partial \lambda} = R \cos \phi_M \sin M \quad (33)$$

where M and S are the interior angles of the triangle PSM. In similar way can form the equations for the other spherical triangles

$$\frac{\partial a_1}{\partial \phi} = - R \cos S_1 \quad (34)$$

$$\frac{\partial a_1}{\partial \lambda} = - R \cos \phi_X \sin X \quad (35)$$

The sign changes in the second equation due to different geometry

$$\frac{\partial a_2}{\partial \phi} = - R \cos S_2 \quad (36)$$

$$\frac{\partial a_2}{\partial \lambda} = R \cos \phi_Y \sin Y \quad (37)$$

$$\frac{\partial a_3}{\partial \phi} = - R \cos S_3 \quad (38)$$

$$\frac{\partial a_3}{\partial \lambda} = R \cos \phi_W \sin W \quad (39)$$

Next let

$$d_1 = a(\phi, \lambda) - a_1(\phi, \lambda) \quad (40)$$

$$d_2 = a(\phi, \lambda) - a_2(\phi, \lambda) \quad (41)$$

$$d_3 = a(\phi, \lambda) - a_3(\phi, \lambda) \quad (42)$$

Suppose that the velocity of the the electromagnetic propagation is constant and equal (C) then:

$$\Delta_{t_1} = \frac{d_1}{C} \quad (43)$$

$$\Delta_{t_2} = \frac{d_2}{C} \quad (44)$$

$$\Delta_{t_3} = \frac{d_3}{C} \quad (45)$$

We propagate the errors into these expressions by forming the Jacobian matrix. We assume here that time is subject to negligible error. This matrix is given by

$$J = \frac{1}{C} \begin{bmatrix} \frac{\partial d_1}{\partial \phi} & \frac{\partial d_1}{\partial \lambda} \\ \frac{\partial d_2}{\partial \phi} & \frac{\partial d_2}{\partial \lambda} \\ \frac{\partial d_3}{\partial \phi} & \frac{\partial d_3}{\partial \lambda} \end{bmatrix} \quad (46)$$

and

$$\begin{aligned} \frac{\partial d_1}{\partial \phi} &= \frac{\partial a(\phi, \lambda)}{\partial \phi} - \frac{\partial a_1(\phi, \lambda)}{\partial \phi} \\ &= -R \cos S + R \cos S_1 \\ &= R(\cos S_1 - \cos S) \end{aligned} \quad (47)$$

$$\begin{aligned} \frac{\partial d_2}{\partial \phi} &= \frac{\partial a(\phi, \lambda)}{\partial \phi} - \frac{\partial a_2(\phi, \lambda)}{\partial \phi} \\ &= -R \cos S + R \cos S_2 \\ &= R(\cos S_2 - \cos S) \end{aligned} \quad (48)$$

$$\begin{aligned} \frac{\partial d_3}{\partial \phi} &= \frac{\partial a(\phi, \lambda)}{\partial \phi} - \frac{\partial a_3(\phi, \lambda)}{\partial \phi} \\ &= -R \cos S + R \cos S_3 \\ &= R(\cos S_3 - \cos S) \end{aligned} \quad (49)$$

$$\begin{aligned}
\frac{\partial d_1}{\partial \lambda} &= \frac{\partial a(\phi, \lambda)}{\partial \lambda} - \frac{\partial a_1(\phi, \lambda)}{\partial \lambda} \\
&= R \cos \phi_M \sin M + R \cos \phi_X \sin X \\
&= R(\cos \phi_M \sin M + \cos \phi_X \sin X)
\end{aligned} \tag{50}$$

$$\begin{aligned}
\frac{\partial d_2}{\partial \lambda} &= \frac{\partial a(\phi, \lambda)}{\partial \lambda} - \frac{\partial a_2(\phi, \lambda)}{\partial \lambda} \\
&= R \cos \phi_M \sin M - R \cos \phi_Y \sin Y \\
&= R(\cos \phi_M \sin M - \cos \phi_Y \sin Y)
\end{aligned} \tag{51}$$

$$\begin{aligned}
\frac{\partial d_3}{\partial \lambda} &= \frac{\partial a(\phi, \lambda)}{\partial \lambda} - \frac{\partial a_3(\phi, \lambda)}{\partial \lambda} \\
&= R \cos \phi_M \sin M - R \cos \phi_W \sin W \\
&= R(\cos \phi_M \sin M - \cos \phi_W \sin W)
\end{aligned} \tag{52}$$

$$C = 3 \times 10^8 (M/\text{sec}) = 3 \times 10^{-1} (M/nsec)$$

Now define the variance covariance matrix of LORAN time differences, assuming that there is no correlation between the three time differences.

$$\Sigma = \begin{bmatrix} \sigma_x^2 & 0 & 0 \\ 0 & \sigma_y^2 & 0 \\ 0 & 0 & \sigma_w^2 \end{bmatrix} \tag{54}$$

The LC 408 is provided with control of the filtering time constant. Selectable time constants are 0 seconds for no filtering, 5 seconds for good response, 10 seconds for slower response, and 20 seconds for slow craft or monitor applications.

In order to measure the standard deviations for the time differences, we recorded data for four days on Spanagel Roof, each day (24 hours) with a different time constant. This resulted in four different variance covariance matrices. There are all given in Appendix A.

From these results we conclude that the filters don't work for the time difference between Master and Secondary Whisky because the standard deviation remains approximately the same for the different time filters. We have no explanation for this beyond it being an instrumental problem. We also conclude

that for monitoring applications, the longer the filtering time, the smaller the standard deviations.

The weight matrix  $P = \Sigma^{-1}$  is given by

$$P = \begin{bmatrix} 1/\sigma_x^2 & 0 & 0 \\ 0 & 1/\sigma_y^2 & 0 \\ 0 & 0 & 1/\sigma_w^2 \end{bmatrix} \quad (55)$$

The variance covariance matrix for the position [Uotila, 1986] will be:

$$\Sigma(\phi, \lambda) = (J^T \times P \times J)^{-1} \quad (56)$$

Define the matrix  $\Sigma_0$  as

$$\Sigma_0 = \begin{bmatrix} 0 & 0 \\ 0 & 0 \end{bmatrix} \quad (57)$$

Now we form the block matrix  $\Sigma(\phi_1, \lambda_1, \phi_2, \lambda_2)$  which is the variance covariance matrix for two positions (the error characteristics are the same for the two positions). If it is assumed that there is no correlation between the two positions, then

$$\Sigma(\phi_1, \lambda_1, \phi_2, \lambda_2) = \begin{bmatrix} \Sigma(\phi_1, \lambda_1) & \Sigma_0 \\ \Sigma_0 & \Sigma(\phi_2, \lambda_2) \end{bmatrix} \quad (58)$$

In order to convert the difference in latitude and difference in longitude (radians) between two positions in meters, apply

$$A = \Delta\phi \times R \quad (59)$$

$$B = \Delta\lambda \times \cos \phi_m \times R \quad (60)$$

where  $\phi_m$  is the mean latitude of the work area, and  $R$  is the mean radius of the earth  $R = 6371$  KM. Let

$$C_1 = R \quad (61)$$

$$C_2 = \cos \phi_m \times R \quad (62)$$

The components of the ship velocity V , U (Northing, Easting) are then given by:

$$V = \frac{A}{\Delta t} = \frac{C_1}{\Delta t} \times (\phi_2 - \phi_1) \quad (63)$$

$$U = \frac{B}{\Delta t} = \frac{C_2}{\Delta t} \times (\lambda_2 - \lambda_1) \quad (64)$$

The Jacobian matrix for the velocity will be

$$J = \frac{1}{\Delta t} \begin{bmatrix} \frac{\partial V}{\partial \phi_1} & \frac{\partial V}{\partial \lambda_1} & \frac{\partial V}{\partial \phi_2} & \frac{\partial V}{\partial \lambda_2} \\ \frac{\partial U}{\partial \phi_1} & \frac{\partial U}{\partial \lambda_1} & \frac{\partial U}{\partial \phi_2} & \frac{\partial U}{\partial \lambda_2} \end{bmatrix} \quad (65)$$

and

$$J = \frac{1}{\Delta t} \begin{bmatrix} -C_1 & 0 & C_1 & 0 \\ 0 & -C_2 & 0 & C_2 \end{bmatrix} \quad (66)$$

Consider time intervals between positions 3 , 6 , 12 , 20 and 40 minutes. The variance covariance matrix for the velocity components will be:

$$\Sigma_{V, U} = J \times \Sigma_{\phi_1, \lambda_1, \phi_2, \lambda_2} \times J^T \quad (67)$$

Appendix B gives 5 tables for standard deviations and covariances of velocity components with different time intervals between positions. From these tables we see clearly that as the time interval between the positions increases the standard deviations for the V and U components decreases (assuming constant course and speed of the ship for the given interval). Also we note that when time averaging over 20 minutes or longer, the choice of filter is not critical.

Appendix C gives a program (DRIVLR FORTRAN) written by the NOAA which calculates the geographic position of the ship from two LORAN Time Differences (TD) and a Dead Reckoning (DR) position of the ship (inverse com-

putation). It can also be used to convert the geographic position of the ship into LORAN Time Differences (forward computation).



## **V. THEORY OF MINI RANGER**

### **A. INTRODUCTION**

The Mini Ranger Falcon was used during the cruise for navigational positioning. The standard Mini Ranger operates at up to 37 kilometers (about 20 nautical miles) with a probable range measurement error of 2 meters.

It operates at microwave frequencies and requires that line of sight be maintained between the reference stations and the receiver transmitter. Significant obstructions such as land masses, buildings, or dense foliage will interfere the operation of the system.

### **B. REFERENCE STATIONS**

The positions of the reference station sites in the UTM coordinate system are [Krioneritis, 1989] listed in Table 4.

**Table 4. REFERENCE STATION SITES**

STATION	X EASTING	Y NORTHING	CODE
TREVOR	585260.161 M	4092490.284 M	15
PACK	609863.128 M	4076611.345 M	1
HAYES	607621.289 M	4055915.264 M	12

### **C. RANGE POSITIONING**

The Mini Ranger determines a two range position when the lengths of all three sides of a triangle are known (trilateration). Suppose that a certain task requires activity between points C , D , E (Figure 15), the reference stations are at points A and B, in the acceptable area the angle of intersection between the two range lines is between 30 and 150 degrees.

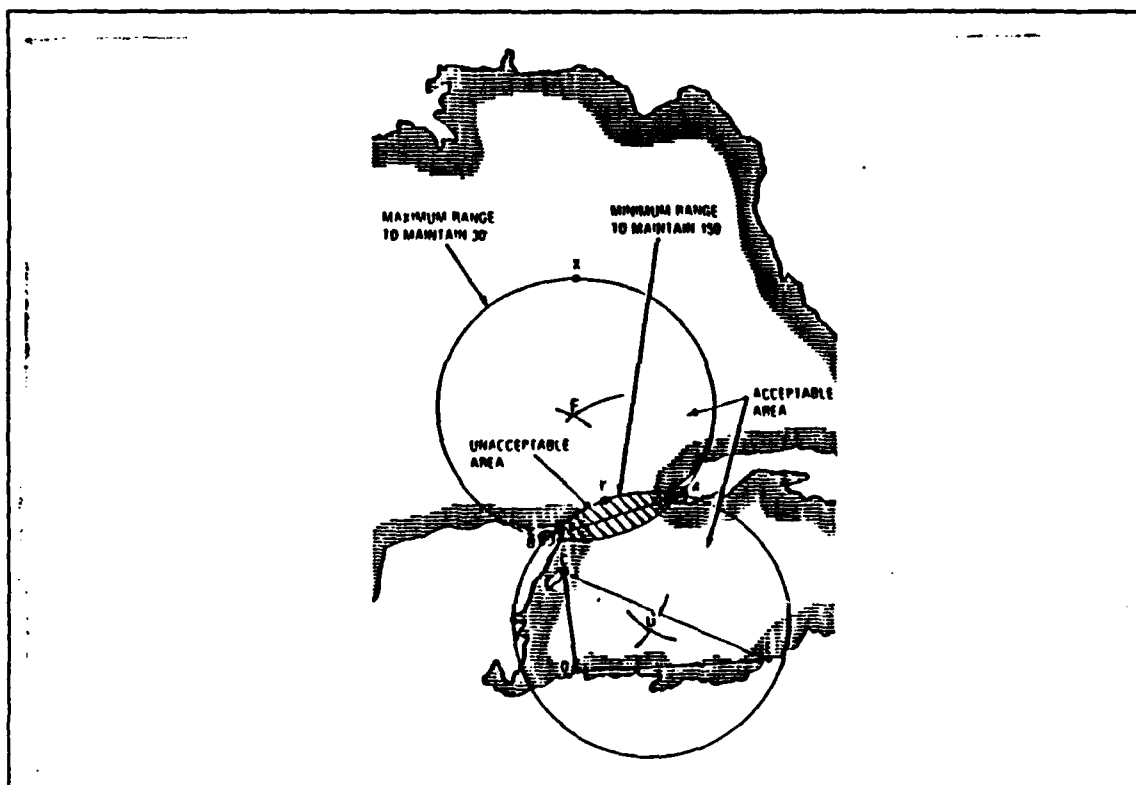


Figure 15. PLANNING THE MOST DESIRABLE SITE

Arcs AXB and AYB define the maximum and minimum distance to maintain between 30 and 150 degrees respectively.

Generally the Mini Ranger uses the method of least squares to calculate positions from three or more reference stations. Operation in areas where the geometry is poor will degrade positional accuracy [Mini Ranger operation manual, 1981].

#### D. ERROR ANALYSIS FOR MINI RANGER

While the Mini Ranger measures ranges well, the actual position error resulting from a set of range readings depends upon a number of contributing factors:

1. system error, and
2. geometry changes.

Figure 16 shows the maximum positional error for two range geometries of 30 , 90 and 150 degrees [Mini Ranger operation manual, 1981].

$$POSITION\ ERROR = \frac{STANDARD\ ERROR}{\sin \theta} \quad (68)$$

The position error for various two range geometries, assuming range error of a single measurement of 2 meters are given in Table 5.

**Table 5. POSITION ERROR FOR DIFFERENT CROSS ANGLES**

CROSSING ANGLE	POSITION ERROR
150 degrees	7.7 meters
120 degrees	4.0 meters
90 degrees	2.8 meters
60 degrees	4.0 meters
30 degrees	7.7 meters

For this experiment we'll take the information for the variance covariance matrix of the positions from the Mini Ranger data processing (see, for example, Krioneritis, 1989). Define the matrix  $\Sigma_0$  as

$$\Sigma_0 = \begin{bmatrix} 0 & 0 \\ 0 & 0 \end{bmatrix} \quad (69)$$

The variance covariance matrix for the position will be

$$\Sigma(X,Y) = \begin{bmatrix} \sigma_x^2 & \sigma_{X,Y} \\ \sigma_{X,Y} & \sigma_y^2 \end{bmatrix} \quad (70)$$

We now form the block matrix  $\Sigma ( X_1,Y_1,X_2,Y_2)$  which is the variance covariance matrix for two positions. If it is assumed there is no correlation between the two positions, then

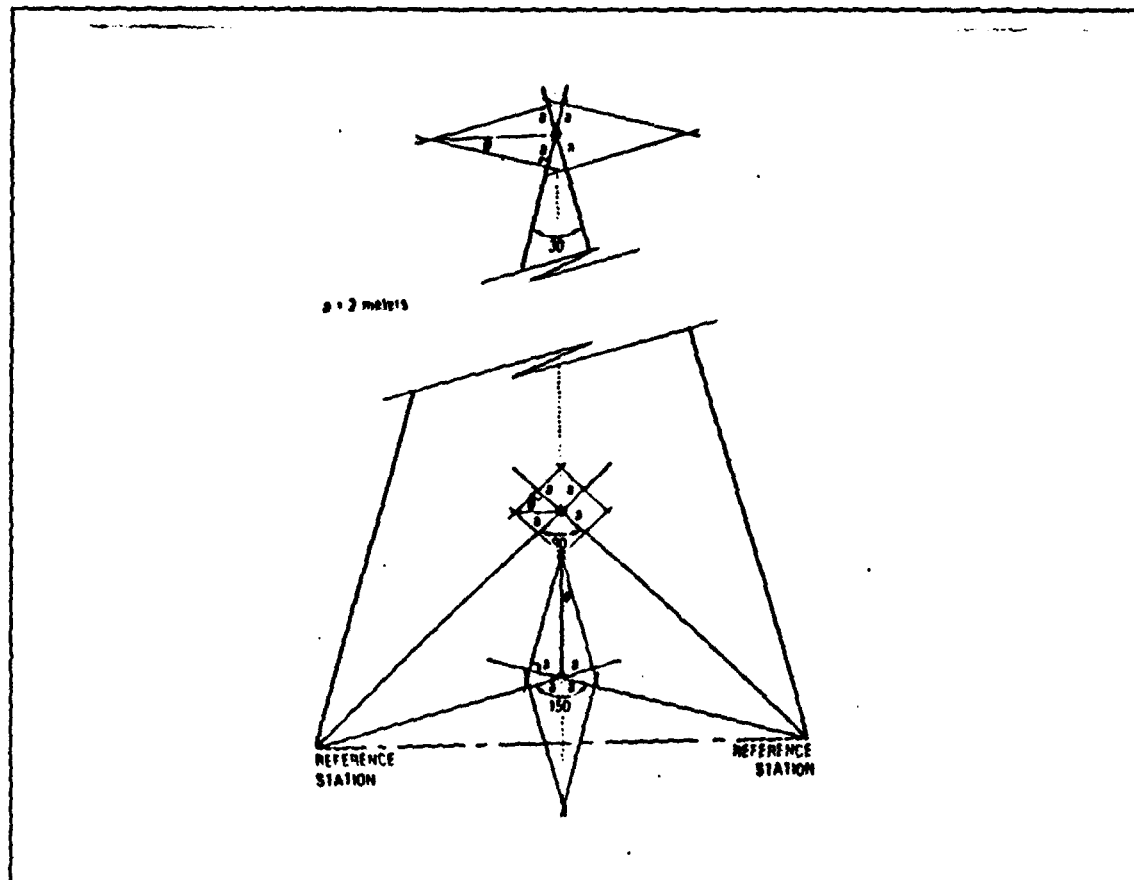


Figure 16. MAXIMUM POSITION ERROR

$$\Sigma(X_1, Y_1, X_2, Y_2) = \begin{bmatrix} \Sigma(X_1, Y_1) & \Sigma_0 \\ \Sigma_0 & \Sigma(X_2, Y_2) \end{bmatrix} \quad (71)$$

Define the velocity components as

$$V = \frac{Y_2 - Y_1}{\Delta t} \quad (72)$$

$$U = \frac{X_2 - X_1}{\Delta t} \quad (73)$$

As we did with LORAN C, we propagate errors into these expressions by forming the jacobian matrix for the velocity components. We again assume that time is subject to negligible error. This matrix is given by

$$J = \frac{1}{\Delta t} \begin{bmatrix} \frac{\partial V}{\partial X_1} & \frac{\partial V}{\partial Y_1} & \frac{\partial V}{\partial X_2} & \frac{\partial V}{\partial Y_2} \\ \frac{\partial U}{\partial X_1} & \frac{\partial U}{\partial Y_1} & \frac{\partial U}{\partial X_2} & \frac{\partial U}{\partial Y_2} \end{bmatrix} \quad (74)$$

OR

$$J = \frac{1}{\Delta t} \begin{bmatrix} 0 & -1 & 0 & 1 \\ -1 & 0 & 1 & 0 \end{bmatrix} \quad (76)$$

The variance covariance matrix for the velocity components will be

$$\Sigma_{V,U} = J \times \Sigma_{X_1,Y_1,X_2,Y_2} \times J^T \quad (77)$$

**Table 6. MAX-MIN VALUES OF STANDARD DEVIATIONS AND COVARIANCES FOR VELOCITY COMPONENTS FOR 3 MINUTE TIME INTERVALS BETWEEN POSITIONS (MINI RANGER)**

MAX-MIN VALUES	$\sigma_V$	$\sigma_U$	$\sigma_{V,U}$
MAXIMUM	1.6 cm/sec	1.8 cm/sec	$2.8 \text{ cm}^2 / \text{sec}^2$
MINIMUM	1.2 cm/sec	1.3 cm/sec	$0.2 \text{ cm}^2 / \text{sec}^2$

Table (6) shows that the the standard error in the velocity components doesn't vary greatly given the geometry in the work area. The results come from 6 different points in the whole work area.

Appendix D gives the velocity error results for different time intervals. Similar to the LORAN (Appendix B), the standard deviations for the velocity com-

ponents decrease when the time interval between the positions increases (assuming constant course and speed of the ship for the given time interval).

Comparing the theoretical results from Appendices B and D, we can see that the MINI RANGER is not only a more stable navigation system than the LORAN C, but also that it provides in 3 minutes the level of accuracy in the U and V velocity components which require 20 minutes to obtain with LORAN C. Because of the practical difficulties in maintaining a constant ship's heading and speed for 20 minutes, and thus the need for an averaging process over such a time interval, the value of using a MINI RANGER wherever possible is even further enhanced.

## VI. RESULTS

In this chapter there are eleven Tables which summarise the results of the computation of the ship velocity components from MINI RANGER, LORAN Time Differences (TD), LORAN (DISPLAY) and Bottom Tracking. We choose to separate the LORAN (TD), and LORAN (DISPLAY) results because of the rounding off which occurs when using the LORAN (DISPLAY).

The LORAN results given here were obtained using different filters (2 - 1, 1 - 3 filter with time constant 5 seconds, 1 - 2 filter with time constant 20 seconds, 3 - 2, 2 - 3 filter with time constant 10 seconds, 3 - 4 filter with time constant 0 seconds ).

**Table 7. SHIP VELOCITY COMPONENTS FOR MINI RANGER, LORAN (TD), LORAN (DISPLAY) FROM POINT 1 TO POINT 2 AT 3 MINUTE TIME INTERVAL.**

TIME	MINI RANGER		LORAN (TD)		LORAN (DISPLAY)	
	U (cm/sec)	V (cm/sec)	U (cm/sec)	V (cm/sec)	U (cm/sec)	V (cm/sec)
14 24 11	-126.5	-277.1	-125.4	-273.5	-126.2	-263.3
14 27 10	-125.9	-276.0	-123.2	-274.8	-124.0	-286.4
14 30 10	-123.3	-277.6	-120.6	-278.1	-115.7	-271.5
14 33 11	-124.4	-280.5	-124.4	-274.6	-124.0	-282.8
14 36 11	-106.3	-282.8	-107.4	-282.5	-109.3	-281.6
14 39 11	-108.7	-285.1	-103.0	-296.2	-105.2	-275.6
14 42 10	-109.3	-280.7	-116.5	-284.5	-113.4	-268.4

**Table 8. SHIP VELOCITY COMPONENTS FOR MINI RANGER, LORAN (TD), LORAN (DISPLAY) FROM POINT 2 TO POINT 1 AT 3 MINUTE TIME INTERVAL**

TIME	MINI RANGER		LORAN (TD)		LORAN (DISPLAY)	
	U (cm/sec)	V (cm/sec)	U (cm/sec)	V (cm/sec)	U (cm/sec)	V (cm/sec)
14 57 10	135.0	265.3	134.3	254.5	135.0	258.0
15 00 10	133.7	261.3	134.4	256.1	132.2	240.7
15 03 10	138.9	255.4	134.7	253.7	138.1	265.0
15 06 10	154.4	252.0	154.0	245.6	148.7	244.1
15 09 10	155.9	253.1	154.7	256.5	151.7	247.9
15 12 10	148.8	255.4	146.2	252.3	154.1	261.3
15 15 10	155.7	251.8	154.9	250.7	143.2	237.2

From Tables 7 and 8 we can see a discontinuity beginning at 14 36 11 near the end of leg 1 - 2 and ending at 15 03 10 at the beginning of leg 2 - 1. This discontinuity occurs at the same position down each leg and is of approximately the same magnitude in each case. While it is tempting to view this discontinuity as being due to a surface current, the inconsistency in sign prohibits such an explanation. It can only be concluded therefore that it is due to a ship navigation correction.

In these tables we see clearly that the LORAN (DISPLAY) results show a much greater variability than the LORAN (TD). Also if we calculate the mean value and the standard deviation of the mean of the absolute difference of the U and V components between the MINI RANGER and LORAN (TD), and the MINI RANGER and LORAN (DISPLAY), we have Table 9.



**Table 9. COMPARISON BETWEEN MINI RANGER AND LORAN (TD) AND THE MINI RANGER AND LORAN (DISPLAY) FOR LEGS 1 - 2 AND 2 - 1.**

LEG	MINI RANGER - LORAN (TD)		MINI RANGER - LORAN (DISPLAY)	
	$\Delta U (\sigma_{\Delta U})$	$\Delta V (\sigma_{\Delta V})$	$\Delta U (\sigma_{\Delta U})$	$\Delta V (\sigma_{\Delta V})$
1 - 2	2.9(0.9)	4.5(2.1)	2.9(0.9)	7.9(1.8)
2 - 1	1.5(0.5)	4.5(1.2)	4.2(1.6)	10.2(2.1)

After using the FISHER-BEHERENS test [Hamilton, 1964] to compare  $\Delta U$  from MINI RANGER-LORAN (TD) against  $\Delta U$  from MINI RANGER-LORAN (DISPLAY) and  $\Delta V$  against  $\Delta V$  we see that these are statistically different at 95% confidence interval in 3 out of 4 cases. This provides strong evidence to suggest that the results from LORAN (TD) and LORAN (DISPLAY) are from different statistical populations.

**Table 10. SHIP VELOCITY COMPONENTS FOR MINI RANGER, LORAN (TD), LORAN (DISPLAY) FROM POINT 1 TO POINT 3 AT 3 MINUTE TIME INTERVAL**

TIME	MINI RANGER		LORAN (TD)		LORAN (DISPLAY)	
	U (cm/sec)	V (cm/sec)	U (cm/sec)	V (cm/sec)	U (cm/sec)	V (cm/sec)
15 30 10	-272.4	-116.1	-272.0	-118.6	-272.8	-123.8
15 33 11	-273.1	-115.8	-274.6	-116.5	-253.5	-106.8
15 36 11	-277.4	-117.8	-276.6	-116.1	-291.8	-126.8
15 39 10	-277.1	-117.9	-276.8	-121.4	-273.7	-104.1
15 42 10	-268.4	-122.7	-269.5	-123.2	-274.8	-130.6
15 45 10	-266.7	-126.4	-268.6	-130.2	-264.4	-134.0

15 48 10	-265.9	-123.9	-264.7	-119.4	-264.7	-123.9
15 51 10	-268.9	-126.7	-265.9	-119.8	-264.3	-113.5
15 54 10	-269.8	-123.9	-263.8	-118.7	-276.3	-123.9
15 57 10	-266.7	-126.1	-267.2	-124.8	-250.8	-125.8
16 00 10	-269.5	-120.5	-269.5	-114.8	-269.9	-101.3
16 03 11	-265.9	-127.2	-259.5	-127.9	-273.8	-140.1
16 06 10	-268.6	-125.5	-267.4	-125.2	-260.6	-123.8

**Table 11. COMPARISON BETWEEN MINI RANGER AND LORAN (TD) AND THE MINI RANGER AND LORAN (DISPLAY) FOR LEG 1 - 3.**

LEG	MINI RANGER - LORAN (TD)		MINI RANGER - LORAN (DISPLAY)	
	$\Delta U (\sigma_{\Delta U})$	$\Delta V (\sigma_{\Delta V})$	$\Delta U (\sigma_{\Delta U})$	$\Delta V (\sigma_{\Delta V})$
1 - 3	1.9(0.6)	2.9(0.6)	7.0(1.7)	7.9(1.7)

Table 10 shows similar results for leg 1 - 3. From Table 11 it is also obvious that the results which comes from the LORAN (TD) and the LORAN (DISPLAY) are different for leg 1 - 3.

**Table 12. SHIP VELOCITY COMPONENTS FOR MINI RANGER, LORAN (TD), LORAN (DISPLAY), BOTTOM TRACKING FROM POINT 3 TO POINT 2 AT 3 MINUTE TIME INTERVAL**

TIME	MINI RANGER		LORAN (TD)		LORAN (DISPLAY)		BOTTOM TRACKING	
	U (cm sec)	V (cm sec)	U (cm sec)	V (cm sec)	U (cm sec)	V (cm sec)	U (cm sec)	V (cm sec)
16 16 18	272.4	-103.5	267.9	-104.4	259.7	-105.4	263.5	-116.5
16 19 18	277.9	-93.2	280.2	-94.6	274.1	-84.0	271.4	-103.5
16 22 18	275.5	-95.3	272.1	-95.5	279.7	-111.8	268.5	-106.0
16 25 18	277.3	-99.2	275.1	-97.5	276.6	-80.7	273.3	-110.1

16 28 17	278.0	-98.2	282.2	-95.4	275.7	-98.7	272.4	-108.1
16 31 19	280.1	-106.6	279.8	-97.7	281.3	-99.1	274.2	-109.5

**Table 13. SHIP VELOCITY COMPONENTS FOR MINI RANGER, LORAN (TD), LORAN (DISPLAY), BOTTOM TRACKING FROM PCINT 2 TO POINT 3 AT 3 MINUTE TIME INTERVAL**

TIME	MINI RANGER		LORAN (TD)		LORAN (DIS- PLAY)		BOTTOM TRACKING	
	U (cm sec)	V (cm sec)	U (cm sec)	V (cm sec)	U (cm sec)	V (cm sec)	U (cm sec)	V (cm sec)
16 52 18	-260.3	124.3	-256.1	124.3	-256.5	124.3	-253.0	128.5
16 55 17	-259.2	118.4	-261.1	114.4	-271.0	121.5	-252.8	124.8
16 58 17	-262.8	116.4	-264.7	115.9	-249.9	108.1	-257.1	125.9
17 01 17	-269.5	122.7	-266.1	118.0	-277.1	126.5	-262.8	128.4
17 04 18	-271.1	117.8	-268.9	120.9	-266.6	118.5	-264.9	125.1
17 07 18	-264.2	116.4	-265.3	108.3	-266.8	114.2	-258.8	123.0
17 10 18	-267.0	115.4	-263.6	119.4	-260.2	120.8	-262.9	123.2
17 13 17	-264.0	121.9	-260.9	120.7	-264.3	116.0	-258.4	128.0

From Tables 12 and 13 we can see that the more consistent results comes from MINI RANGER. The variability of the LORAN (TD) results are smaller than the variability of the LORAN (DISPLAY) results. We also see that the Bottom Tracking, while giving values to the same internal consistency as the MINI RANGER, gives results which are systematically biased.

**Table 14. COMPARISON BETWEEN MINI RANGER AND LORAN (TD) AND THE MINI RANGER AND LORAN (DISPLAY) FOR LEGS 3 - 2 AND 2 - 3.**

LEG	MINI RANGER - LORAN (TD)		MINI RANGER - LORAN (DISPLAY)		MINI RANGER - BOT- TOM TRACKING	
	$\Delta U (\sigma_{\Delta U})$	$\Delta V (\sigma_{\Delta V})$	$\Delta U (\sigma_{\Delta U})$	$\Delta V (\sigma_{\Delta V})$	$\Delta U (\sigma_{\Delta U})$	$\Delta V (\sigma_{\Delta V})$

3 - 2	2.8(0.6)	2.6(1.3)	4.1(1.8)	9.1(3.1)	6.3(0.7)	9.6(1.4)
2 - 3	2.6(0.4)	3.2(0.9)	6.3(1.6)	3.7(1.0)	5.9(0.4)	6.7(0.6)

From Table 14, after using the FISHER-BEHERENS test to compare  $\Delta U$  from MINI RANGER-LORAN (TD) against  $\Delta U$  from MINI RANGER-LORAN (DISPLAY) and  $\Delta V$  against  $\Delta V$  we see that these are statistically different at a 95% confidence interval in 2 out of 4 cases.

**Table 15. SHIP VELOCITY COMPONENTS FOR MINI RANGER, LORAN (TD), LORAN (DISPLAY), BOTTOM TRACKING FROM POINT 3 TO POINT 4 AT 3 MINUTE TIME INTERVAL**

TIME	MINI RANGER		LORAN (TD)		LORAN (DISPLAY)		BOTTOM TRACKING	
	U (cm sec)	V (cm sec)	U (cm sec)	V (cm sec)	U (cm sec)	V (cm sec)	U (cm sec)	V (cm sec)
17 22 17	-9.4	286.1	-12.1	283.2	-10.2	275.7	0.5	282.2
17 25 17	-11.7	288.0	-12.8	284.2	-10.6	288.9	-1.4	285.9
17 28 17	-12.5	289.3	-9.8	285.3	-10.9	287.5	-4.1	287.0
17 31 17	-4.9	295.7	-8.7	295.9	-15.1	293.5	1.5	290.6
17 34 17	-8.7	293.5	-11.7	292.8	-7.1	293.0	-1.9	288.4
17 37 19	-19.4	293.5	-18.3	286.7	-23.6	274.5	-11.8	290.1
17 40 18	-21.6	297.3	-20.0	296.2	-20.0	307.0	-15.1	293.2
17 43 18	-16.2	288.6	-15.9	288.8	-7.9	288.8	-9.2	286.6
17 46 18	-24.9	292.2	-26.4	290.5	-29.5	299.3	-20.2	287.9
17 49 18	-37.5	290.6	-42.0	284.7	-41.6	278.8	-33.7	286.8
17 52 18	-32.2	288.7	-34.5	291.0	-41.3	287.5	-27.7	286.4
17 55 17	-28.0	286.0	-29.9	281.1	-23.4	287.0	-21.4	282.5
17 58 18	-22.2	281.3	-13.6	286.1	-16.6	247.7	-15.3	278.6
18 01 18	-22.3	281.0	-23.4	276.0	-25.7	280.0	-18.5	276.7
18 04 18	-25.3	275.4	-26.1	275.1	-20.0	283.2	-17.7	273.9
18 07 18	-23.4	274.6	-24.9	272.2	-28.3	266.3	-18.2	271.6

18 10 18	-22.3	271.0	-19.2	273.1	-22.3	258.7	-14.8	268.9
18 13 18	-28.7	267.2	-30.2	267.5	-23.8	285.7	-23.1	266.0
18 16 18	-29.8	262.8	-37.4	257.3	-37.7	262.5	-21.4	265.1
18 19 18	-30.9	264.3	-20.7	269.9	-20.0	268.3	-17.1	262.9
18 22 47	-25.8	261.2	-33.0	257.9	-32.3	256.5	-	-
18 25 47	-31.3	256.1	-37.8	253.8	-41.2	247.6	-	-
18 28 47	-26.8	266.0	-29.1	262.2	-26.1	262.7	-	-
18 31 47	-29.1	263.0	-25.7	264.4	-28.0	251.7	-	-
18 34 47	-29.1	264.7	-30.2	263.2	-24.5	281.2	-	-
18 37 47	-27.5	263.9	-27.2	262.0	-24.9	245.9	-	-
18 40 47	-33.6	261.1	-35.8	257.6	-32.8	264.4	-	-
18 43 46	-39.4	256.5	-38.2	261.5	-32.5	251.1	-	-
18 46 46	-32.9	259.8	-34.4	256.8	-45.4	269.8	-	-
18 49 46	-41.9	257.5	-40.8	258.9	-41.9	258.0	-	-
18 52 46	-43.3	256.0	-43.3	257.9	-44.9	262.8	-	-
18 55 47	-37.7	257.9	-36.2	255.3	-33.2	248.9	-	-
18 58 47	-32.5	255.4	-31.0	259.6	-32.5	262.2	-	-
19 01 47	-33.9	252.4	-32.8	251.9	-20.7	231.4	-	-
19 04 47	-32.4	255.7	-32.4	253.1	-49.4	274.3	-	-
19 07 46	-32.1	253.1	-32.1	253.1	-28.7	237.3	-	-
19 10 46	-43.5	253.2	-41.2	255.3	-41.6	273.4	-	-
19 13 47	-47.8	256.5	-48.1	253.2	-49.3	252.9	-	-
19 16 46	-53.7	255.4	-56.4	251.4	-41.2	232.0	-	-
19 19 46	-57.1	256.5	-56.3	253.0	-65.8	273.3	-	-
19 22 47	-46.2	259.8	-51.9	254.7	-45.5	242.7	-	-
19 25 46	-42.0	263.6	-45.8	259.4	-53.3	257.7	-	-
19 28 46	-47.7	268.0	-49.6	264.9	-49.6	274.2	-	-
19 31 46	-50.9	270.9	-57.6	263.3	-49.7	262.8	-	-
19 34 47	-59.5	267.2	-60.6	262.5	-65.9	258.0	-	-
19 37 46	-54.9	268.8	-59.0	262.9	-53.4	252.9	-	-

19 40 47	-52.7	272.5	-51.9	268.0	-65.9	283.8	-	-
19 43 47	-60.4	276.0	-66.0	270.3	-66.0	273.6	-	-
19 46 46	-57.9	279.1	-64.4	272.7	-61.7	273.4	-	-
19 49 46	-45.2	273.9	-52.7	268.4	-52.3	264.4	-	-
19 52 47	-39.1	276.8	-36.9	266.9	-34.2	266.9	-	-
19 55 47	-21.1	278.8	-23.0	275.8	-28.6	273.6	-	-
19 58 46	-21.6	281.4	-25.0	276.6	-16.3	273.3	-	-
20 01 47	-21.8	276.8	-26.7	274.2	-33.1	278.7	-	-
20 04 47	-19.5	277.7	-22.2	271.3	-20.7	268.3	-	-
20 07 47	-26.8	279.4	-30.5	269.9	-24.5	268.5	-	-
20 10 46	-23.4	274.2	-24.6	274.9	-25.0	268.5	-	-

**Table 16. COMPARISON BETWEEN MINI RANGER AND LORAN (TD) AND THE MINI RANGER AND LORAN (DISPLAY) FOR LEG 3 - 4.**

LEG	MINI RANGER - LORAN (TD)		MINI RANGER - LORAN (DISPLAY)		MINI RANGER - BOTTOM TRACKING	
	$\Delta U (\sigma_{\Delta U})$	$\Delta V (\sigma_{\Delta V})$	$\Delta U (\sigma_{\Delta U})$	$\Delta V (\sigma_{\Delta V})$	$\Delta U (\sigma_{\Delta U})$	$\Delta V (\sigma_{\Delta V})$
3 - 4	2.8(0.3)	3.5(0.3)	5.1(0.5)	8.6(0.8)	7.1(0.5)	3.1(0.3)

Table 15 again yields similar results for leg 3 - 4. From Table 16 it is again obvious that the results which comes from the LORAN (TD) and the LORAN (DISPLAY) are different.

In Table 17 are the average velocity components for the different positioning systems and for the bottom tracking for each leg. From this table we can see:

- Data averaged over times of about 18 minutes (minimum) show no statistically significant difference between MINI RANGER, LORAN (TD) and LORAN (DISPLAY). Any one of these positioning systems can be used for these averaged times. This is due to the fact that the variations of the ship course and speed in the averaged period of time completely swamp the different precision which the different navigation systems have in their calculation of the U and V components of the ship. The minimum time interval from which the averaged data over the different navigation systems become the same statistically depends upon the ship's variations in course and speed.

- The results from Bottom Tracking are clearly systematically different from those of the others systems. They do, however, show the same level of internal consistency as both the MINI RANGER and the LORAN (TD) results.
- The much larger standard deviations on the LORAN (DISPLAY) results are indicative of the much greater variability in computed U and V components when using this system.

**Table 17. AVERAGE VELOCITY COMPONENTS FOR MINI RANGER, LORAN (TD), LORAN (DISPLAY), BOTTOM TRACKING**

	MINI RANGER		LORAN (TD)		LORAN (DIS- PLAY)		BOTTOM TRACK- ING	
	U ( $\sigma_U$ )	V ( $\sigma_V$ )	U ( $\sigma_U$ )	V ( $\sigma_V$ )	U ( $\sigma_U$ )	V ( $\sigma_V$ )	U ( $\sigma_U$ )	V ( $\sigma_V$ )
1 - 2	-117.7(3.4)	-279.9(1.2)	-117.2(3.3)	-276.7(2.1)	-116.8(3.1)	-275.6(3.2)	-	-
2 - 1	146.1(3.7)	256.3(1.9)	144.7(3.8)	252.7(1.4)	143.3(3.2)	250.6(4.1)	-	-
1 - 3	-270.1(1.1)	-122.3(1.1)	-268.9(1.4)	-121.2(1.3)	-268.5(2.9)	-121.4(3.2)	-	-
3 - 2	276.8(1.1)	-99.3(2.1)	276.2(2.2)	-97.5(1.5)	274.5(3.1)	-96.6(4.9)	270.5(1.6)	-108.9(1.8)
2 - 3	-264.7(1.4)	119.1(1.1)	-263.3(1.4)	117.7(1.7)	-264.1(3.0)	118.7(2.1)	-258.8(1.6)	125.8(0.8)
3 - 4	-32.5(1.8)	271.1(1.7)	-33.8(1.9)	269.1(1.7)	-33.6(2.1)	268.7(2.1)	-	-
3 - 4A	-21.6(1.9)	283.3(2.4)	-21.8(2.1)	281.8(2.3)	-21.8(2.3)	282.1(2.7)	-14.5(2.1)	280.6(2.1)

In Appendix E there are 12 figures which show the average current profiles from point 1 - 3, 3 - 2, 2 - 3, 3 - 4 with the three different navigation data from MINI RANGER, LORAN (TD), LORAN (DISPLAY). These plots show us the same thing as the Table 17 i.e. no significant difference between the navigation systems when we average over times of about 20 - 30 minutes.

In Appendix F there are 6 plots for points 1 - 2, 2 - 1 but not averaged for the whole length (just plots for specific times between the points). These plots

show, as expected, that the  $U$  and  $V$  components of the current are different for different navigation systems.



## VII. CONCLUSIONS AND RECOMMENDATIONS

From this thesis we can conclude that:

- Because of the variability in the LORAN (DISPLAY) results and the need for a reasonable measure of statistical strength, it is not recommended that LORAN (DISPLAY) be used for giving averaged results of under 20 minutes. Indeed, it is preferable to use LORAN (TD) rather than LORAN (DISPLAY) whenever possible. Furthermore, LORAN (DISPLAY) results not only show a much greater variability than the LORAN (TD) results, but also at a 95% confidence interval consistently fail the statistical hypothesis that they come from the same population.
- MINI RANGER results as expected are very consistent. It is felt that good ADCP current estimates could be derived using MINI RANGER observations for periods as short as 3 minutes.
- When averaging for 20 - 30 minutes all the navigation systems give the same results.
- Without averaging we recommended that the MINI RANGER be used whenever possible. If this system is not available, LORAN (TD) should be the next choice.
- The theoretical investigation revealed that when time averaging over 20 minutes or longer, the choice of the filter to be used for the LORAN system was not critical. The cruise results appear to support this contention.
- Bottom Tracking results are systematically biased, but have the same standard deviation as the MINI RANGER results.

In looking to the future work on this subject it is recommended that:

- Further work is required to understand and resolve the Bottom Tracking bias problem.
- If this cruise is done again we suggest checking the LORAN filters by making one long run, dividing it into 30 minute segments, and using a different filter on each segment.

## APPENDIX A. STATISTICAL ANALYSIS FOR THE LC 408 DATA

The provided numbers are in *nanoseconds* .

### (1) TIME CONSTANT 0 SECONDS (NO FILTERING)

STATION	N	MEAN	STANDARD DEVIATION	MINIMUM VALUE	MAXIMUM VALUE	STD ERROR OF MEAN
WHISKY	1440	16312005.09	46.85663572	16311760.00	16312180.00	1.23478077
X-RAY	1440	27511618.59	22.27564796	27511540.00	27511720.00	0.58701487
YANKEE	1440	42735925.76	24.94991412	42735810.00	42736030.00	0.65748797

### (2) TIME CONSTANT 5 SECONDS (GOOD RESPONSE)

STATION	N	MEAN	STANDARD DEVIATION	MINIMUM VALUE	MAXIMUM VALUE	STD ERROR OF MEAN
WHISKY	1440	16312033.94	51.75565604	16311860.00	16312180.00	1.36388129
X-RAY	1440	27511616.71	19.82896815	27511560.00	27511680.00	0.52253919
YANKEE	1440	42735928.43	23.39278554	42735860.00	42736020.00	0.61645403

### (3) TIME CONSTANT 10 SECONDS (SLOWER RESPONSE)

STATION	N	MEAN	STANDARD DEVIATION	MINIMUM VALUE	MAXIMUM VALUE	STD ERROR OF MEAN
WHISKY	1440	16311981.04	49.40674807	16311790.00	16312110.00	1.30198213
X-RAY	1440	27511616.56	13.76653231	27511580.00	27511680.00	0.36277998
YANKEE	1440	42735918.06	18.02041879	42735850.00	42735990.00	0.47487973

### (4) TIME CONSTANT 20 SECONDS (MONITOR

APPLICATIONS)

STATION	N	MEAN	STANDARD DEVIATION	MINIMUM VALUE	MAXIMUM VALUE	STD ERROR OF MEAN
WHISKY	1417	16311990.54	46.87615596	16311800.00	16312130.00	1.24528015
X-RAY	1417	27511618.80	12.99066592	27511570.00	27511680.00	0.34510122
YANKEE	1417	42735915.31	16.74596778	42735850.00	42735980.00	0.44486202

**APPENDIX B. TABLES FOR STANDARD DEVIATIONS AND  
COVARIANCES OF VELOCITY COMPONENTS FOR LORAN C (LC 408)**

**Table 18. TIME INTERVAL BETWEEN POSITIONS 3 MINUTES**

FILTER	$\sigma_v$	$\sigma_u$	$\sigma_{v,u}$
0 sec	11.6 cm/sec	6.8 cm/sec	-61.184 $cm^2/sec^2$
5 sec	10.8 cm/sec	6.1 cm/sec	-51.047 $cm^2/sec^2$
10 sec	8.2 cm/sec	4.3 cm/sec	-27.447 $cm^2/sec^2$
20 sec	7.7 cm/sec	4.1 cm/sec	-24.029 $cm^2/sec^2$

**Table 19. TIME INTERVAL BETWEEN POSITIONS 6 MINUTES**

FILTER	$\sigma_v$	$\sigma_u$	$\sigma_{v,u}$
0 sec	5.8 cm/sec	3.4 cm/sec	-15.296 $cm^2/sec^2$
5 sec	5.4 cm/sec	3.0 cm/sec	-12.761 $cm^2/sec^2$
10 sec	4.1 cm/sec	2.1 cm/sec	-6.861 $cm^2/sec^2$

20 sec	3.8 cm/sec	2.0 cm/sec	-6.007 $cm^2/sec^2$
--------	------------	------------	---------------------

**Table 20. TIME INTERVAL BETWEEN POSITIONS 12 MINUTES**

FILTER	$\sigma_v$	$\sigma_u$	$\sigma_{v,u}$
0 sec	2.9 cm/sec	1.7 cm/sec	-3.824 $cm^2/sec^2$
5 sec	2.7 cm/sec	1.5 cm/sec	-3.190 $cm^2/sec^2$
10 sec	2.1 cm/sec	1.1 cm/sec	-1.715 $cm^2/sec^2$
20 sec	1.9 cm/sec	1.0 cm/sec	-1.502 $cm^2/sec^2$

**Table 21. TIME INTERVAL BETWEEN POSITIONS 20 MINUTES**

FILTER	$\sigma_v$	$\sigma_u$	$\sigma_{v,u}$
0 sec	1.7 cm/sec	1.0 cm/sec	-1.376 $cm^2/sec^2$
5 sec	1.6 cm/sec	0.9 cm/sec	-1.148 $cm^2/sec^2$

10 sec	1.2 cm/sec	0.7 cm/sec	$-0.617cm^2/sec^2$
20 sec	1.1 cm/sec	0.6 cm/sec	$-0.540cm^2/sec^2$

**Table 22. TIME INTERVAL BETWEEN POSITIONS 40 MINUTES**

FILTER	$\sigma_V$	$\sigma_U$	$\sigma_{V,U}$
0 sec	0.9 cm/sec	0.5 cm/sec	$-0.344cm^2/sec^2$
5 sec	0.8 cm/sec	0.4 cm/sec	$-0.287cm^2/sec^2$
10 sec	0.6 cm/sec	0.3 cm/sec	$-0.154cm^2/sec^2$
20 sec	0.5 cm/sec	0.3 cm/sec	$-0.135cm^2/sec^2$

## **APPENDIX C. PROGRAM DRIVLR FORTRAN**

### **A. GENERAL REMARKS**

This program calculate the hyperbolic coordinates of a ship expressed in LORAN time differences from geographic positions forward computation , and the inverse computation.

Forward computation:

- Input parameters - ALAT, ALON, L, DEL, ISYS, IB, IVEL.
- Output parameters - TD, BETA, BLEN, BLEM, IER.

Inverse computation:

- Input parameters - ALAT, ALON, L, DEL, TD, ISYS, ISENT, ISW, IB, IVEL.
- Output parameters - ALAT, ALON, BETA, BLEN, BLEM, ISENT, IER, IT.

### **B. DESCRIPTION OF PARAMETERS:**

ALAT - Latitude array in seconds of arc:

- ALAT(1) - Latitude of master station.
- ALAT(2) - Latitude of slave 1 station.
- ALAT(3) - Latitude of master station.
- ALAT(4) - Latitude of slave 2 station.
- ALAT(5) - Latitude of ship position.
- ALON(1) - Longitude of master station.
- ALON(2) - Longitude of slave 1 station.
- ALON(3) - Longitude of master station.
- ALON(4) - Longitude of slave 2 station.
- ALON(5) - Longitude of ship position.

L - Spheroid code array.

L(1) - Spheroid code array for first rate:

- L(1) = 1 WGS 1984.

- L(1) = 2    Bessel spheroid.
- L(1) = 3    Clarke 1858 spheroid.
- L(1) = 4    Clarke 1866 spheroid.
- L(1) = 5    Clarke 1880 spheroid.
- L(1) = 6    Everest spheroid.
- L(1) = 7    Fischer spheroid.
- L(1) = 8    International spheroid.
- L(1) = 9    WGS 1972 spheroid.

L(2) - Spheroid code for second rate:

- L(2) = 1    WGS 1984.
- L(2) = 2    Bessel spheroid.
- L(2) = 3    Clarke 1858 spheroid.
- L(2) = 4    Clarke 1866 spheroid.
- L(2) = 5    Clarke 1880 spheroid.
- L(2) = 6    Everest spheroid.
- L(2) = 7    Fischer spheroid.
- L(2) = 8    International spheroid.
- L(2) = 9    WGS 1972 spheroid.

DEL - Coding delay array, in microseconds:

- DEL(1)    Coding delay for first rate.
- DEL(2)    Coding delay for second rate.

TD - Time difference array, in microseconds:

- TD(1)    Time difference for first rate.
- TD(2)    Time difference for second rate.

ISYS - Loran system array:

- ISYS(1)    Loran system for first rate.  
ISYS(1) = A: Loran A  
ISYS(1) = c: Loran C
- ISYS(2)    Loran system for second rate.  
ISYS(2) = A: Loran A  
ISYS(2) = c: Loran C

BETA - Baseline delay array:

- BETA(1) Baseline delay for first rate.
- BETA(2) Baseline array for second rate.

BLN - Minimum time difference array, in microseconds:

- BLN(1) Minimum time difference for first rate.
- BLN(2) Minimum time difference for second rate.

BLEM - Maximum time difference array, in microseconds:

- BLEM(1) Maximum time difference for first rate.
- BLEM(2) Maximum time difference for second rate.

ISENT - Sentinel for DR position:

- ISENT = 0 DR position not given.
- ISENT = 1 DR position given.

ISW Operation code:

- ISW = 1 Forward computation.
- ISW = 2 Inverse computation.

IB - Switch for baseline computation:

- IB = 0 Baseline computation off.
- IB = 1 Baseline computation on.

IER - Error code:

- IER = 1 Invalid velocity of propagation code.
- IER = 2 Invalid spheroid code.
- IER = 3 Invalid configuration.
- IER = 4 Invalid operation code.
- IER = 5 Invalid readings.
- IER = 6 Invalid DR position.

IT - Iteration code.

IVEL - Velocity of propagation code array:

IVEL(1) - Velocity of propagation code for first rate:



- 0 = 299.6929 kilometers per microsecond
- 1 = 299.6911624 kilometers per microsecond
- 2 = 299.708 kilometers per microsecond

IVEL(2) - VElocity of propagation code for second rate:

- 0 = 299.6929 kilometers per microsecond
- 1 = 299.6911624 kilometers per microsecond
- 2 = 299.708 kilometers per microsecond

```

C          *****
C          * PROGRAM DRIVLR FORTRAN SOURCE CODE *
C          *****
C          DESCRIPTION OF PARAMETERS
C          DATA DECLARATION
C          IMPLICIT REAL*8(A-H,O-Z)
C          REAL*8 ALAT(5),ALON(5),DEL(2),TD(2),BETA(2),BLEN(2),BLEM(2),LN
C          CHARACTER*1 ISYS(2)
C          INTEGER H,M,L(2),IVEL(2),ISYS(2)
C          ALAT(1)=3600.0D0*39.0D0 + 33.0D0*60.0D0 + 6.740D0
C          ALAT(2)=3600.0D0*38.0D0 + 46.0D0*60.0D0 + 57.110D0
C          ALAT(3)=3600.0D0*39.0D0 + 33.0D0*60.0D0 + 6.740D0
C          ALAT(4)=3600.0D0*35.0D0 + 19.0D0*60.0D0 + 18.3050D0
C          ALAT(5)=3600.0D0*36.0D0 + 45.0D0*60.0D0 + 0.0D0
C          ALON(1)=3600.0D0*118.0D0 + 49.0D0*60.0D0 + 55.8160D0
C          ALON(2)=3600.0D0*122.0D0 + 29.0D0*60.0D0 + 43.9750D0
C          ALON(3)=3600.0D0*118.0D0 + 49.0D0*60.0D0 + 55.8160D0
C          ALON(4)=3600.0D0*114.0D0 + 48.0D0*60.0D0 + 16.8810D0
C          ALON(5)=3600.0D0*121.0D0 + 55.0D0*60.0D0 + 0.0D0
C          L(1) = 1
C          L(2) = 1
C          DEL(1) = 27000.0D0
C          DEL(2) = 40000.0D0
C          ISYS(1)=1
C          ISYS(2)=1
C          ISENT=1
C          ISW=2
C          IVEL(1)=1
C          IVEL(2)=1
C          IB=1
C          CALL LORAN (ALAT,ALON,L,DEL,TD,ISYS,BETA,BLEN,BLEM,ISENT,ISW,IB,
C          *IER,IT,IVEL)
C          DO 200 I=1,914
C          READ(7,10) H,M,S,TD(1),TD(2)
10  FORMAT(I2,1X,I2,1X,F5.2,21X,F8.2,1X,F8.2)
C          IER=0
C          CALL LORAN (ALAT,ALON,L,DEL,TD,ISYS,BETA,BLEN,BLEM,ISENT,ISW,IB,
C          *IER,IT,IVEL)
C          WRITE(9,20) I,H,M,S,ALAT(5),ALON(5),IT,IER
20  FORMAT(I3,1X,I2,1X,I2,1X,F5.2,2X,F10.2,2X,F10.2,2X,I2,2X,I1)
C          F=ALAT(5)/3600.0D0
C          LN=-ALON(5)/3600.0D0

```

```

WRITE(10,30) I,H,M,S,F,LN
30 FORMAT(I3,1X,I2,1X,I2,1X,F5.2,2X,F10.7,2X,F12.7)
   READ(8,40) F1, LNI
40 FORMAT(9X,F10.7,1X,F12.7)
   DF=F-F1
   DL=LN-LN1
   WRITE(6,*) DF,DL,LN1
200 CONTINUE
   STOP
   END
   SUBROUTINE LORAN ( ALAT,ALON,L,DEL,TD,ISYS,BETA,BLEN,BLEM,
*ISENT,ISW,IB,IER,IT,IVEL)

```

C  
C  
C

#### DATA DECLARATION

```

IMPLICIT REAL*8(A-H,O-Z)
INTEGER SOUTH,EAST,WEST

```

C  
C  
C

#### STORAGE ALLOCATION

```

DIMENSION DEL(2),TD(2),BETA(2),BLEN(2),BLEM(2),ISYS(2),H(2),R(2),
*IVEL(2),VELL(2),L(2)
DIMENSION VEL(3)
DIMENSION TEMP1(4),TEMP2(4)
DIMENSION ALAT(5),ALON(5)
DIMENSION A(9),B(9)
DATA A/ 6378137.0D0 , 6377397.1550D0 , 6378293.6450D0 ,
* 6378206.4000D0 , 6378249.1450D0,6377276.3450D0,6378166.0000D0,
*6378388.0000D0,6378135.0000D0/
DATA B/6356752.31420D0,6356078.9628D0,6356617.9376D0,
*6356583.8000D0,6356514.8695D0,6356075.4131D0,6356784.2836D0,
*6356911.9461D0,6356750.5200D0/
DATA A1/24.0305D0/,A2/-0.40758D0/,A3/0.00346776D0/
DATA B1/0.510483D0/,B2/-0.011402D0/,B3/0.001760D0/
DATA ARC1/0.484813681110D-5/
DATA LORANC/1/
DATA FAZ/0.0D0/,IK/0/,TEMP1/4*0.0D0/,TEMP2/4*0.0D0/
DATA ZERO/0.0D0/
DATA NORTH,SOUTH,EAST,WEST/1HN,1HS,1HE,1HW/
DATA MINUS/1H-/
DATA VEL/299.6929D0,299.6911624D0,299.708D0/
DATA BAZ/0.0D0/,JER/0/
DATA ALATS/0.0D0/,ALONS/0.0D0/,N/0/

```

C  
C  
C

#### INITIALIZE ERROR CODE

```

IER=0

```

C  
C  
C

#### TEST SWITCH FOR BASELINE COMPUTATION

```

IF (IB) 5,150,5

```

C  
C  
C  
C

#### BASELINE COMPUTATION

```

C      TEST FOR VALID VFLOCITY OF PROPAGATION CODE FOR BOTH CHAINS
C
5      DO 10 I=1,2
      IF (IVEL(I).GT.2) GO TO 15
10     CONTINUE
      GO TO 20
15     IER=1
      GO TO 320

C      DETERMINE VELOCITY OF PROPAGATION FOR BOTH CHAINS
C
20     DO 25 I=1,2
      IVEL(I)=IVEL(I)+1
      KK=IVEL(I)
25     VELL(I)=VEL(KK)
      A4A=VELL(1)
      A4B=VELL(2)

C      TEST FOR CHANGE IN SPHEROID CODE, FOR VALID SPHEROID CODE
C      AND DETERMINE APPROPRIATE SPHEROID COSTANTS
C
      DO 30 J=1,2
      IF (L(J).GE.1.AND.L(J).LE.9) GO TO 30
      GO TO 55
30     CONTINUE
      IF (L(1).EQ.L(2)) GO TO 35
      GO TO 55
35     K=L(1)
      IF (IK-K) 40,60,40
40     DO 50 I=1,9
      IF (I-K) 50,45,50
45     A5=A(I)
      A6=B(I)
      A55=A5*A5
      A10=(A55-A6*A6)/A55
      IK=K
      GO TO 60
50     CONTINUE
55     IER=2
      GO TO 320

C      TEST FOR CHANGE IN FIXED STATIONS
C
60     DO 80 I=1,4
      IF (TEMP1(I)-ALAT(I)) 70,65,70
65     IF (TEMP2(I)-ALON(I)) 70,80,70
70     DO 75 J=1,4
      TEMP1(J)=ALAT(J)
75     TEMP2(J)=ALON(J)
      GO TO 85
80     CONTINUE
      GO TO 145

C      TEST FOR TRIAD OR TETRAD CONFIGURATION AND ACTIVATE
C      APPROPRIATE SENTINEL
C

```

```

85  A12=ALAT(1)-ALAT(3)+ALON(1)-ALON(3)
    A12=DABS(A12)
    A13=ALAT(2)-ALAT(4)+ALON(2)-ALON(4)
    A13=DABS(A13)
    IF (A12-0.001D0) 90,90,105
90  IF (A13-0.001D0) 95,95,100
95  IER=3
    GO TO 320
100 A11=-1.0D0
    GO TO 110
105 A11=1.0D0
C
C      TEST FOR VALID OPERATION CODE
C
110 IF (ISW-1) 120,125,115
115 IF (ISW-2) 125,125,120
120 IER=4
    GO TO 320
C
C      COMPUTE GEODETIC DISTANCE AND SALT-WATER RETARDATION FROM
C      MASTER 1 STATION TO SLAVE 1 STATION
C
125 CALL SODIN (ALAT(1),ALON(1),ALAT(2),ALON(2),L,A35,FAZ,BAZ,JER)
    AA10=A35/A4A
    M=1
    I=1
    GO TO 295
130 AA11=A47
C
C      COMPUTE GEODETIC DISTANCE AND SALT-WATER RETARDATION FROM
C      MASTER 2 STATION TO SLAVE 2 STATION
C
    CALL SODIN (ALAT(3),ALON(3),ALAT(4),ALON(4),L,A35,FAZ,BAZ,JER)
    CC10=A35/A4B
    M=2
    I=2
    GO TO 295
135 CC11=A47
C
C      COMPUTATION OF BASELINE DATA
C
    BETA(1)=AA10+AA11
    BETA(2)=CC10+CC11
    DO 140 I=1,2
    BLEN(I)=DEL(I)
140 BLEM(I)=2.0D0*BETA(I)+DEL(I)
C
C      TURN SWITCH FOR BASELINE COMPUTATION OFF
C
145 IB=0
    RETURN
C
C      TEST SWITCH FOR FORWARD OR INVERSE COMPUTATION
C
150 GO TO (155,190),ISW
C
C      FORWARD COMPUTATION

```

```

C
C
C      COMPUTE GEODETIC DISTANCE AND SALT-WATER RETARDATION FROM
C      SHIP TO MASTER 1 STATION
C
155 CALL SODIN (ALAT(5),ALON(5),ALAT(1),ALON(1),L,A35,FAZ,BAZ,JER)
    A76=A35/A4A
    A72=A76
    M=1
    I=7
    GO TO 295
160 A77=A47
    A73=A77
C
C      COMPUTE GEODETIC DISTANCE AND SALT-WATER RETARDATION FROM
C      SHIP TO SLAVE 1 STATION
C
    CALL SODIN (ALAT(5),ALON(5),ALAT(2),ALON(2),L,A35,FAZ,BAZ,JER)
    A74=A35/A4A
    M=1
    I=8
    GO TO 295
165 A75=A47
C
C      COMPUTE GEODETIC DISTANCE AND SALT-WATER RETARDATION FROM
C      SHIP TO SLAVE 2 STATION
C
    CALL SODIN (ALAT(5),ALON(5),ALAT(4),ALON(4),L,A35,FAZ,BAZ,JER)
    A70=A35/A4B
    M=2
    I=9
    GO TO 295
170 A71=A47
C
C      COMPUTE GEODETIC AND SALT-WATER RETARDATION FROM
C      SHIP TO MASTER 2 STATION
C
    IF (A11) 185,175,175
175 CALL SODIN (ALAT(5),ALON(5),ALAT(3),ALON(3),L,A35,FAZ,BAZ,JER)
    A72=A35/A4B
    M=2
    I=10
    GO TO 295
180 A73=A47
C
C      COMPUTE LORAN TIME DIFFERENCES OF FIX
C
185 TD(1)=AA10+AA11+A74+A75-A76-A77+DEL(1)
    TD(2)=CC10+CC11+A70+A71-A72-A73+DEL(2)
    RETURN
C
C      INVERSE COMPUTATION
C
C      STORE DR POSITION OF SHIP
C

```

```

190 ALATDR=ALAT(5)
   ALONDR=ALON(5)
C
C     TEST FOR VALID MICROSECOND READINGS
C
DO 195 I=1,2
  IF (TD(I).LE. BLEM(I).AND. TD(I).GE. BLEN(I)) GO TO 195
  IER=5
  GO TO 320
195 CONTINUE
C
C     CONVERT SHIPS POSITION TO RADIANs
C
  IF (ISENT) 205,205,200
200 ALATR=ALAT(5)*ARC1
   ALONR=ALON(5)*ARC1
C
C     INITIALIZE IETRATION COUNTER
C
205 IT=0
   GO TO 215
C
C     TEST ITERATION COUNTER
C
210 IF (IT.LT.30) GO TO 215
   IER=6
   GO TO 320
C
C     COMPUTE SINES AND COSINES OF SHIPS POSITION
C
215 SINS=DSIN(ALATR)
   COSS=DCOS(ALATR)
C
C     COMPUTE GEODETIC DISTANCE, SIN AND COSINE OF AZIMUTH, AND
C     SALT-WATER RETARDATION FROM SHIP TO SLAVE 2 STATION
C
  CALL SODIN (ALAT(5),ALON(5),ALAT(4),ALON(4),L,A35,FAZ,BAZ,JER)
  M=2
  I=3
  GO TO 280
220 C1=A35
   D1=C1/A4B
   C2=DSIN(FAZ)
   C3=DCOS(FAZ)
   C101=A47
C
C     COMPUTE GEODETIC DISTANCE, SIN AND COSINE OF AZIMUTH, AND
C     SALT-WATER RETARDATION FROM SHIP TO MASTER 2 STATION
C
  CALL SODIN (ALAT(5),ALON(5),ALAT(3),ALON(3),L,A35,FAZ,BAZ,JER)
  M=2
  I=4
  GO TO 280
225 C4=A35
   D4=C4/A4B
   C5=DSIN(FAZ)

```

```

C6=DCOS(FAZ)
C104=A47

C
C      COMPUTE GEODETIC DISTANCE, SIN AND COSINE OF AZIMUTH, AND
C      SALT-WATER RETARDATION FROM SHIP TO SLAVE 1 STATION
C

CALL SODIN (ALAT(5),ALON(5),ALAT(2),ALON(2),L,A35,FAZ,BAZ,JER)
M=1
I=5
GO TO 280
230 C7=A35
E7=C7/A4A
C8=DSIN(FAZ)
C9=DCOS(FAZ)
C107=A47
IF (A11) 245,235,235

C
C      COMPUTE GEODETIC DISTANCE, SIN AND COSINE OF AZIMUTH, AND
C      SALT-WATER RETARDATION FROM SHIP TO MASTER 1 STATION
C      (FOR TETRAD CONFIGURATIONS ONLY)
C

235 C10=C7
C11=C8
C12=C9
CALL SODIN (ALAT(5),ALON(5),ALAT(1),ALON(1),L,A35,FAZ,BAZ,JER)
M=1
I=6
GO TO 280
240 C7=A35
D7=C7/A4A
C8=DSIN(FAZ)
C9=DCOS(FAZ)
C108=A47

C
C      DETERMINATION OF TIME DIFFERENCE COSTANTS AND DIFFERENTIAL
C      CORRECTIONS IN Y AND X
C      (FOR TETRAD CINFIGURATIONS ONLY)
C

C13=TD(2)-CC10-CC11-C101+C104-DEL(2)
C17=C13*A4B
C18=TD(1)-AA10-AA11-C107+C108-DEL(1)
C22=C18*A4A
C23=C1-C17
C24=C4
C25=C7+C22
C26=C10
C27=((C2-C5)*(C25-C26)*(C23-C24)*(C11-C8))
C29=((C2-C5)*(C12-C9)*(C3-C6)*(C8-C11))
C30=C27/C29
C28=(C23-C24+C30*(C3-C6))/(C5-C2)
GO TO 250

C
C      DETERMINATION OF TIME DIFFERENCE COSTANTS AND DIFFERENTIAL
C      CORRECTIONS IN Y AND X
C      (FOR TRIAD CINFIGURATIONS ONLY)
C

```

```

245 C13=TD(2)-CC10-CC11-C101+C104-DEL(2)
    C17=C13*A4B
    C18=TD(1)-AA10-AA11-C107+C104-DEL(1)
    C22=C18*A4A
    C23=C1-C17
    C24=C4
    C25=C7-C22
    C27=C2*(C25-C24)+C23*(C5-C8)+C8*C24-C5*C25
    C29=C2*(C6-C9)+C3*(C8-C5)+C5*C9-C8*C6
    C30=C27/C29
    C28=(C23-C24+C30*(C3-C6))/(C5-C2)

```

```

C
C      DETRMINATION OF DIFFERENTIAL CORRECTIONS IN LATITUDE AND
C      LONGITUDE AND PRELIMINARY GEOGRAPHIC POSITION OF SHIP
C

```

```

250 C100=1.0D0-A10*SINS*SINS
    C102=DSQRT(C100)
    C32=A5/C102
    C31=C32*((1.0D0-A10)/C100)
    C33=C30/C31
    C34=(-C28/(C32*COSS))
    ALATR=ALATR+C33
    ALONR=ALONR+C34
    ALAT(5)=ALATR/ARC1
    ALON(5)=ALONR/ARC1
    WRITE(13,*) ALAT(5),ALON(5),'ALAT ALON FM LORAN'

```

```

C
C      TEST OF CONVERGENCE OF SOLUTION
C

```

```

    IF (A11) 260,255,255
255 H(1)=AA10+AA11+E7+C107-D7-C108+DEL(1)
    GO TO 265
260 H(1)=AA10+AA11+E7+C107-D4-C104+DEL(1)
265 H(2)=CC10+CC11+D1+C101-D4-C104+DEL(2)
    DO 270 I=1,2
270 R(I)=TD(I)-H(I)
    ANUM=DABS(R(1))+DABS(R(2))
    IF (ANUM.LT.0.0001D0) GO TO 275
    IT=IT+1
    GO TO 210
275 RETURN

```

```

C
C      CONVERSION OF AZIMUTHS FROM NORTH TO SOUTH ORIENTATION
C

```

```

280 IF (FAZ-648000.0D0) 285,285,290
285 FAZ=(FAZ+648000.0D0)*ARC1
    GO TO 295
290 FAZ=(FAZ-648000.0D0)*ARC1

```

```

C
C      FORWARD AND INVERSE COMPUTATION
C      OF SALT-WATER RETARDATION (FOR LORAN C ONLY)
C

```

```

295 IF (ISYS(M).EQ.LORANC) GO TO 300
    A47=0.0D0
    GO TO 315

```



```

300 A46=A35/1609.349D0
    IF (A46-100.0D0) 305,310,310
305 A47=(B1/A46)+B2+B3*A46
    GO TO 315
310 A47=(A1/A46)+A2+A3*A46
C
C     BRANCHING FOR QUANTITIES TO BE USED IN SOLUTION
C
315 GO TO (130,135,220,225,230,240,160,165,170,180),I
C
C     PRINT ROUTINE FOR INVALID DATA
C
320 IF (IER.LE.4) GO TO 340
    CALL ANGLE (N,ALONDR,ISGN,LOND,LONM,ALONS)
    CALL ANGLE (N,ALATDR,ISGM,LATD,LATM,ALATS)
    IF (ISGM.EQ.MINUS) GO TO 325
    KLA=NORTH
    GO TO 330
325 KLA=SOUTH
330 IF (ISGN.EQ.MINUS) GO TO 335
    KLO=WEST
    GO TO 340
335 KLO=EAST
340 GO TO (345,350,355,360,365,370),IER
345 PRINT 375
    RETURN
350 PRINT 380
    RETURN
355 PRINT 385
    RETURN
360 PRINT 390
    RETURN
365 PRINT 395,LATD,LATM,KLA,LOND,LONM,KLO,TD(1),TD(2)
    RETURN
370 PRINT 400,LATD,LATM,KLA,LOND,LONM,KLO,TD(1),TD(2)
    RETURN
C
C     FORMAT STATEMENTS
C
375 FORMAT(1H1,1X,'INVALID VELOCITY OF PROPAGATION CODE, DATA NOT PROC
*ESSED')
380 FORMAT(1H1,1X,'INVALID SPHEROID CODE,DATA NOT PROCESSED')
385 FORMAT(1H1,1X,'INVALID CONFIGURATION, DATA NOT PROCESSED')
390 FORMAT(1H1,1X,'INVALID OPERATION CODE, DATA NOT PROCESSED')
395 FORMAT(18X,2I3,A1,6X,I4,I3,A1,16X,F9.2,13X,F9.2,3X,'INVALID READIN
*GS')
400 FORMAT(18X,2I3,A1,6X,I4,I3,A1,16X,F9.2,13X,F9.2,3X,'INVALID DR POS
*ITION')
    END
C
C
C     SUBROUTINE SODIN (ALAT1,ALON1,ALAT2,ALON2,L,S,FAZ,BAZ,IER)
C
C     IMPLICIT REAL*8(A-H,O-Z)
C
C     DIMENSION X(2),E(2),F(2),L(2)

```

```

DATA PI/3.14159265359D0/,ARC1/0.484813681110D-5/
DATA A,B/6378137.0D0,6356752.3142D0/

C
C
C   INITIALIZE ERROR CODE AND DETERMINE COSTANTS

A14=1.0D0-(B/A)
A56=A14*A14
A50=1.0D0+A14+A56
A51=A50-1.0D0
A52=A56/2.0D0
A53=-A51/2.0D0
A54=A56/16.0D0
A55=A56/8.0D0
A57=A56*1.25D0
A58=A56/4.0D0

C
C
C   TEST FOR IDENTICAL STATIONS

30 IF(ALAT1-ALAT2) 45,35,45
35 IF(ALON1-ALON2) 45,40,45
40 IER=2
   GO TO 255

C
C
C   COMPUTATION OF PARAMETRIC LATITUDE OF STATIONS

45 X1=ALAT1*ARC1
   Y1=ALON1*ARC1
   X2=ALAT2*ARC1
   Y2=ALON2*ARC1
   X(1)=X1
   X(2)=X2
   DO 50 I=1,2
     BETA=DATAN((1.0D0-A14)*DSIN(X(I))/DCOS(X(I)))
     E(I)=DSIN(BETA)
50  F(I)=DCOS(BETA)

C
C
C   COMPUTATION OF SPHERICAL DIFFERENCE OF LONGITUDES

A59=-Y2
A60=-Y1
C35=A59-A60
C36=DABS(C35)
IF(C36-PI) 60,55,55
55 A16=2.0D0*PI-C36
   GO TO 65
60 A16=C36
65 IF(A16) 75,70,75
70 A16=0.5D-7

C
C
C   COMPUTATION OF GEODETIC DISTANCE

75 A17=DSIN(A16)
   A18=DCOS(A16)
   A19=E(1)*E(2)
   A20=F(1)*F(2)
   A21=A19+A20*A18

```

```

A80=A17*F(2)
A81=A80*A80
A82=E(2)*F(1)-E(1)*F(2)*A18
A83=A82*A82
A84=A81+A83
A22=DSQRT(A84)
A23=(A20*A17)/A22
A24=1.0D0-A23*A23
A90=A22/A21
A25=DATAN(A90)
IF(A25) 80,85,85
80 A25=(PI/2.0D0)+A25
85 A26=A25*A25
A27=1.0D0/A22
A91=A21/A22
A29=A24*A24
A30=(A50*A25)+A19*(A51*A22-A52*A26*A27)
A31=A24*(A53*A25+A53*A22*A21+A52*A26*A91)
A32=A19*A19*(-A52*A21*A22)
A33=A29*(A54*A25+A54*A22*A21-A52*A26*A91-A55*A22*A21**3)
A34=A19*A24*(A52*A26*A27+A52*A22*A21*A21)
S=(A30+A31+A32+A33+A34)*B

C
C
C COMPUTATION OF DIFFERENCE OF LONGITUDE ON THE REDUCED SPHERE

A36=(A51*A25)+A19*(-A52*A22-A56*A26*A27)
A37=A24*(-A57*A25+A58*A22*A21+A56*A26*A91)
A38=(A36+A37)*A23+A16

C
C
C COMPUTATION OF GEODETIC FORWARD AZIMUTH

A39=DSIN(A38)
A40=DCOS(A38)
A41=(E(2)*F(1)-A40*E(1)*F(2))/(A39*F(2))
IF(A41) 95,90,95
90 A41=0.5D0-7
95 A42=1.0D0/A41
A43=DATAN(A42)
IF(C35) 120,100,100
100 IF(C35-PI) 105,115,115
105 IF(A41) 110,140,140
110 A43=PI+A43
GO TO 140
115 IF(A41) 130,135,135
120 IF(C35+PI) 105,105,125
125 IF(A41) 130,135,135
130 A43=PI-A43
GO TO 140
135 A43=2.0D0*PI-A43
140 A43=A43+PI
A43=A43-2.0D0*PI
IF(A43) 145,150,150
145 A43=A43+2.0D0*PI
150 FAZ=A43/ARC1
FAZ=FAZ+648000.0D0
IF(FAZ-1296000.0D0) 160,155,155

```

```

155 FAZ=FAZ-1296000.0D0
C
C   COMPUTATION OF BACK AZIMUTH NOT INCLUDED IN THIS VERSION
C
160 BAZ=0.0D0
    RETURN
C
C   PRINT ROUTINE FOR INVALID DATA
C
255 PRINT 270
    CALL ANGLE(3,ALAT1,ISGN1,LAT1D,LAT1M,ALAT1S)
    CALL ANGLE(3,ALON1,ISGN2,LON1D,LON1M,ALON1S)
    CALL ANGLE(3,ALAT2,ISGN3,LAT2D,LAT2M,ALAT2S)
    CALL ANGLE(3,ALON2,ISGN4,LON2D,LON2M,ALON2S)
265 PRINT 280,ISGN1,LAT1D,LAT1M,ALAT1S,ISGN2,LON1D,LON1M,ALON1S,ISGN3,
    *LAT2D,LAT2M,ALAT2S,ISGN4,LON2D,LON2M,ALON2S
    RETURN
C
C   FORMAT STATEMENTS
270 FORMAT(1H1,51X,'SUBROUTINE SODIN INVALID DATA'/)
280 FORMAT(1X,4(2X,A1,2I3,F7.3),2X,I2,2X,'IDENTICAL STATIONS')
    END
C
C
    SUBROUTINE ANGLE (N,ARGS,ISIGN,IDEG,MIN,SEC)
C
C
    IMPLICIT REAL*8(A-H,O-Z)
    DIMENSION ASEC(6)
    DATA ASEC/59.45D0,59.945D0,59.9945D0,59.99945D0,59.999945D0,
    *59.9999945D0/
    DATA MINUS/1H-/,IBLANK/1H /
C
C   ANGLE CONVERSION
C
    IF (ARGS) 10,5,5
5    ISIGN=IBLANK
    BRGS=ARGS
    GO TO 15
10   ISIGN=MINUS
    BRGS=-ARGS
15   IDEG=BRGS/3600.0D0
    ARGT=IDEG*3600
    AMIN=BRGS-ARGT
    MIN=AMIN/60.0D0
    AMINT=MIN*60
    SEC=AMIN-AMINT
    M=N+1
    IF (SEC-ASEC(M)) 30,20,20
20   SEC=0.0D0
    MIN=MIN+1
    IF (MIN-60) 30,25,25
25   MIN=0
    IDEG=IDEG+1
30   RETURN
    END

```

**APPENDIX D. TABLE FOR STANDARD DEVIATIONS AND  
COVARIANCES OF VELOCITY COMPONENTS FOR MINI RANGER**

TIME IN- TERVAL	$\sigma_v$	$\sigma_u$	$\sigma_{v,u}$
3 MIN	1.3 cm/sec	1.3 cm/sec	0.1234 $cm^2/sec^2$
6 MIN	0.64 cm/sec	0.64 cm/sec	0.0386 $cm^2/sec^2$
12 MIN	0.32 cm/sec	0.32 cm/sec	0.0116 $cm^2/sec^2$
20 MIN	0.19 cm/sec	0.19 cm/sec	$10^{-1} \times 0.0486 cm^2/sec^2$
40 MIN	$10^{-3} \times 0.98 cm/sec$	$10^{-3} \times 0.97 cm/sec$	$10^{-2} \times 0.17 cm^2/sec^2$
60 MIN	$10^{-3} \times 0.67 cm/sec$	$10^{-3} \times 0.66 cm/sec$	$10^{-2} \times 0.1080 cm^2/sec^2$

## APPENDIX E. AVERAGE CURRENT PROFILES

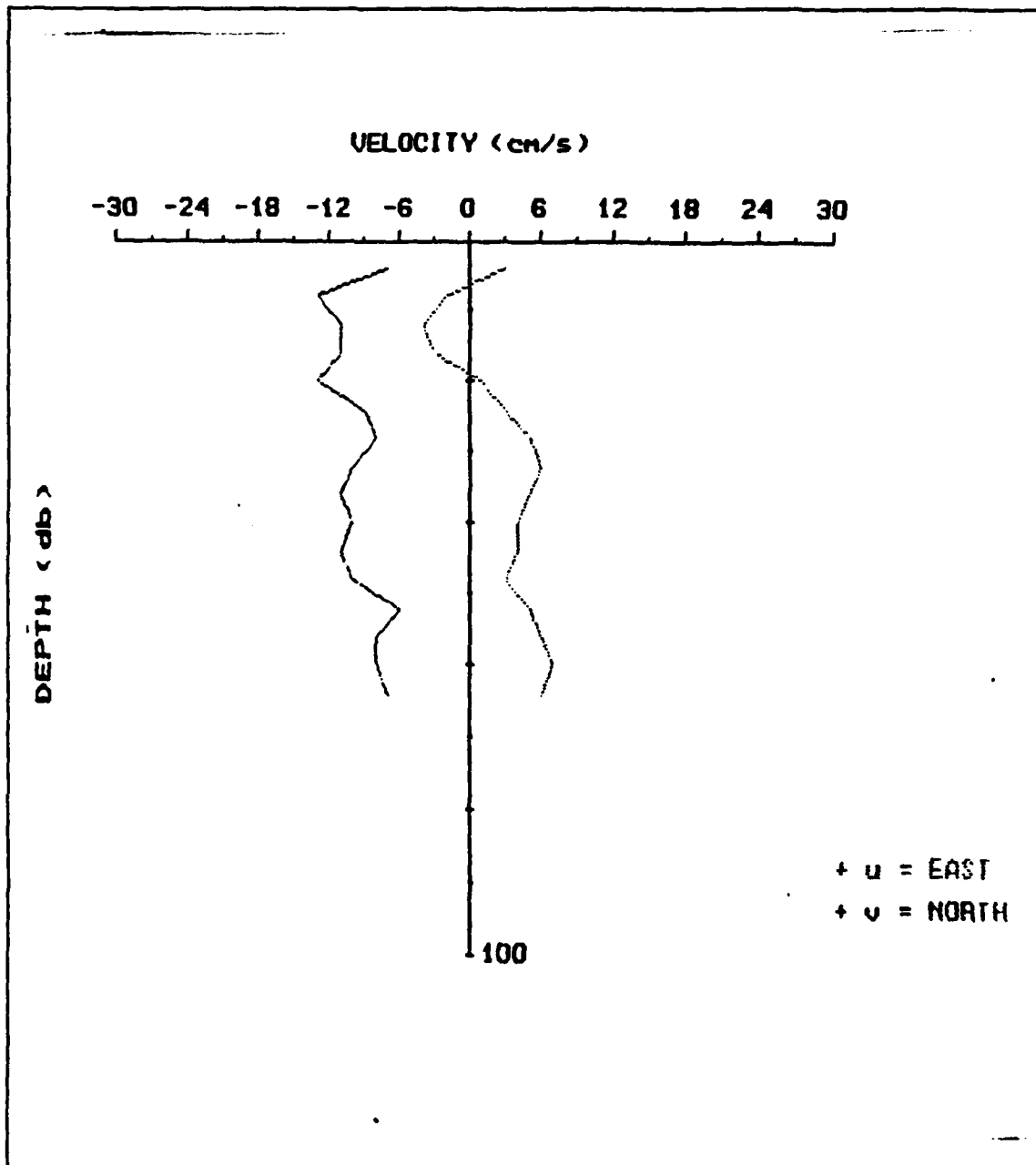


Figure 17. AVERAGE CURRENT PROFILE FROM POINT 1 TO POINT 3  
USING NAVIGATION DATA FROM MINI RANGER

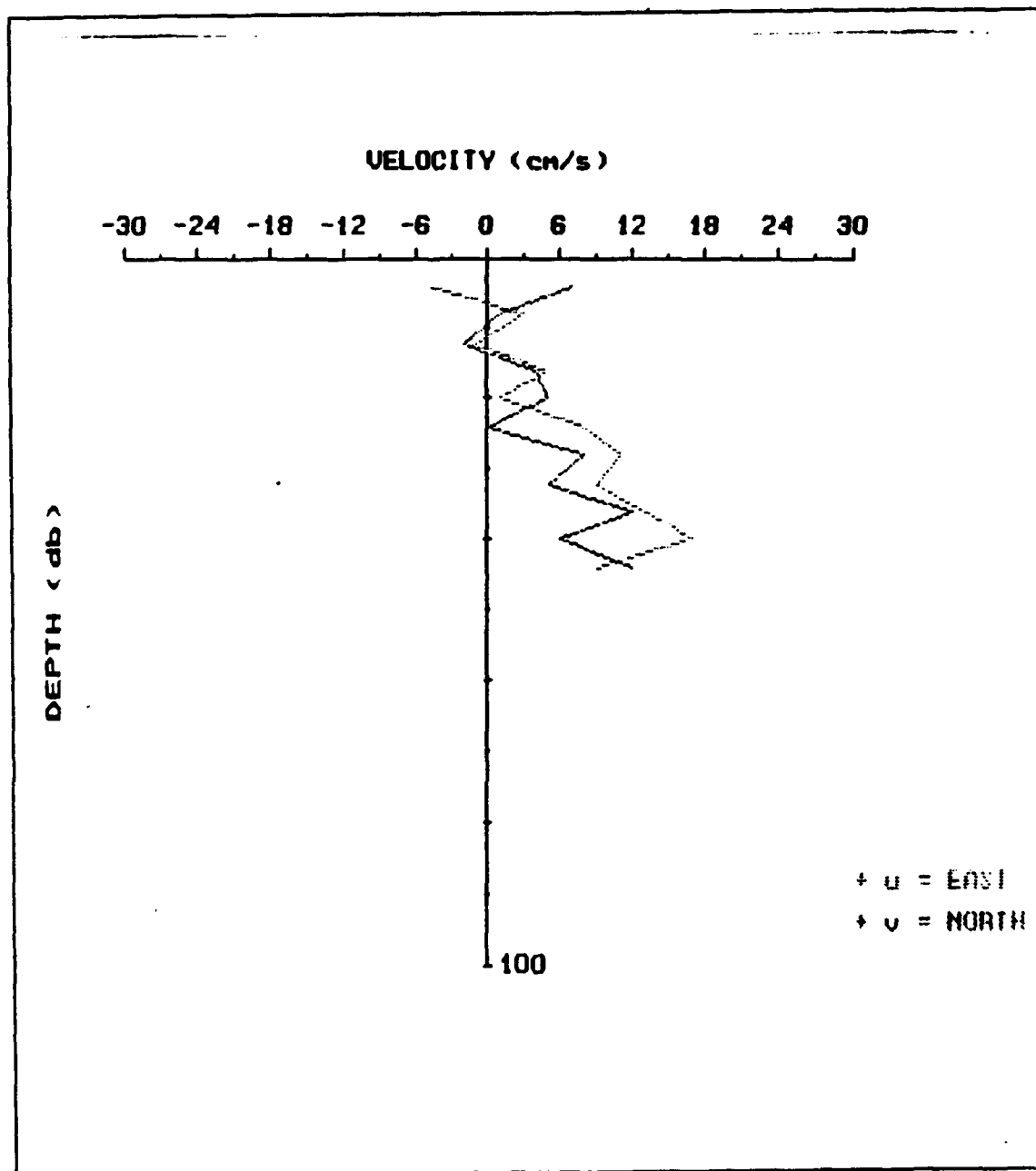


Figure 18. AVERAGE CURRENT PROFILE FROM POINT 3 TO POINT 2  
USING NAVIGATION DATA FROM MINI RANGER

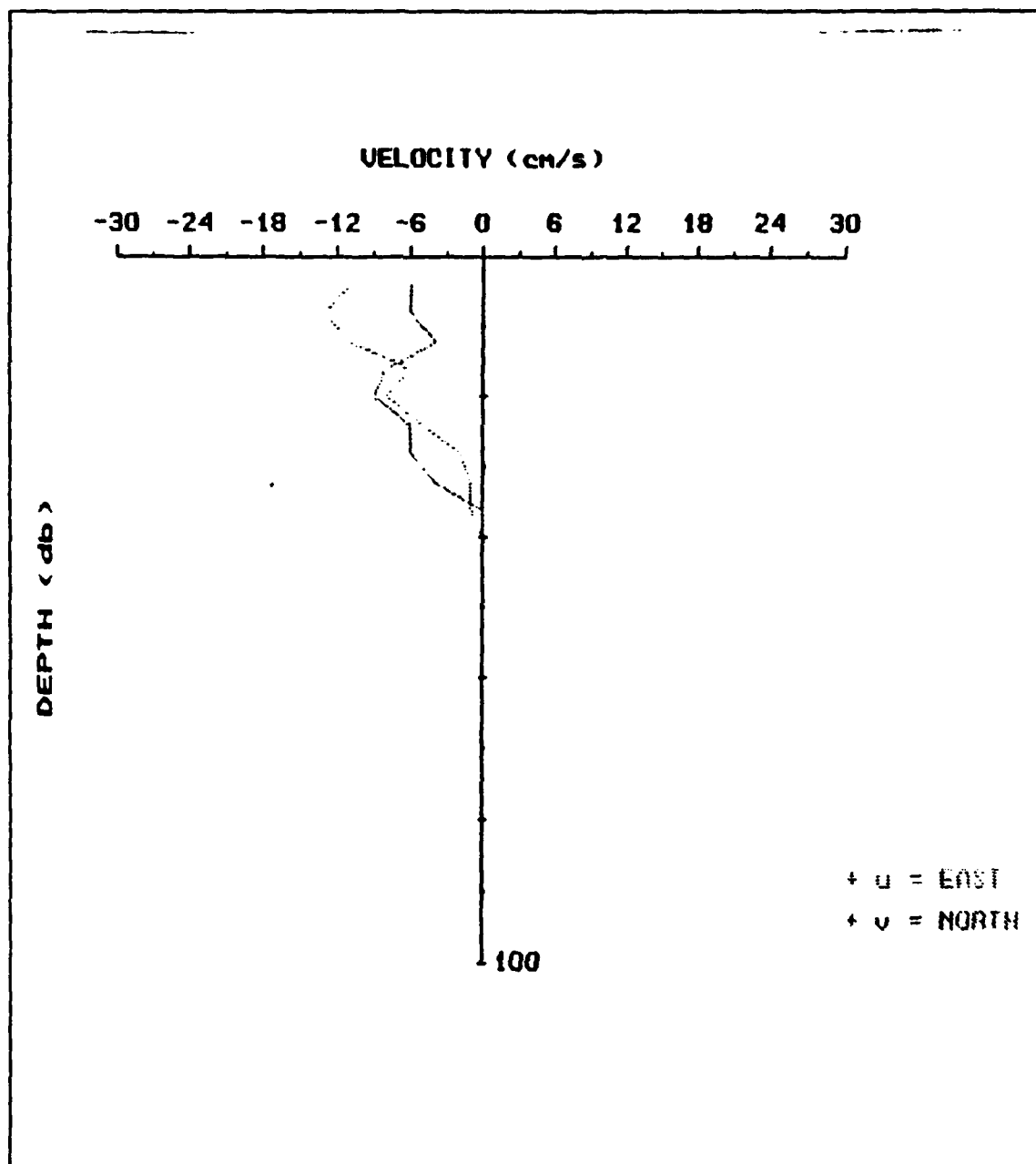


Figure 19. AVERAGE CURRENT PROFILE FROM POINT 2 TO POINT 3  
USING NAVIGATION DATA FROM MINI RANGER



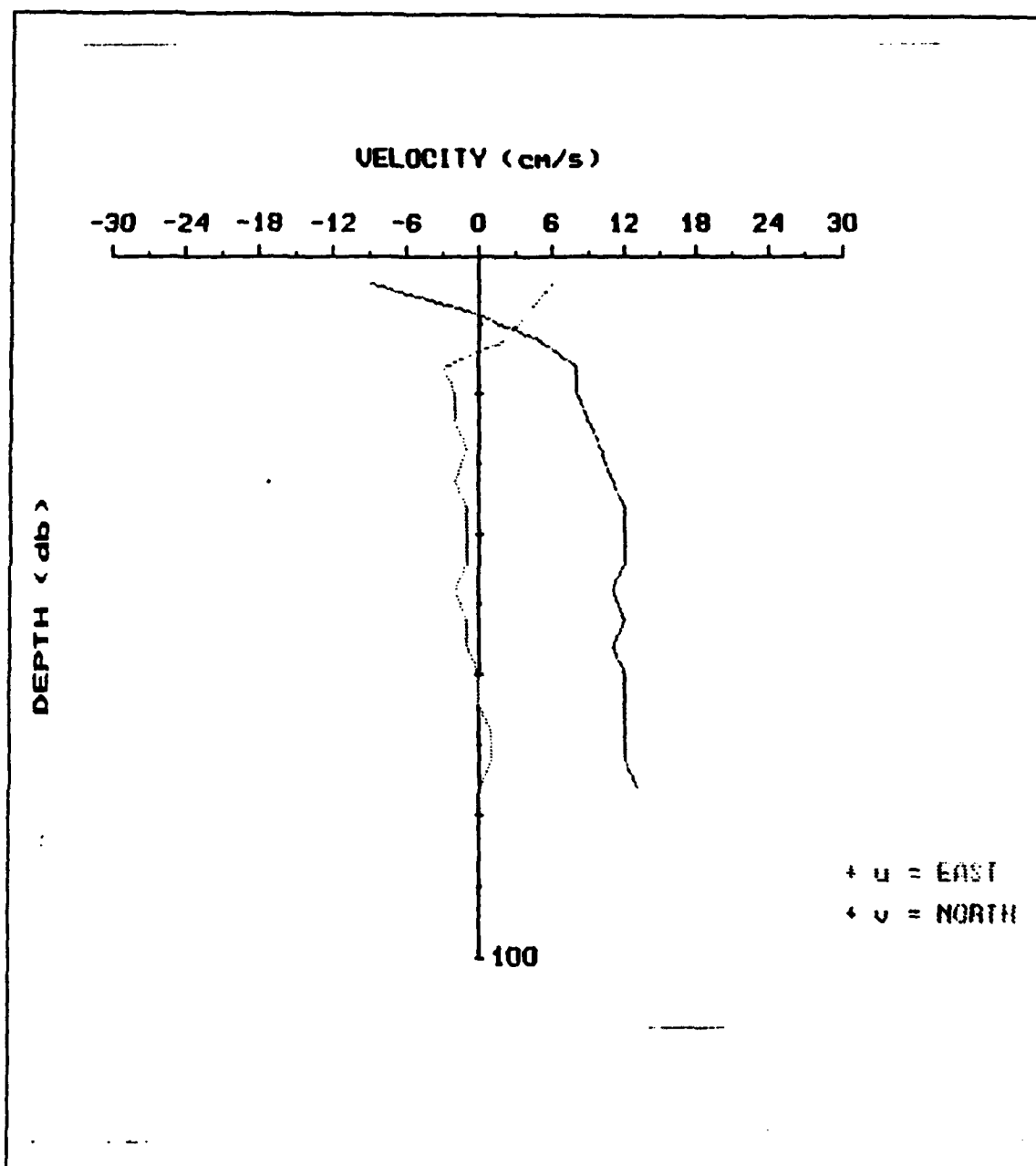


Figure 20. AVERAGE CURRENT PROFILE FROM POINT 3 TO POINT 4  
USING NAVIGATION DATA FROM MINI RANGER

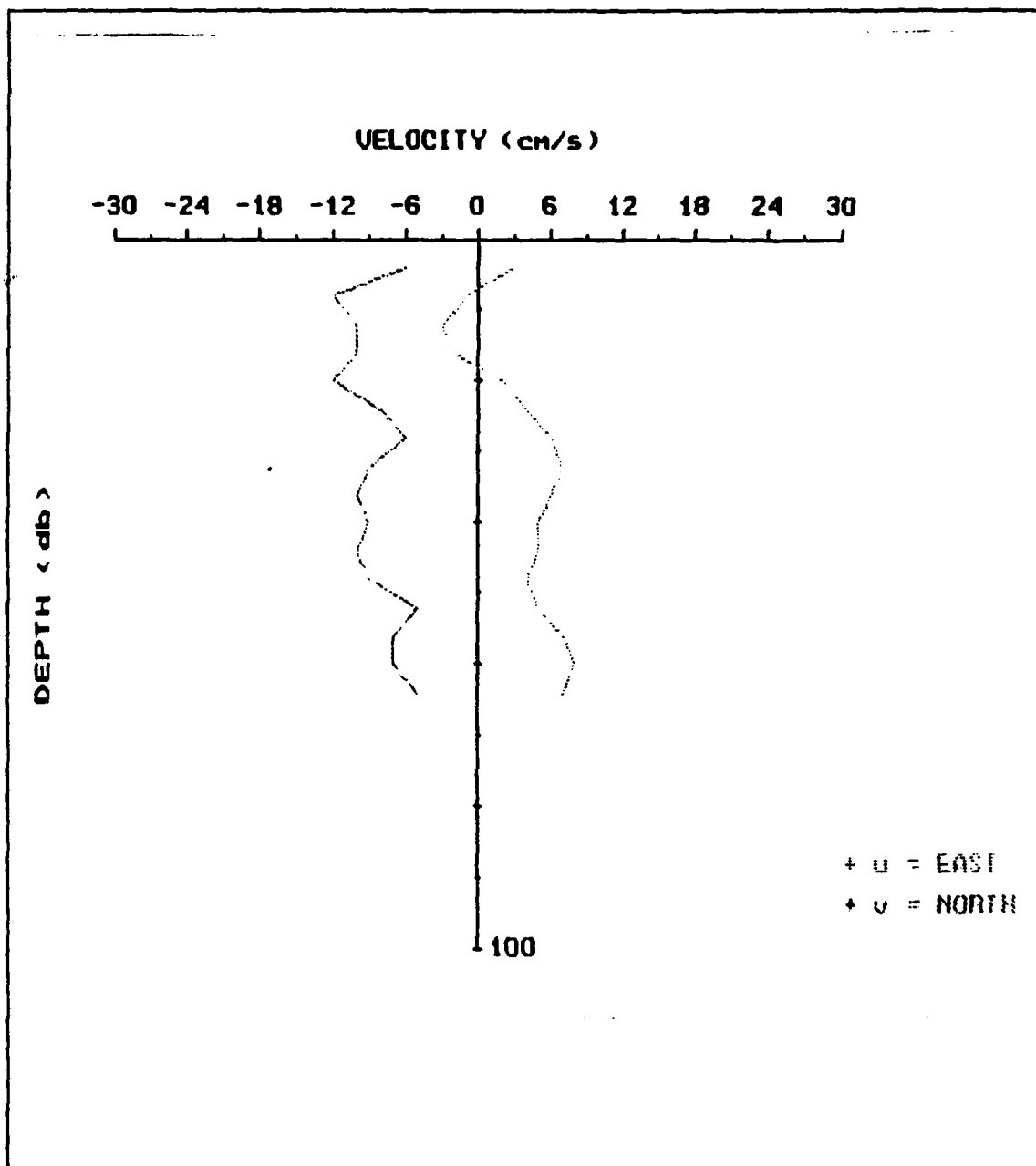


Figure 21. AVERAGE CURRENT PROFILE FROM POINT 1 TO POINT 3  
USING NAVIGATION DATA FROM LORAN (TD)

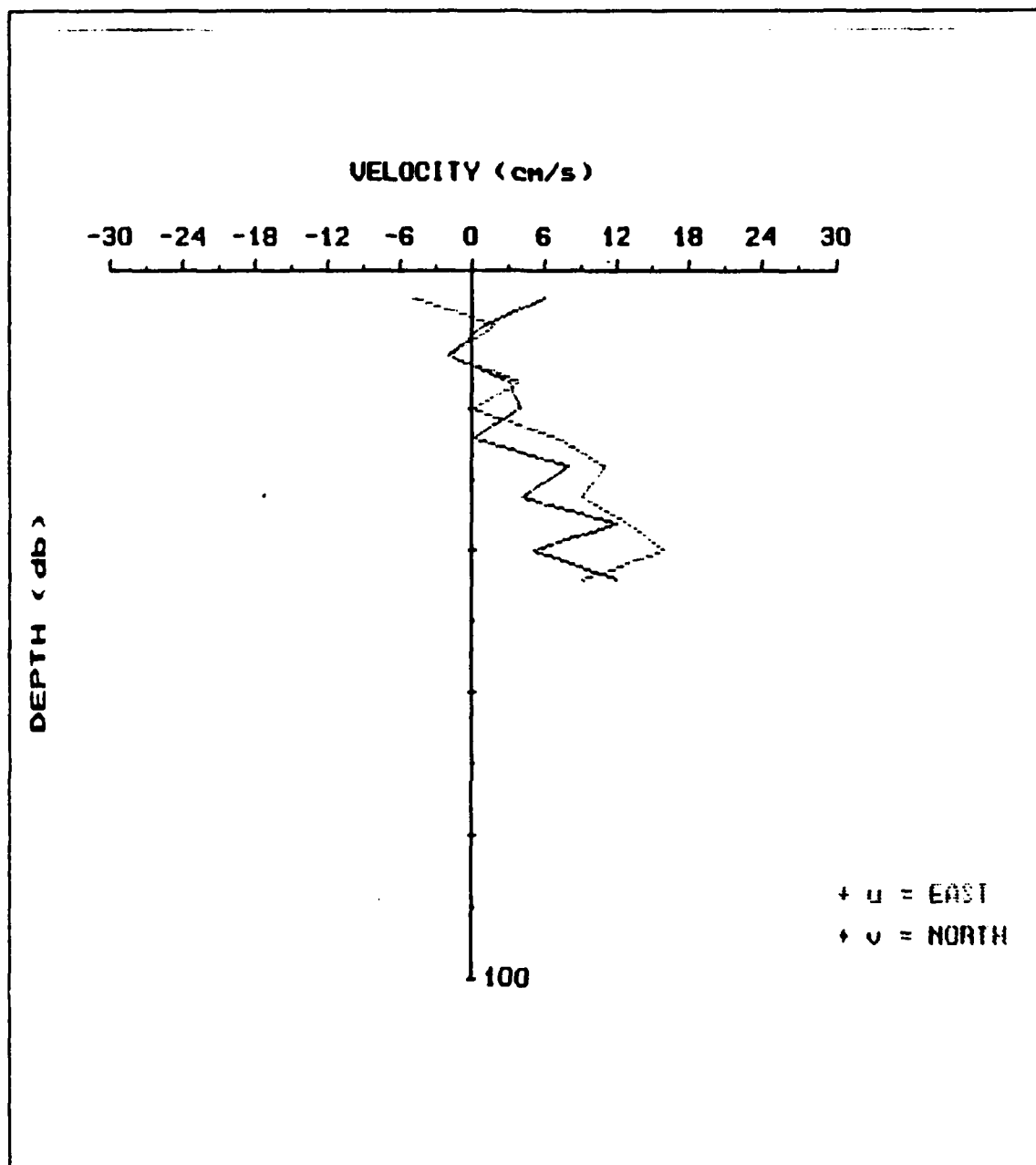


Figure 22. AVERAGE CURRENT PROFILE FROM POINT 3 TO POINT 2  
USING NAVIGATION DATA FROM LORAN (TD)

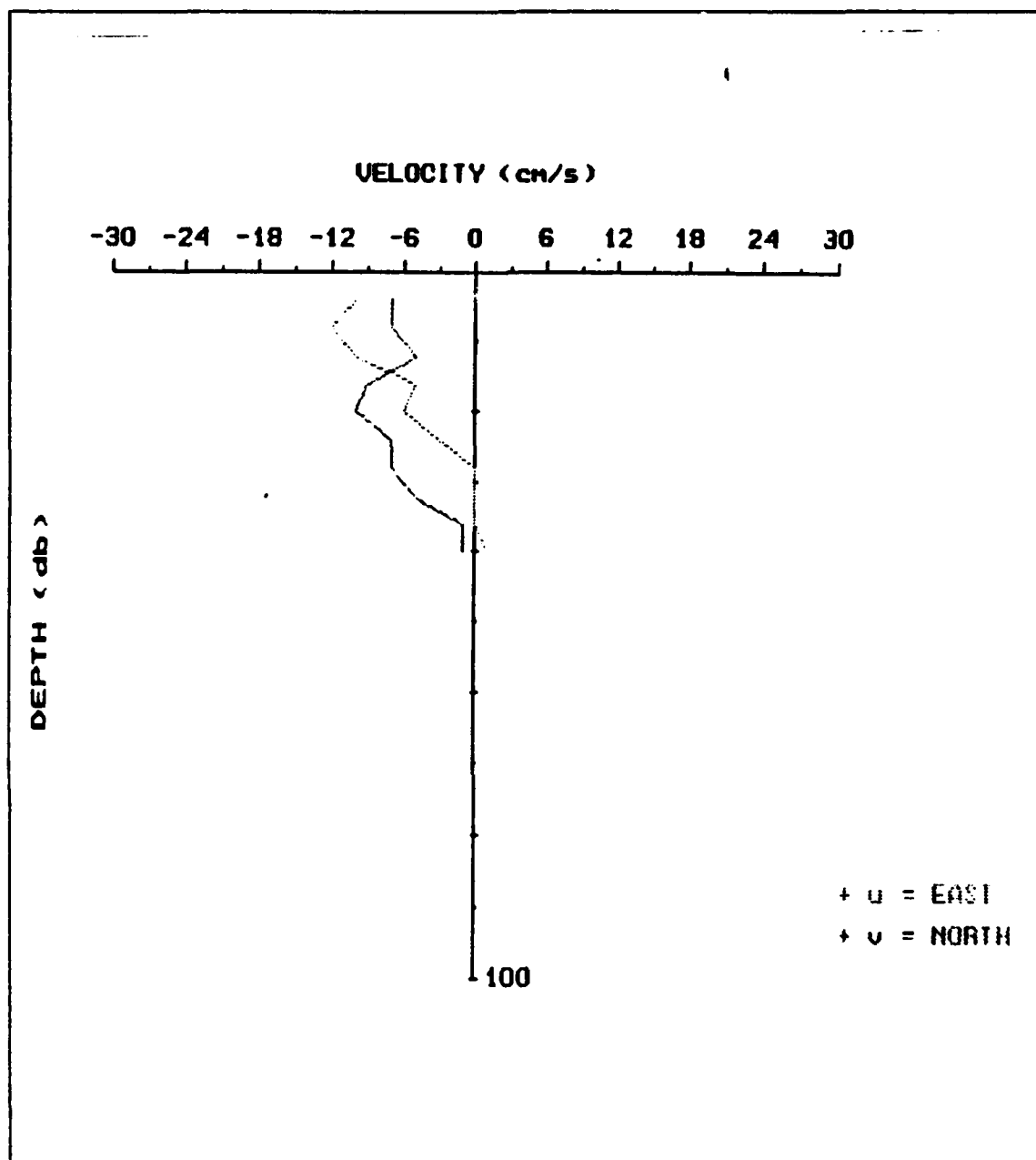


Figure 23. AVERAGE CURRENT PROFILE FROM POINT 2 TO POINT 3  
USING NAVIGATION DATA FROM LORAN (TD)

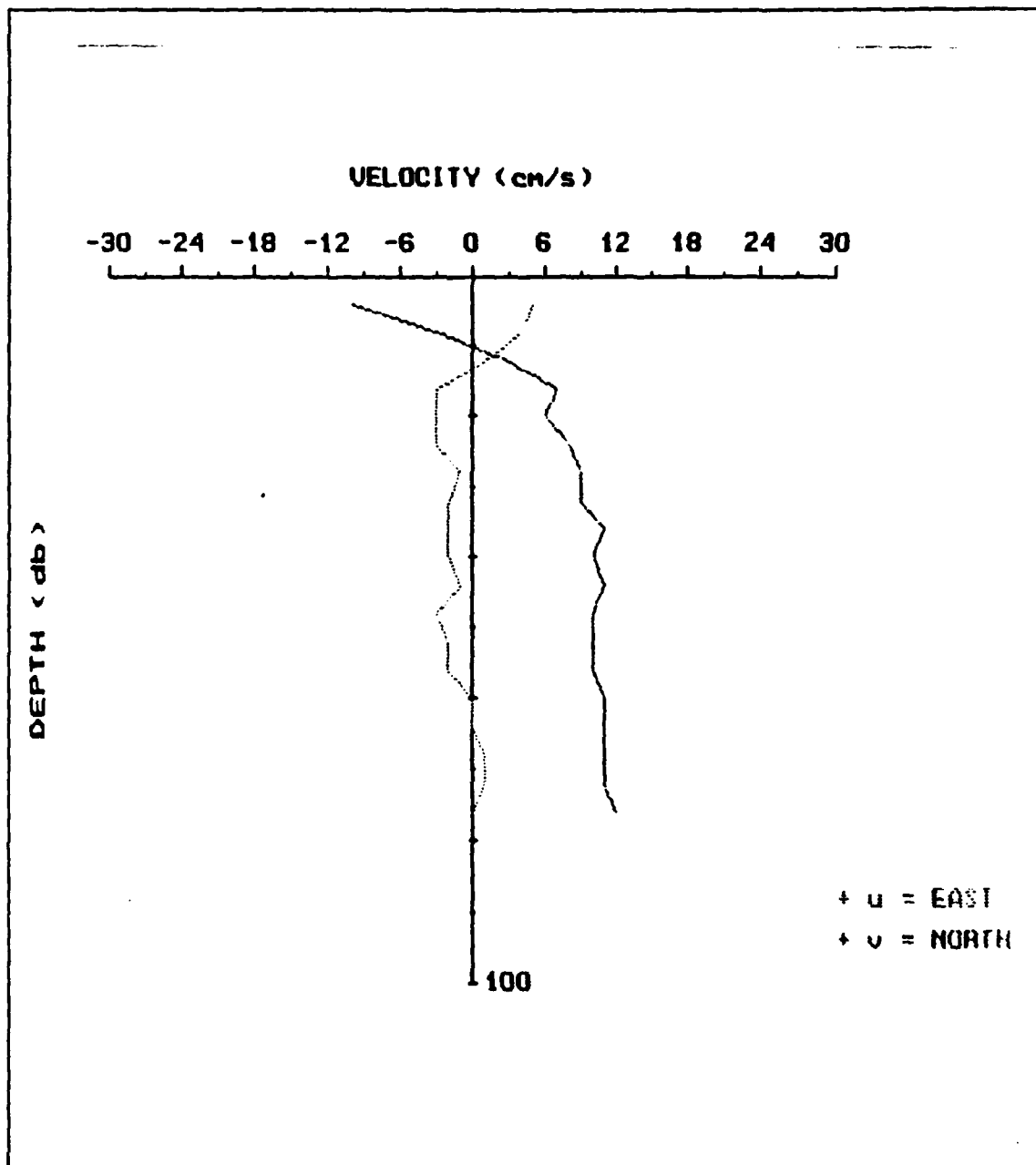


Figure 24. AVERAGE CURRENT PROFILE FROM POINT 3 TO POINT 4  
USING NAVIGATION DATA FROM LORAN (TD)

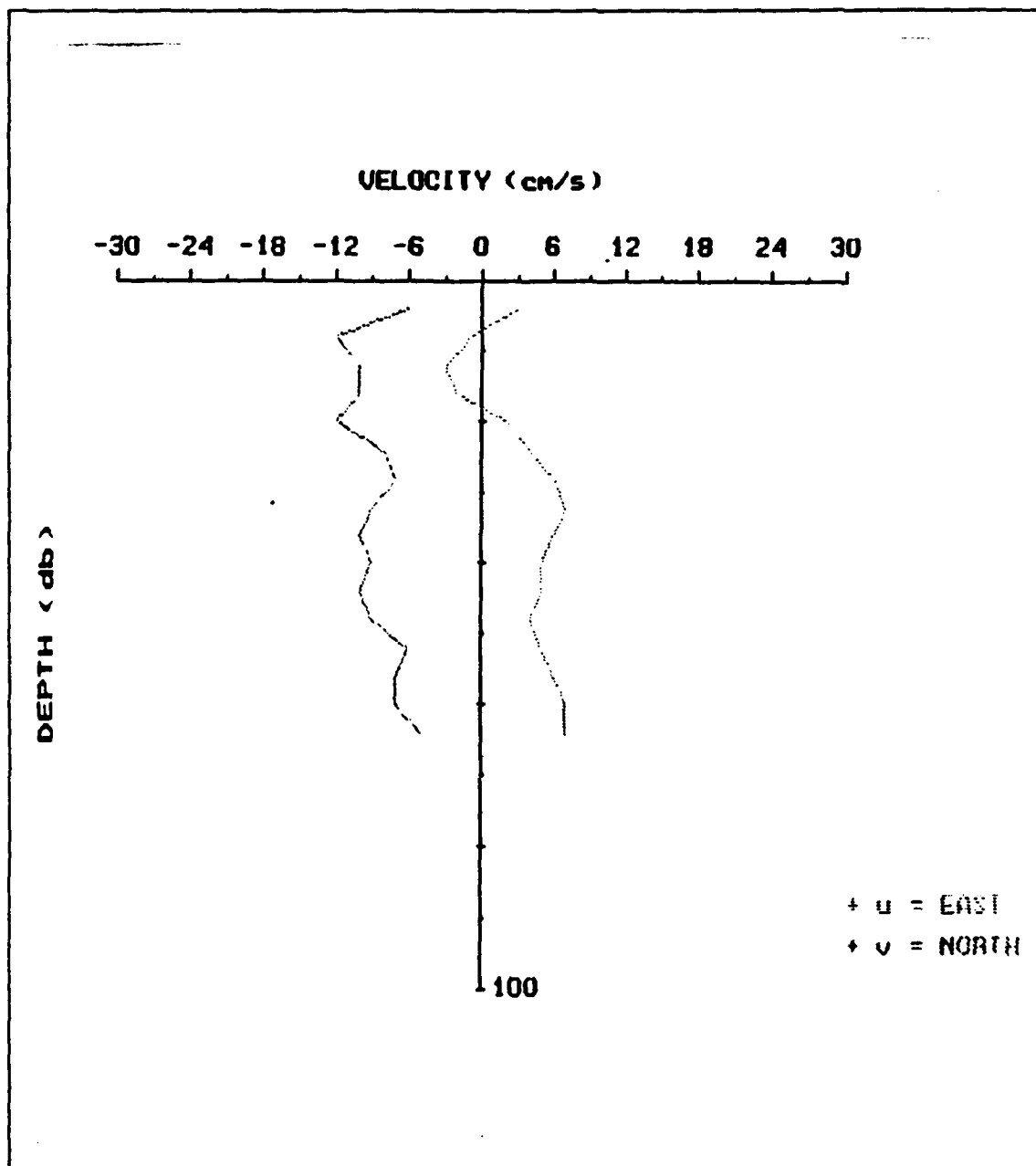


Figure 25. AVERAGE CURRENT PROFILE FROM POINT 1 TO POINT 3  
USING NAVIGATION DATA FROM LORAN (DISPLAY)

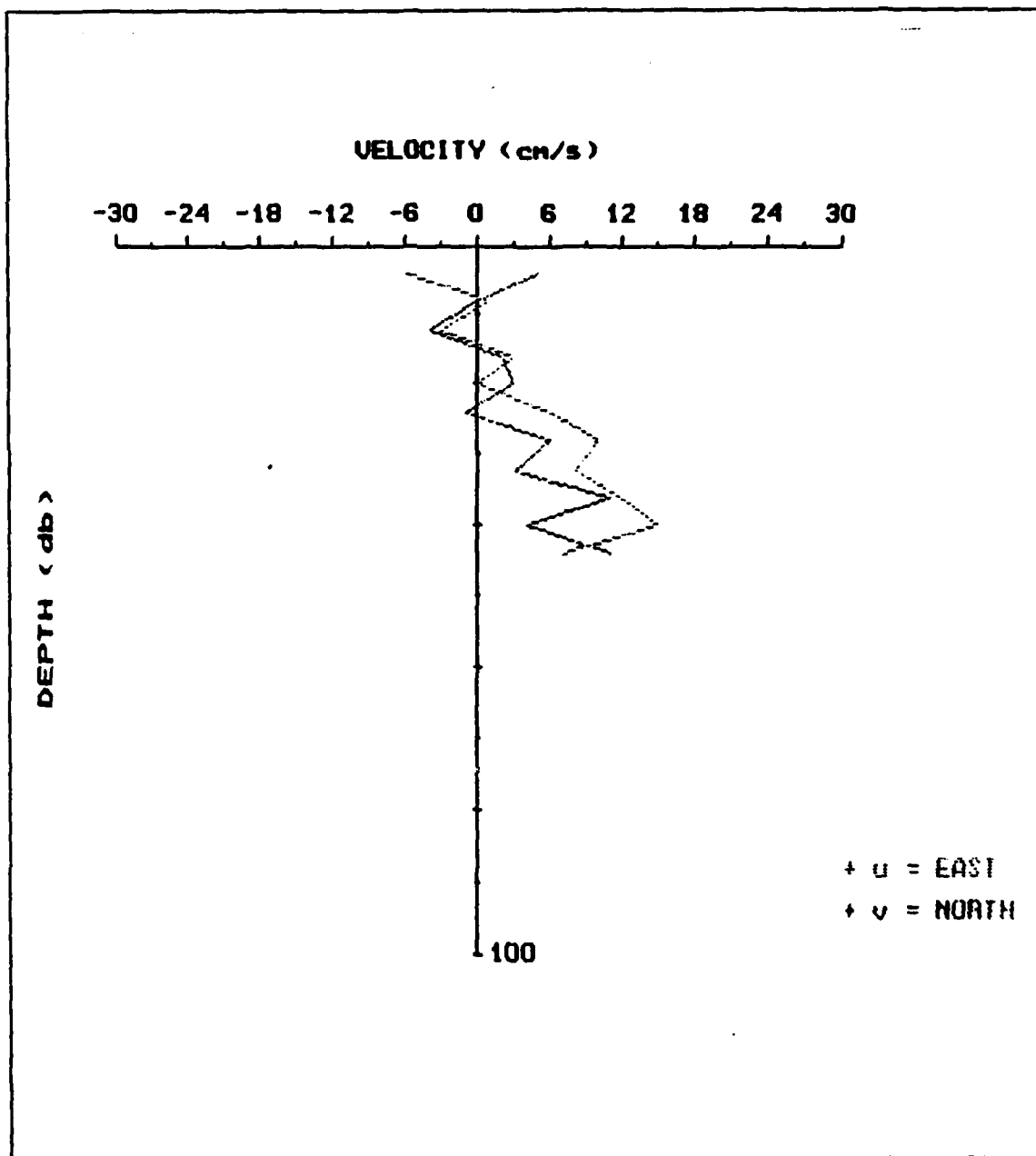


Figure 26. AVERAGE CURRENT PROFILE FROM POINT 3 TO POINT 2  
USING NAVIGATION DATA FROM LORAN (DISPLAY)

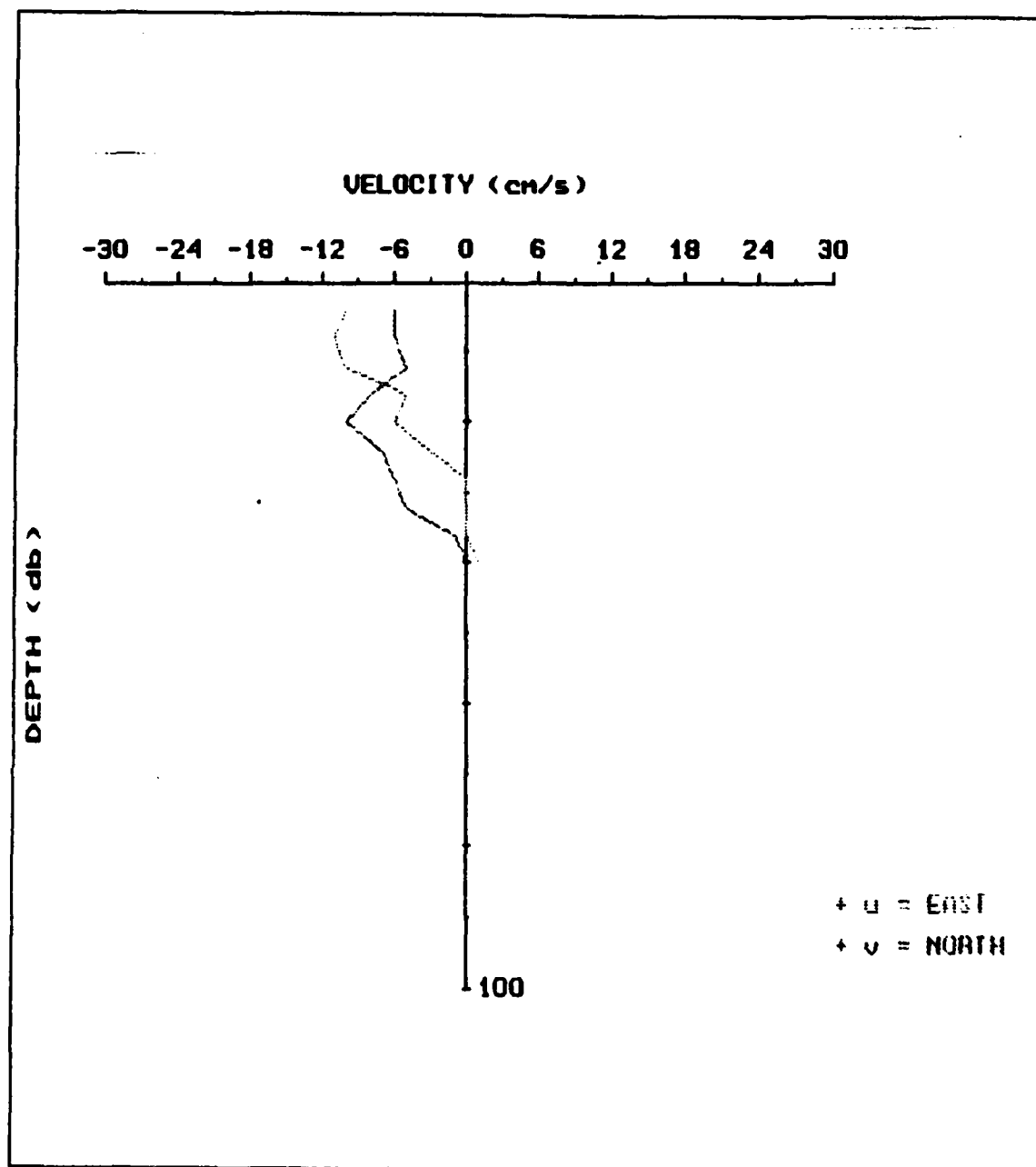


Figure 27. AVERAGE CURRENT PROFILE FROM POINT 2 TO POINT 3  
USING NAVIGATION DATA FROM LORAN (DISPLAY)



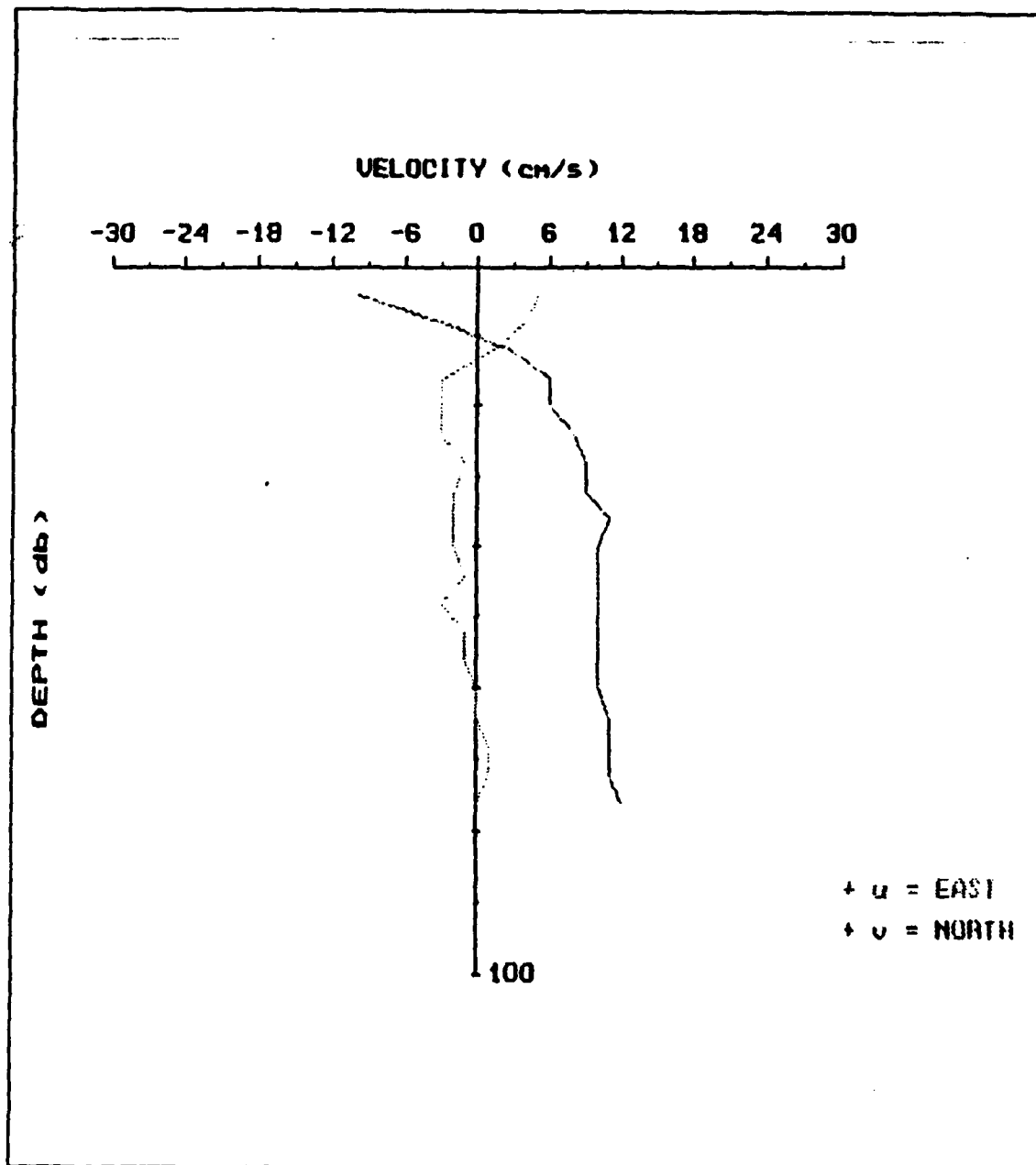


Figure 28. AVERAGE CURRENT PROFILE FROM POINT 3 TO POINT 4  
USING NAVIGATION DATA FROM LORAN (DISPLAY)

## APPENDIX F. CURRENT PROFILES FOR SPECIFIC TIMES

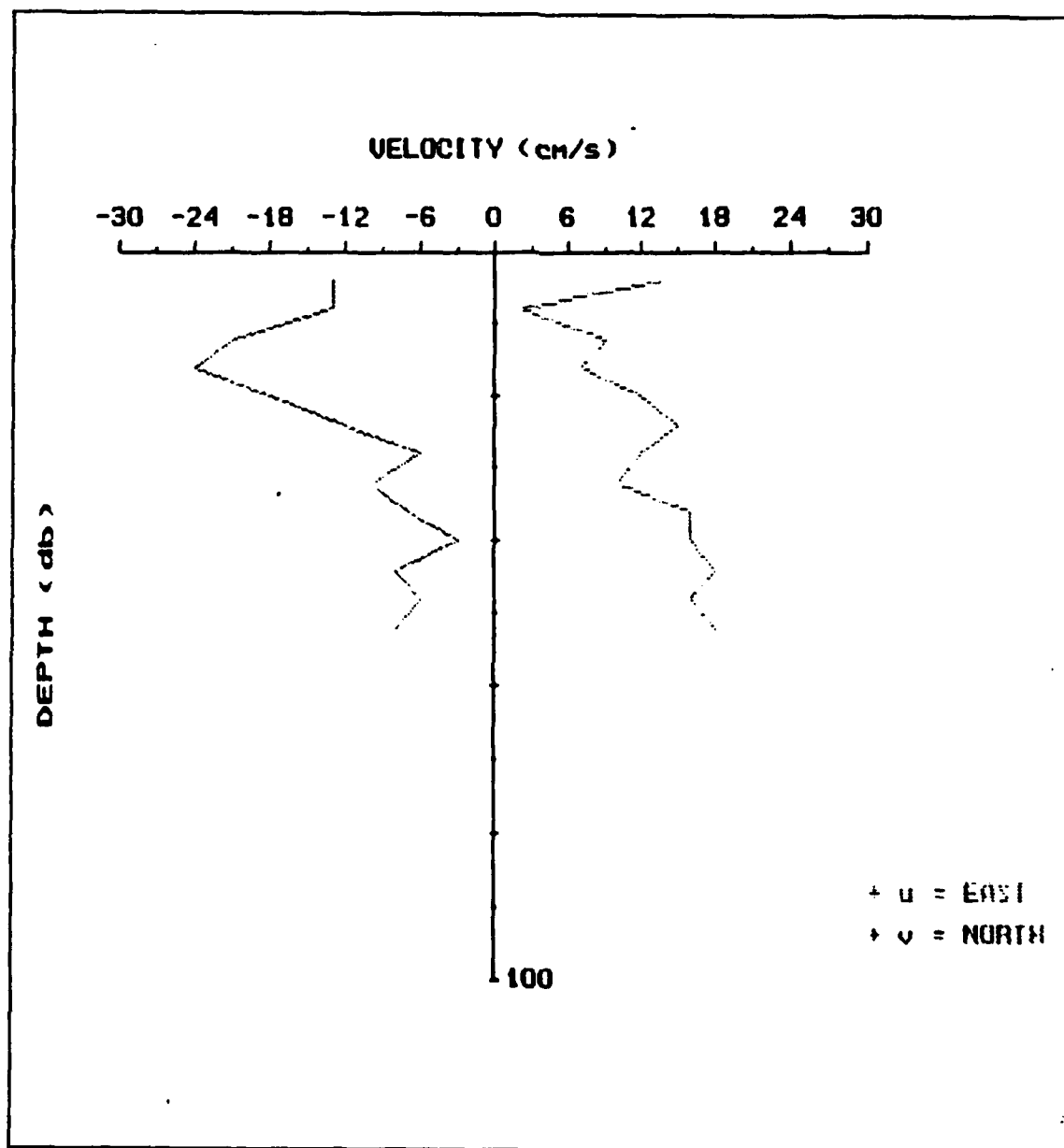


Figure 29. CURRENT PROFILE FROM POINT 1 TO POINT 2 USING NAVIGATION DATA FROM MINI RANGER FOR A SPECIFIC TIME (14 33 11)

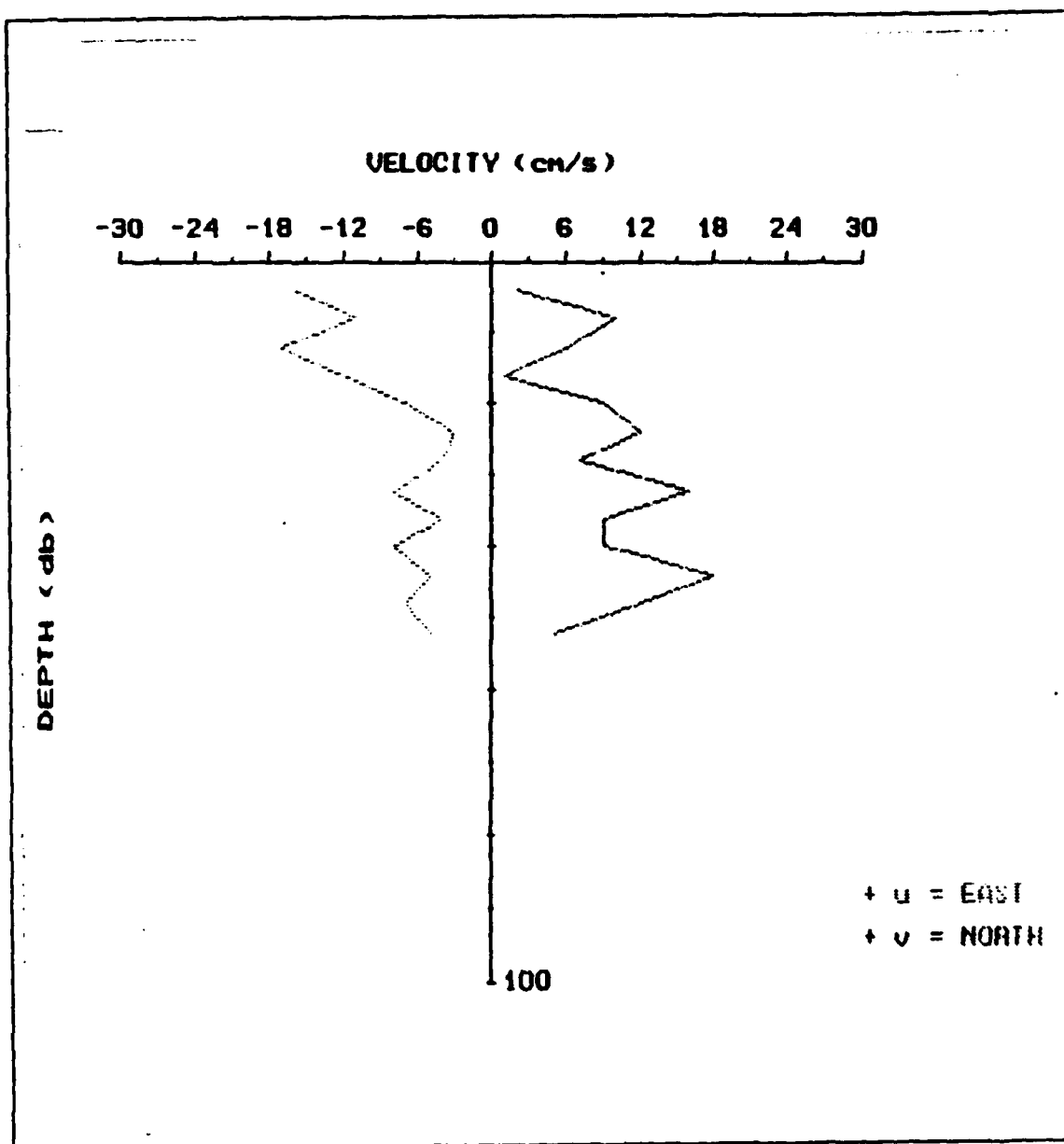


Figure 30. CURRENT PROFILE FROM POINT 2 TO POINT 1 USING NAVIGATION DATA FROM MINI RANGER FOR A SPECIFIC TIME (15 06 10)

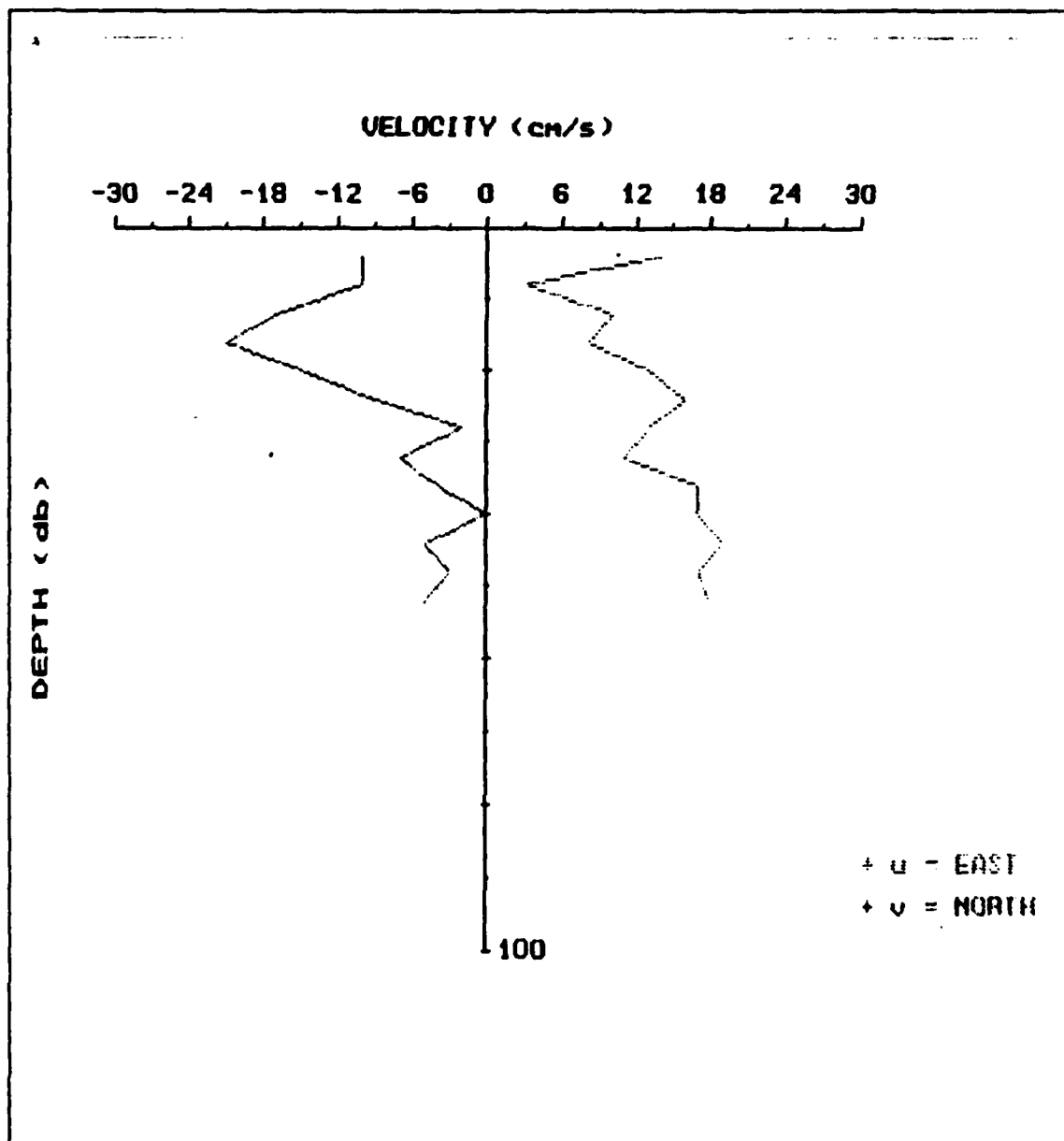


Figure 31. CURRENT PROFILE FROM POINT 1 TO POINT 2 USING NAVIGATION DATA FROM LORAN (TD) FOR A SPECIFIC TIME (14 33 11)

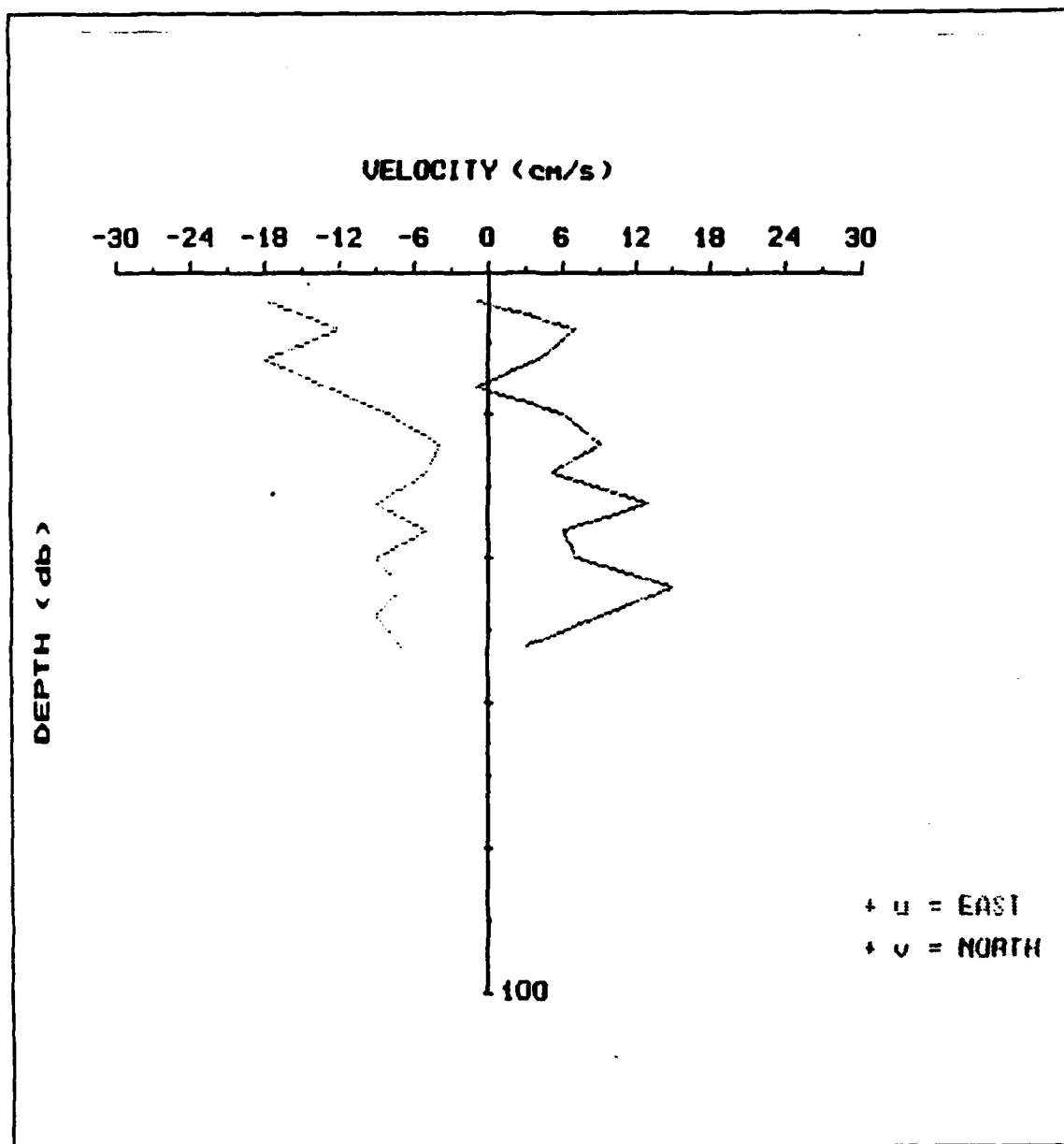


Figure 32. CURRENT PROFILE FROM POINT 2 TO POINT 1 USING NAVIGATION DATA FROM LORAN (TD) FOR A SPECIFIC TIME (15 06 10)

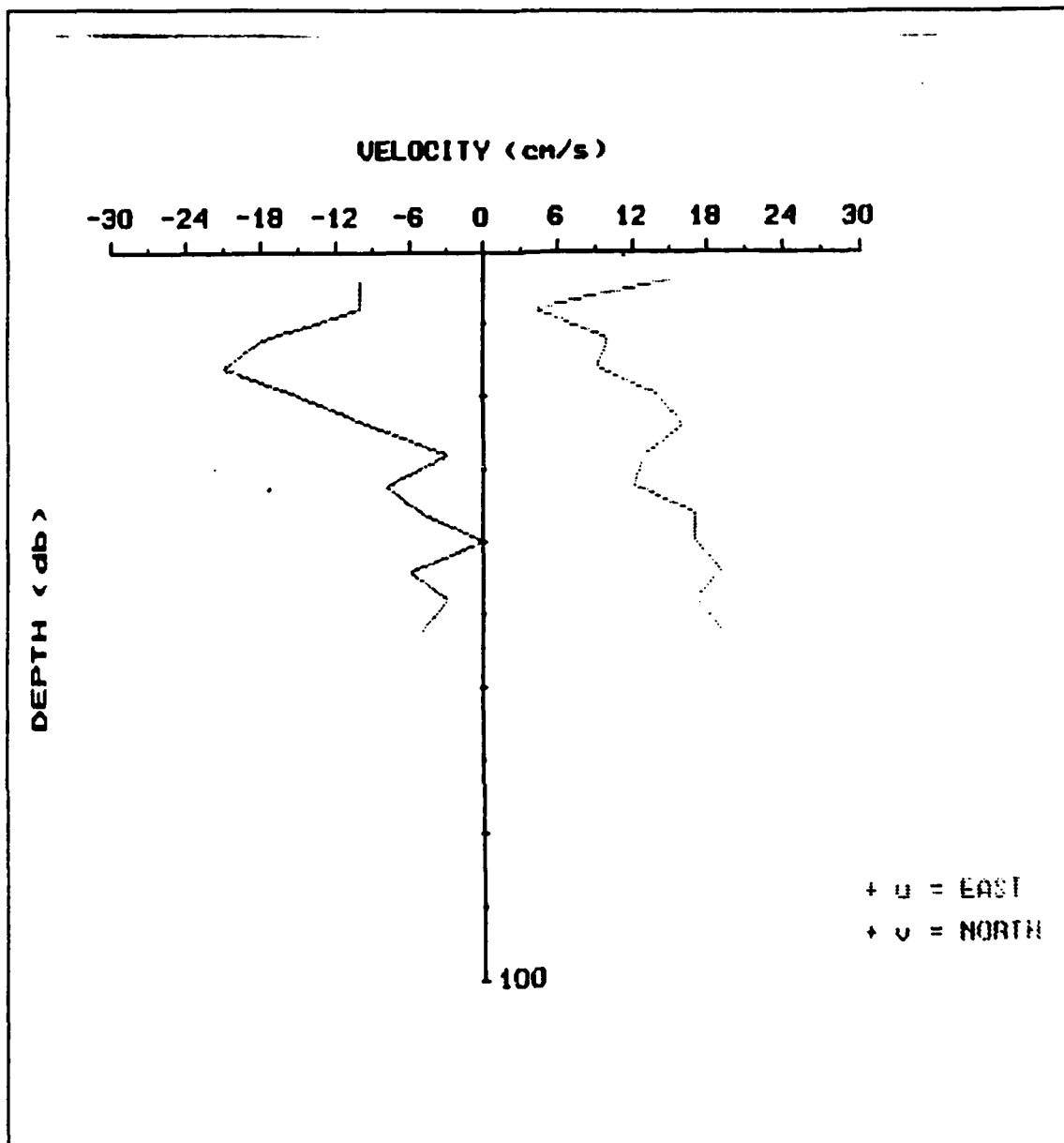


Figure 33. CURRENT PROFILE FROM POINT 1 TO POINT 2 USING NAVIGATION DATA FROM LORAN (DISPLAY) FOR A SPECIFIC TIME (14 33 11)

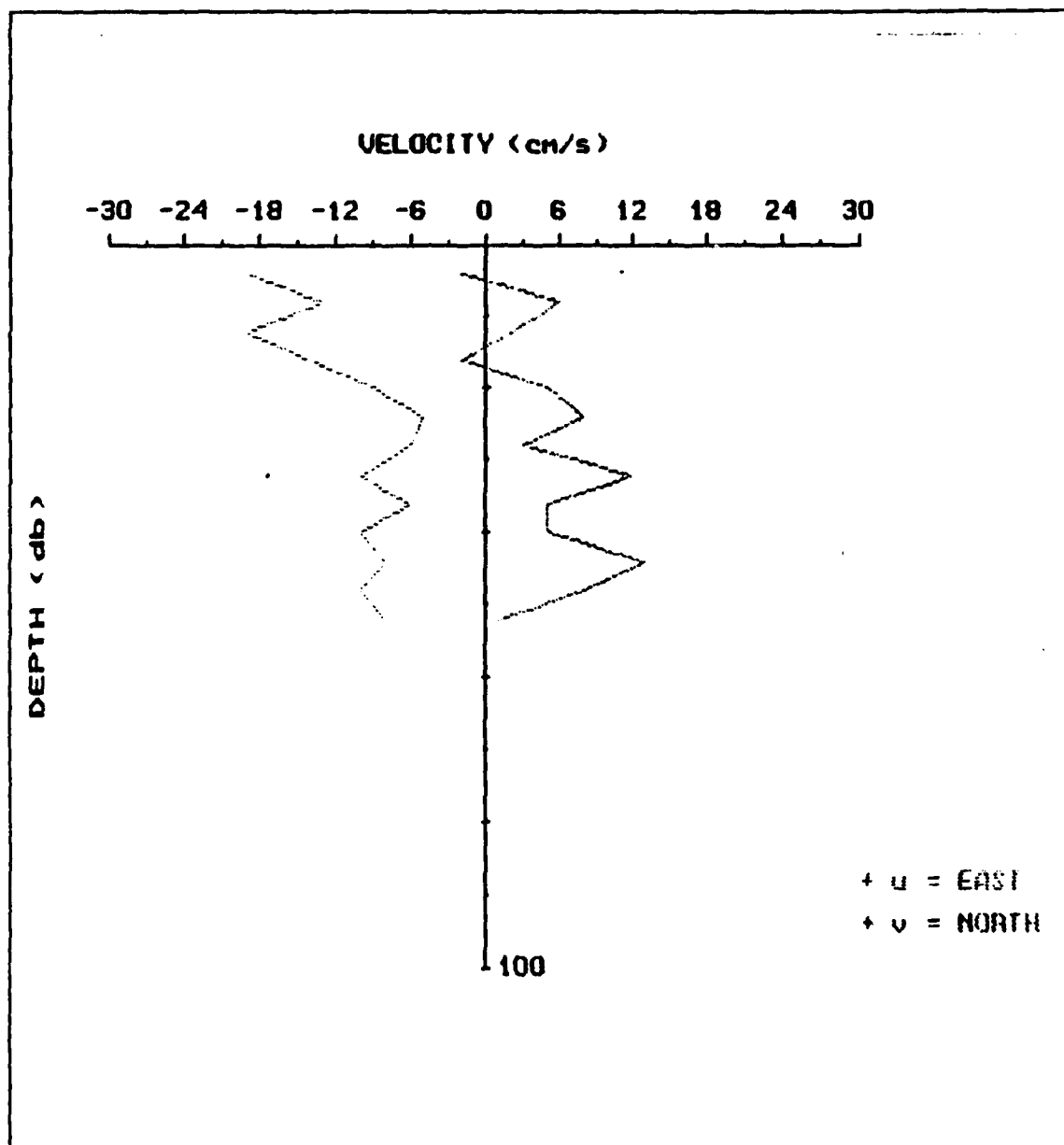


Figure 34. CURRENT PROFILE FROM POINT 2 TO POINT 1 USING NAVIGATION DATA FROM LORAN (DISPLAY) FOR A SPECIFIC TIME (15 06 10)

### LIST OF REFERENCES

Bowditch, "American Practical Navigator", *Defence Mapping Agency Hydrographic/Topographic Center*, 1984.

Kurt J. Schenebele, "Application of LORAN C Positioning to Hydrographic Surveying", *Thesis*, September 1979.

John T. Gann, "Integrated GPS, Range-Range and Hyperbolic Loran C Marine Navigation System for Use on IBM AT or Compatible Microcomputer", *Department of the Interior U.S Geological survey*.

Nickolaos G. Krieneritis, "Evaluation and Improvement of Mini Ranger Network in Monterey Bay for Oceanography Purposes", *Thesis*, December 1989.

Cross P.A, "The Computation of Position at Sea", *The Hydrographic Journal*, No.20, April 1981.

Mini-Ranger III, "Positioning system maintenance Manual", *Motorola Inc.*, February 1981.

RD Instruments, "Acoustic Doppler Current Profiles, Principles of Operation: A Practical Primer", 1989.

LC 408, "Operation Manual".

Walter Clark Hamilton, "Statistics in Physical science", *Ronald Press Company*, 1964.



# INITIAL DISTRIBUTION LIST

	No. Copies
1. Defense Technical Information Center Cameron Station Alexandria, VA 22304-6145	2
2. Library, Code 0142 Naval Postgraduate School Monterey, CA 93943-5002	2
3. Chairman, Department of Oceanography Code 68Co Naval Postgraduate School Monterey, CA 93943-5000	3
4. Dr. John Hannah Code 68Hn Naval Postgraduate School Monterey, CA 93943-5000	3
5. Dr. Donald Danielson Code 53Dd Naval Postgraduate School Monterey, CA 93943-5000	3
6. Cdr Kurt J. Schnebele Code 68Sn Naval Postgraduate School Monterey, CA 93943-5000	1
7. Dr. Stevens P. Tucker Code 68Tx Naval Postgraduate School Monterey, CA 93943-5000	1
8. Dr. Von Schwind Code 68Vs Naval Postgraduate School Monterey, CA 93943-5000	1

- |     |   |   |
|-----|---|---|
| 9.  | Dr. Tim Stanton<br>Code 68St<br>Naval Postgraduate School<br>Monterey, CA 93943-5000                                  | 1 |
| 10. | Mr. James R. Cherry<br>Code 68Ch<br>Naval Postgraduate School<br>Monterey, CA 93943-5000                              | 1 |
| 11. | Mr. Jim Stockel<br>Code 68Si<br>Naval Postgraduate School<br>Monterey, CA 93943-5000                                  | 1 |
| 12. | Embassy of Greece<br>Naval Attache<br>2228 Massachusetts Av. NW<br>Washington DC 20008                                | 4 |
| 13. | Mr. Ioannis S. Moschovos<br>Korifi Pyrgou Hlias<br>GREECE   | 5 |
| 14. | Mr. George Tziagidis<br>961 mc clellan<br>Monterey CA 93940   | 1 |
| 15. | Dr. Mike Kosro<br>College of Oceanography<br>Oregon State University<br>Corvallis, OR 97331                           | 1 |
| 16. | Dr. Eric Firing<br>Department of Oceanography<br>University of Hawaii<br>Honolulu, HI 96844                           | 1 |
| 17. | Dr. Terry Joyce<br>Physical Oceanography<br>WHOI<br>Woods Hole, MA 02543  | 1 |
| 18. | Director Naval Oceanography Division<br>Naval Observatory<br>34th and Massachusetts Avenue NW<br>Washington, DC 20390 | 1 |

19. Commanding Officer  
Naval Oceanographic Office  
NSTL Station  
Bay st. Louis, MS 39522